ANALYSIS OF NUCLEON - NUCLEUS SCATTERING WITH THE WKB METHOD

THESIS FOR THE DEGREE OF Ph. D.

MICHIGAN STATE UNIVERSITY

BY

HYANG KEY LEE

1966

This is to certify that the

thesis entitled

ANALYSIS OF NUCLEON-NUCLEUS

SCATTERING WITH THE WKB METHOD

presented by

Hyang Key Lee

has been accepted towards fulfillment
of the requirements for

Ph. D. degree in Physics

H. McManus
Major professor

Date 5-19-66

O-169

ABSTRACT

ANALYSIS OF NUCLEON-NUCLEUS SCATTERING
WITH THE WKB METHOD

by Hyang Key Lee

The WKB method together with the impulse approximation is applied to the inelastic scattering of 156 MeV nucleons from the nuclei C^{12}, O^{16} and Ca^{40}. The optical potential employed includes a spin-orbit part. In general, the agreement between prediction and experiment for the cross-sections is impressive. The predictions by the WKB compare favorably with the results of the DWIA, although the WKB appears to predict slightly larger cross-sections than the DWIA.

For normal parity states, the effect of the spin-orbit potential on the polarization is as expected. In the cases where spin-flip is important, the polarization is sensitive to the spin-orbit term. For Ca^{40}, the imaginary part of the spin-orbit potential contributes little to the polarization.

The WKB method is applied also to the cases where the incident energy of the projectile is 40 MeV. In place of the impulse approximation, a two-body potential of the Yukawa type is assumed. The agreement between data and prediction is qualitative only. The WKB is clearly inadequate at this low energy.

ANALYSIS OF NUCLEON-NUCLEUS SCATTERING WITH THE WKB METHOD

By

Hyang Key Lee

A THESIS

Submitted to
Michigan State University
in partial fulfillment of the requirements
for the degree of

DOCTOR OF PHILOSOPHY

Department of Physics and Astronomy

1966

ACKNOWLEDGMENTS

The author wishes to express deep gratitude to his parents and brother, who made it possible for him to study in this country by personal sacrifices on their part.

Sincere appreciation is felt for the patient guidance and understanding provided by Professor Hugh McManus throughout this work.

The author gives special thanks to his wife for her unceasing encouragement and personal endeavors in preparing this manuscript.

TABLE OF CONTENTS

		Page
ACKNOWLEDGMENTS		ii
LIST OF ILLUSTRATIONS		v
LIST OF TABLES		viii
LIST OF APPENDICES		ix
Chapter		
I.	INTRODUCTION	1
II.	DISTORTED WAVE THEORY	6
	Cross Sections and Polarizations	6
	Optical Potential; Perturbation Theory	9
	Impulse Approximation	12
III.	WKB APPROXIMATION	16
IV.	FORM FACTORS	21
	Nuclear States	21
	Isospin Dependence	24
	Form Factors	24
	Final State for Spin $S = 0$	25
	Final State for Spin $S = 1$, $J = L$	27
	Final State for Spin $S = 1$, $J = L \pm 1$	29
V.	DETAILED CALCULATIONS	32
	Reduction of the Scattering Amplitudes	32
	Scattering Amplitudes for $S = 0$	32
	Scattering Amplitudes for $S = 1$	37
	Numerical Calculations	39
VI.	DISCUSSION	44
	C^{12}	44
	O^{16}	48
	Ca^{40}	50

Page

VII. THE WKB METHOD AT 40 MEV 52

VIII. CONCLUSION 60

LIST OF REFERENCES 95

LIST OF ILLUSTRATIONS

Figure		Page
1.	Cross-Section for 4.43 MeV level of C^{12}	98
2.	Polarization " " " " " "	99
3.	Cross-Section for 9.7 MeV level of C^{12}	100
4.	Polarization " " " " " "	101
5.	Cross-Section for 12.7 MeV level of C^{12}	102
6.	Polarization " " " " " "	103
7.	Cross-Section for 15.1 MeV level of C^{12}	104
8.	Polarization " " " " " "	105
9.	Cross-Section for 16.1 MeV level of C^{12}	106
10.	Polarization " " " " " "	107
11.	Cross-Section for 18.2 MeV level of C^{12}	108
12.	Polarization " " " " " "	109
13.	Cross-Section for 19.3 MeV level of C^{12}	110
14.	Polarization " " " " " "	111
15.	Cross-Section for 21 MeV level of C^{12}	112
16.	Polarization " " " " " "	113
17.	Cross-Section for 22.3 MeV level of C^{12}	114
18.	Polarization " " " " " "	115
19.	Cross-Section for 21.2 MeV level of C^{12}	116
20.	Polarization " " " " " "	117
21.	Cross-Section for 19.5 MeV level of C^{12}	118
22.	Polarization " " " " " "	119

Page

23. Cross-Section for 23.2 MeV level of C^{12} 120

24. Cross-Section for 19.2 MeV level of C^{12} 121

25. Polarization " " " " " " 122

26. Cross-Section for 24.2 MeV level of C^{12} 123

27. Cross-Section for 6.15 MeV level of O^{16} 124

28. Polarization " " " " " " 125

29. Cross-Section for 11.5 MeV level of O^{16} 126

30. Polarization " " " " " " 127

31. Cross-Section for 13.1 MeV level of O^{16} 128

32. Polarization " " " " " " 129

33. Cross-Section for 15.3 MeV level of O^{16} 130

34. Polarization " " " " " " 131

35. Cross-Section for 18.7 MeV level of O^{16} 132

36. Cross-Section for 20.2 MeV level of O^{16} 133

37. Polarization for 19.1 MeV level of O^{16} 134

38. Cross-Section for 13.5 MeV level of O^{16} 135

39. Cross-Section for 16.6 MeV level of O^{16} 136

40. Polarization for 17 MeV level of O^{16} 137

41. Cross-Section for 17.3 MeV level of O^{16} 138

42. Polarization " " " " " " 139

43. Cross-Section for 17.6 MeV level of O^{16} 140

44. Polarization " " " " " " 141

45. Cross-Section for 20 MeV level of O^{16} 142

46. Polarization " " " " " " 143

47. Cross-Section for 20.2 MeV level of O^{16} 144

48. Polarization " " " " " " 145

49. Cross-Section for 3.7 MeV level of Ca^{40} 146

Page

50. Polarization for 3.7 MeV level of Ca^{40} 147

51. Polarization " " " " " " 148

52. Cross-Section for 4.4 MeV level of Ca^{40} . . . 149

53. Polarization " " " " " " 150

54. Cross-Section for 7.15 MeV level of Ca^{40} . . . 151

55. Polarization " " " " " " 152

56. Cross-Section for 7.73 MeV and 8.34 MeV levels of Ca^{40} 153

57. Polarization for 8.34 MeV level of Ca^{40} . . . 154

58. Cross-Section for 8 MeV level of Ca^{40} 155

59. Cross-Section for 12 MeV level of Ca^{40} 156

60. Cross-Section for 4.43 MeV level of C^{12} with 40 MeV 157

61. Cross-Section for 9.6 MeV level of C^{12} with 40 MeV 158

62. Cross-Section for 6 MeV level of O^{16} with 40 MeV 159

LIST OF TABLES

Table		Page
1.	Optical Parameters	40
2.	Central Absorption	42
3.	Spin-orbit Integration	42
4.	Effective Form Factors for C^{12} 2^+, T = 0 . . .	57
5.	Parameters for the Distorted Wave	57
6.	Effective Form Factors for C^{12} 3^-, T = 0 . . .	59
7.	Effective Form Factors for O^{16} 3^-, T = 0 . . .	59
8.	Identification of the Final States	63

LIST OF APPENDICES

Appendix	Page
I.	64
II.	69
III.	71
IV.	73
V.	76
VI.	89
VII.	91

CHAPTER I

INTRODUCTION

The theory of the scattering of high energy nucleons by the nucleus as developed by Kerman, McManus and Thaler (1) (hereafter referred to as KMT), often called the distorted wave impulse approximation (or DWIA), has been very useful in the study of the nuclear reactions. In DWIA the incoming nucleon is considered to be scattered by an essentially free nucleon in the target nucleus while traversing an average (or optical) potential due to the presence of other nucleons in the nucleus before and after the collision. The calculation of the wave function (distorted wave) of the beam nucleon (as the optical potential is of complicated functional form) has to be carried out numerically using a high-speed computer. Since this procedure is long and complicated, it is difficult to keep the essential physics in sight. Therefore it is hoped that the calculation of the distorted wave can be simplified by making further approximations and thereby bringing out the essential features of the nuclear reactions. The Eikonal or WKB method is used for such purpose.

Several authors have applied the WKB method to nuclear reactions with high energy beam particles above 100 MeV. Squires (2) used WKB to calculate the cross section and polarization of the inelastically scattered nucleons leaving the target C^{12} in 2^{+} state. Squires' optical potential was of Gaussian form and had no spin-orbit potential. The particle-hole interaction was not taken into account in the nuclear wave functions. Agreement with the existing data was good if an effective charge correction was made to the cross-section. Making use of WKB, Sanderson was reasonably successful in reproducing the broad peak in the cross sections observed at the excitation energy near 20 MeV for C^{12}. (3) The optical potential Sanderson used was purely absorptive and had no spin-orbit part. Sanderson's nuclear wave functions were linear combinations of the particle-hole states.

D. Jackson used WKB to study the scattering of a nucleon with incoming energies of 40 MeV, 90 MeV and 150 MeV from Li^{6}, exciting the target to 2.18 MeV above the ground state. (4) The theoretical prediction was compared with the experimental cross section for a beam energy of 40 MeV. The experimental cross-section was greater than the theoretical prediction by a factor of 1.5 and peaked at smaller angles. This is not surprising as DWIA and WKB are high energy approximations. However, the polarization agreed with the experiment reasonably well. This is because the polarization for excited states of normal parity is essentially given by the Born approximation. D. Jackson also used a complex optical potential of the Gaussian form. She showed that the effect of the real part of the optical potential was very small at energies above 90 MeV. T. Erickson calculated the cross section for incoming nucleons of 180 MeV exciting the O^{16} nucleus to 2^- state at 12.5 MeV. He obtained good agreement with the experiment for the cross section although he was less successful with the polarization. The optical potential used was purely absorptive and central. The nuclear wave functions Erickson used were combinations of particle-hole states. (5)

There is now much more experimental information about the inelastic scattering of high energy protons (around 150 MeV) from C^{12}, O^{16}, and Ca^{40}. DeBouard et al. (6) at Orsay measured the polarization of inelastically scattered nucleons from C^{12}. Jacmart et al. (7) at Orsay published results on the inelastic cross sections of the light nuclei. More recently, Hasselgren et al. (8) measured a large number of inelastic cross sections again from the light nuclei. Roos (9) measured a few scattering cross sections from Ca^{40}.

Looking at existing theoretical calculations by the WKB method, one is impressed with its reasonable success at high energy. The present investigation applies the WKB method to nuclear reactions involving an inelastically scattered nucleon with an incident energy of 156 MeV and many excited states of the nuclei, C^{12}, O^{16}, and Ca^{40}. The optical potential used has a Wood-Saxon form and a spin-orbit part as given by Haybron and Satchler from analysis of elastic scattering. (10) The nuclear wave functions are taken from calculations of Gillet et al. (11) Cross sections and polarizations are compared with experiment and also with the results of DWIA calculations. (19) Particular attention is given to the effect of the spin-orbit potential on the polarization as it is suspected that for some states, the spin-orbit term may be very important. The same calculations are done for the inelastic scattering of incident nucleons of 40 MeV from C^{12} and O^{16}. As the use of the WKB method is not entirely justified at this low incident energy, one would be gratified to get qualitative agreement with the experiments.

In Chapter II, the distorted wave formalism is outlined. Expressions for the scattering cross-sections and polarizations are given. The definition of the optical potential is also given, along with the definition of the scattering amplitude. Then follows the discussion of the impulse approximations.

In Chapter III, the distorted wave is calculated by the WKB method.

Chapter IV deals with the nuclear state functions in the particle-hole formalism. Form Factors are defined for spins $S = 0$ and $S = 1$.

Further reduction of the S-matrix is carried out in the first part of Chapter V. A typical integral that is involved is carried out. The most general expressions for the scattering amplitudes are given both for spin $S = 0$ and $S = 1$. In the second part of Chapter V, the data for the optical potentials are given. The results of the numerical calculations of the distorted waves are shown.

In Chapter VI, the results are discussed and compared with recent experiments and also with DWIA calculations.

WKB is applied to the incoming energy of 40 MeV in Chapter VII. The main features of the calculations are the same as for 156 MeV except that the two-body interaction is of the Yukawa type. The numerical work involved has been carried out again with a computer.

The conclusions are drawn in Chapter VII.

CHAPTER II

DISTORTED WAVE THEORY

Cross Sections and Polarizations

Assume that the Hamiltonian H of the system of a nucleon and a nucleus can be separated into two parts:

$$H = H_o + V$$

where $H_o = H_n + \mathcal{k}$ and $V = \sum_{i=1}^{\mathcal{N}} \quad V(\vec{r}, \vec{\sigma}; \vec{r}_i, \vec{\sigma}_i \quad)$.

The symbols have the following meanings:

$\mathcal{k}$ is the kinetic energy operator of the incident nucleon.

H_n is the Hamiltonian of the target nucleus.

$\vec{r}, \vec{\sigma}$ are the position vector and the spin operator, respectively, of the incident nucleon.

$\vec{r}_i, \vec{\sigma}_i$ are the position vector and the spin operator of the i^{th} nucleon in the nucleus.

$\mathcal{N}$ is the total number of the nucleons in the target.

$V\ (\vec{r}, \vec{\sigma}; \vec{r}_i, \vec{\sigma}_i\ )$ is the interaction operator between the incident nucleon and i^{th} nucleon in the target.

Let H_n have the iegenfunctions (ϕ_o, ϕ_1 , -- ϕ_n--) with corresponding eigenvalues (ε_o, ε_1, --ε_n--). Assume (ϕ_o, ε_o) represent the ground state eigenfunction and energy, which we shall take as zero. Let k_o be the wave number of the incident particle when it is far away from the target. m is the mass of the nucleon.

$$H_o \frac{e^{i\vec{K}_0\cdot\vec{r}}}{(2\pi)^{3/2}} U_\nu \phi_n(\vec{r}_1, \cdots \vec{r}_N; s_1, \cdots s_N)$$

$$= E_n \frac{e^{i\vec{K}_0\cdot\vec{r}}}{(2\pi)^{3/2}} U_\nu \phi_n(\vec{r}_1, \cdots \vec{r}_N; s_1 \cdots s_N) \tag{2.1}$$

where $E_n = \frac{k_o^2}{2m} + \mathcal{E}_n$ and $(s_1 --- s_n)$ denote the spins of the nucleons in the target; U_ν is the spin wave function of incident nucleons with projection ν.

For the scattering of a nucleon of energy E by a ground state nucleus,

$$(H_o + v)\ \psi(\vec{r}, \zeta) = E\psi(\vec{r}, \zeta) \tag{2.2}$$

with the boundary conditions of incoming plane wave and outgoing spherical wave (ζ represents the variables of the target). We can rewrite (2.2) as:

$$\psi(\vec{r}, \zeta) = \frac{e^{i\vec{K}_0\cdot\vec{r}}}{(2\pi)^{3/2}} U_\nu \phi_o(\zeta) + \frac{1}{E - H_o + i\epsilon} V\psi(\vec{r}, \zeta) \tag{2.3}$$

corresponding to outgoing spherical wave.

The asymptotic form is

$$\psi(\vec{r}, \zeta) = \left(\frac{e^{i\vec{K}_0\cdot\vec{r}}}{(2\pi)^{3/2}} \phi_o(\zeta) + S_o \frac{e^{iK_o r}}{r} \phi_o(\zeta) + \sum_{n=1} \sqrt{\frac{K_o}{k_n}} \frac{S_n e^{iK_n r}}{r} \phi_n(\zeta) \right) U_\nu \tag{2.4}$$

where $k_n^2 = k_o^2 - 2mE_n$ and summation over n is to be carried out for all possible excited states of the nucleus. The coefficients S_o, and S_n respectively, are called the elastic and inelastic scattering amplitudes and are to be calculated from (2.3) and (2.4).

One gets in the center-of-mass system of the nucleon-nucleus,

$$S_n = -(2\pi)^2 \frac{m}{\hbar^2} \sqrt{\frac{k_n}{k_o}} \left(\frac{\mathcal{N}}{1+\mathcal{N}}\right) \langle n, k_n | T | k_o, o \rangle \qquad (2.5)$$

$$\text{with } T = V + V \frac{1}{E-H_o + i\epsilon} T \qquad (2.6)$$

k_o and k_n are the wave numbers of the free particles before and after the collision. $|o\rangle$ represents the ground state of the target nucleus. Since we are concerned with closed shell nuclei, the ground states have the total angular momentum $J = 0$ and isotopic spin $T = 0$. n is a set of radial quantum number, J, T, and projection of J, μ, for the excited state. Since we will be concerned with a specific final state one at a time, only μ will be kept in writing S_n as $S(\mu)$.

$S(\mu)$ is an operator in the spin space of the beam and hence can be expanded as

$$S(\mu) = S^o(\mu) \times 1 + S^x(\mu)\sigma_x + S^y(\mu)\sigma_y + S^z(\mu)\sigma_z \qquad (2.7)$$

where 1, σ_x, σ_y and σ_z are the unit and Pauli matrices. The cross section for the nucleon with any spin state after the scattering of an initially unpolarized nucleon against the target nucleus is

$$\frac{d\sigma}{d\Omega} = \frac{1}{2} \sum_{\mu} \sum_{\nu'} \sum_{\nu} \left| \langle u_{\nu'} | S(\mu) | u_\nu \rangle \right|^2$$

$$= \sum_{\mu} \sum_{\hat{r}} | S^{\hat{r}}(\mu) |^2 \tag{2.8}$$

The polarization of an initially unpolarized particle after the scattering is

$$P = \sum_{\mu} \mathrm{Tr}\,[\,S^{+}(\mu)\,\sigma_y\,S(\mu)\,] \Big/ \mathrm{Tr}\,[\,S^{+}(\mu)\,S(\mu)\,]$$

$$= \frac{2\sum_{\mu}[\,\mathrm{Re}\,(S^{0*}(\mu)\,S^{y}(\mu)) + \mathrm{Im}\,(S^{z*}(\mu)\,S^{x}(\mu))\,]}{\sum_{\mu}\mathrm{Tr}\,[\,S^{+}(\mu)\,S(\mu)\,]} \tag{2.9}$$

where Re and Im mean the real and imaginary parts, respectively. The scattering plane is taken to be the xz plane.

Optical Potential; Perturbation Theory

Our job is now the calculation of the T matrix as defined in (2.6). Because the interaction potential V is not well known and whatever is known at present about V has a complicated functional form, it is not possible to calculate T completely. The approach taken in this paper was developed in Reference 1.

The interaction potential V is split into two parts; one that is responsible for the elastic scattering and the other for the inelastic scattering. As the elastic scattering is generally much more pronounced than the inelastic scattering, the part responsible for the inelastic scattering is treated as a perturbation.

Let P and Q be the projection operators to the ground state and the excited states respectively.

$$P + Q = 1 \tag{2.10}$$

Operating with P on (2.6) from the left,

$$PT = PV + PVG\ (P+Q)T \tag{2.11}$$

where $G = \dfrac{1}{E_o - H_o + i\epsilon}$

Likewise with Q,

$$QT = QV + QVG\ (P+Q)T \tag{2.12}$$

From (2.11) and (2.12), one deduces

$$PT = PV\ (1+G\ \frac{1}{1-QVG}\ QV)\ (1+GPT) \tag{2.13}$$

Define $T_0 = PT$, (2.14)

$$U = PV + PVG\ \frac{1}{1-QVG}\ QV \tag{2.15}$$

(2.13) can be rewritten as

$$T_0 = U + UGT_o \tag{2.16}$$

Since we start out with the nuclei in the ground states, T_o is that part of the T matrix which is responsible for the elastic scattering. Then U is that part of the interaction potential responsible for the elastic scattering. We call U the optical potential. U in general is, as defined by (2.15), neither local nor hermitian.

Let $V = U + \theta$. Then T can be written in T_0 and θ which is assumed to be small,

$$T = T_o + (1+T_oG)\ \theta\ (1+GT)$$

$$T_o + (1+T_oG)\ \theta\ (1+GT_o). \tag{2.17}$$

The matrix element of T between the initial state $|k_o, 0\rangle$ and the final state $|k, n\rangle$ is

$$\langle K, n|T|K_0, 0\rangle = \langle K, n|\ (1+T_0G)\,\theta\ \ (1+G_0T)|\ K_0, 0\rangle \qquad (2.18)$$

$(1+GT_0)\ |K_0, 0\rangle$ is with (2.16)

$$(1+GT_0)|K_0,0\rangle = |K_0,0\rangle + G(U+UGU+UGUGU+---)\ |K_0,0\rangle \qquad (2.19)$$

That (2.19) is the solution of the equation

$$(H_0 + U)\chi^{(+)}_{K_0}\phi_0(\xi) = E_0\,\chi^{(+)}_{K_0}\phi_0(\xi) \qquad (2.20)$$

with the incident plane wave and outgoing spherical wave can be seen by rewriting (2.20) as

$$\begin{aligned}\chi^{(+)}_{K_0}\phi_0 &= \frac{e^{i\vec{K}_0\cdot\vec{r}}}{(2\pi)^{3/2}}\phi_0 + \frac{1}{E_0 - H_0 + i\epsilon}U\chi^{(+)}_{K_0}\phi_0 \\ &= \frac{e^{i\vec{K}_0\cdot\vec{r}}}{(2\pi)^{3/2}}\phi_0 + G(U + UGU + \cdots)\frac{e^{i\vec{K}_0\cdot\vec{r}}}{(2\pi)^{3/2}}\phi_0\end{aligned} \qquad (2.21)$$

To simplify (2.20), we assume that U is local. Multiplying from the left side of (2.20) by $\phi_0^*(\xi)$ and integrating over the variables of ξ

$$\left(-\frac{\hbar^2}{2m}\nabla^2 + U_{00}(r)\right)\chi^{(+)}_{K_0} = E_0\,\chi^{(+)}_{K_0} \qquad (2.22)$$

where $U_{00} = \int \phi_0^*(\xi)\,U\,\phi_0(\xi)\,d\xi$

Likewise one can find $(1+T_0G)^{\dagger}\ |K,n\rangle$ by solving

$$\left(-\frac{\hbar^2}{2m}\nabla^2 + U^{\dagger}_{nn}\right)\chi^{(-)}_{K} = E_n\chi^{(-)}_{K}$$

$$U^{\dagger}_{nn} = \int \phi_n^*(\xi)\,U^{\dagger}\,\phi_n(\xi)\,d\xi \qquad (2.23)$$

where $E_k = \varepsilon_n + \frac{K^2}{2m}$ and $\dagger$ means "adjoint". The reason we have U_{nn} in place of U_{oo} is because if we have our $|n\rangle$ as the initial state, then the elastic scattering will leave the target nucleus at $|n\rangle$. Then P and Q of (2.10) will be the projection operators on the state $|n\rangle$ and all other states respectively. We approximate U_{nn} by U_{oo}. As long as our projectile does not disturb the nucleus too much, this certainly will be reasonable. In practice, U_{oo} is found from the analysis of the elastic nucleon-nucleus scattering and is in general complex and has a central as well as spin-orbit part. The parameters for the U_{oo} are listed in Chapter V. Hereafter, U_{oo} will be referred to as U.

Combining (2.23), (2.20) and (2.18), we get

$$\langle K,n|T|K_0,0\rangle = \langle \phi_n, \chi_K^{(-)}|\,\theta\,|\chi_{K_0}^{(+)}, \phi_0\rangle \tag{2.24}$$

$$= \langle \phi_n, \chi_K^{(-)}|\,V\,|\chi_{K_0}^{(+)}, \phi_0\rangle \tag{2.25}$$

(2.25) is possible as $\langle \phi_n|U|\phi_0\rangle = 0$.

Impulse Approximation

The objective of this section is to approximate V with nucleon-nucleon scattering amplitudes. To reduce the complexity of (2.25), consider a term, suppressing the spins and using f in place of n,

$$\langle \phi_f\, \chi_K^{(-)}|\,V(\vec{r}-\vec{r}_i)\,|\chi_{K_0}^{(+)}\, \phi_i\rangle$$

$$= \int \phi_f^*(\varsigma,\vec{r}_i)\,\chi_k^{(-)}(\vec{r})\;V(\vec{r}-\vec{r}_i)\,\chi_{k_0}^{(+)}\;\phi_0(\varsigma,\vec{r}_i)\;d\vec{r}_i\,d\varsigma\,d\vec{r}$$

(2.26)

denotes the coordinates of $\eta-1$ nucleons.

Using the Fourier transforms

$$\chi_{k_0}^{(+)} = \frac{1}{(2\pi)^{3/2}}\int \chi^{(+)}(k_1)\;e^{i\vec{k}_1\cdot\vec{r}}\;d\vec{k}_1$$

$$\phi_0(\vec{r}_i,\varsigma) = \frac{1}{(2\pi)^{3/2}}\int \phi_0(\varsigma,\;k_i)\;e^{i\vec{k}_i\cdot\vec{r}_i}\;d\vec{k}_i$$

etc. (2.27)

and also changing the variables

$$\frac{\vec{r}+\vec{r}_i}{2} = \vec{R} \qquad \vec{r}_s = \vec{r}-\vec{r}_i$$

integration over R yields

$$= \frac{1}{(2\pi)^3}\int \phi_f^*(\varsigma,\vec{k}_1-\vec{k}_i+\vec{k}_i')\,\chi^{(-)*}(k_1')\;V(\vec{r}_s)\,e^{i(\vec{k}_1-\vec{k}_1')\cdot\vec{r}_s}\,\chi^{(+)}(k_1)\;\phi_0(\varsigma,\vec{k}_i)\,d\vec{R}_1\,d\vec{k}_i\,d\vec{k}_1'\,d\vec{r}_s\,d\varsigma$$

$$= \int \phi_f^*(\varsigma,\vec{k}_1-\vec{k}_i+\vec{k}_i')\,\chi^{(-)*}(k_1')\;\langle k_1'|\,V|k_1\rangle\,\chi^{(+)}(k_1)\;\phi_0(\varsigma,\vec{k}_i)\;d\vec{k}_i\,d\vec{k}_1\,d\vec{k}_1'\,d\varsigma$$

(2.28)

But $\langle k_1'|\,V\,|\,k_1\rangle = V_i\,(q',\;q'^2+p'^2,\;\vec{p}'\cdot\vec{q}')$

where $\vec{q} = \vec{k}_1'-\vec{k}_1,\quad \vec{P}' = \vec{k}_1'+\vec{k}_1$ (2.29)

Experiences in two-body scattering show that V is insensitive to the energy. So we assume that V = V (q'). Furthermore, assume

$$V\,(q') = V\,(q) \tag{2.30}$$

where $q = |\vec{k}-\vec{k}_0|$, the momentum change of the incident particle.

Substituting (2.30) into (2.28) and using the inverse Fourier transform of (2.27), (2.25) is written now

$$\langle f,k \mid T \mid k_0, 0\rangle = (2\pi)^3 \int \phi_f^*(\xi,\vec{r}_i)\, \chi_k^{(-)*}(\vec{r}) \sum_{i=1}^{\mathcal{N}} \left[V_i(q)\, \delta(\vec{r}-\vec{r}_i) \right]$$
$$\chi_{k_0}^{(+)}\, \phi_0(\xi,\vec{r}_i)\, d\xi\, d\vec{r}_i\, d\vec{r}$$

(2.31)

Approximate the Fourier transform of V as

$$-\frac{2\pi}{\hbar^2}\cdot\frac{m}{2}\langle k \mid V \mid k_0\rangle = t_i(q)$$

(2.32)

where $t_i(q)$ is the scattering amplitude of two free nucleons as listed in Reference 1.

Charge independence, invariance against time reversal and space inversion, and finally rotational invariance restrict the general form of two-body scattering to the following expression (15)

$$t = A + B\sigma_n\cdot\sigma_{1n} + c(\sigma_n+\sigma_{1n}) + E\sigma_q\cdot\sigma_{1q} + F\sigma_p\cdot\sigma_{1p}$$

(2.33)

where $(\hat{q}, \hat{n}, \hat{p})$ are unit vectors as shown below,

$$\hat{q} = \frac{\vec{k}-\vec{k}_0}{|\vec{k}-\vec{k}_0|}, \quad \hat{n} = \frac{\vec{k}_0\times\vec{k}}{|\vec{k}_0\times\vec{k}|}, \quad \hat{p} = \frac{\vec{k}_0+\vec{k}}{|\vec{k}_0+\vec{k}|} \qquad (2.34)$$

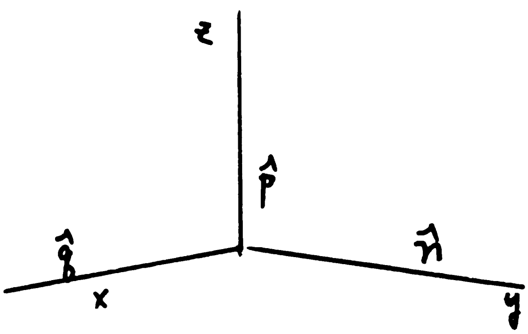

The coefficients A's are the operators in the isotopic spin space as shown below:

$$A = \tfrac{1}{4}(3A_1+A_0) + \tfrac{1}{4}(A_1-A_0)\,\tau\cdot\tau_i \tag{2.35}$$

with corresponding expressions for B, C, E and F. τ refers to the incoming nucleon and τ_i to the nucleon in the target. A_0 and A_1 are the coefficients for the singlet and triplet states.

(2.31) can be written as

$$\langle f, k|\, T\, |k_0, o\rangle = -\frac{\hbar^2}{(2\pi)^2}\cdot\frac{2}{m}(2\pi)^3 \int \phi_f^*(\vec{r}_i,\xi)\,\chi_k^{(-)*}(\vec{r})$$

$$\left[\sum_{i=1}^{N} t_i(q)\,\delta(\vec{r}-\vec{r}_i)\right]\chi_{k_0}^{(+)}(\vec{r})\,\phi_0(\vec{r},\vec{r}_i)\,d\vec{r}_i\,d\vec{r}\,d\xi \tag{2.37}$$

(2.37) is still an operator in the spin space of the incident particle. ϕ_f's are given by Gillet et al. So the remaining task is to calculate $\chi^{(\pm)}$, which is done in the next chapter.

CHAPTER III

WKB APPROXIMATION

The differential equation (2.22) is, in the center of the mass of the nucleon-nucleus system,

$$\left[-\frac{\nabla^2}{2\rho} + U_c(r) + U_s(r)\,\vec{\sigma}\cdot\vec{L} \right] \chi_{k_0}^{(+)}(\vec{r}) = E_0\, \chi_{k_0}^{(+)}(\vec{r}) \tag{3.1}$$

with the incident plane wave of the wave number k_0 and the outgoing spherical wave. U_c and U_s are the scalar functions of Wood-Saxon type which vary very slowly and have short ranges. In practice $U_c \gg U_s$. $\vec{\sigma}\cdot\vec{L}$ is a spin-orbit operator acting on the incoming particle. ρ is the reduced mass and $\hbar = c = 1$.

Using Green's function, one can write

$$\chi_{k_0}^{(+)} = \frac{e^{i\vec{k}_0\cdot\vec{r}}}{(2\pi)^{3/2}} - \frac{2\rho}{4\pi}\int \frac{e^{ik_0|\vec{r}-\vec{r}'|}}{|\vec{r}-\vec{r}'|} \left[U_c(r') + U_s(r')\,\vec{\sigma}\cdot\vec{L} \right] \chi_{k_0}^{(+)}(\vec{r}')\, d\vec{r}' \tag{3.2}$$

where U_ν, the spin wave function of the beam, is suppressed. With McCauley and Brown (12) and Glauber (13), we write

$$\chi_{k_0}^{(+)} = \chi'(\vec{r})\, \frac{e^{i\vec{k}_0\cdot\vec{r}}}{(2\pi)^{3/2}} \tag{3.3}$$

$\chi'(r)$ is an operator in the spin space and has to be determined by (3.2) and (3.3). Assume that the potential is very smooth and varies very little within a distance d and the incident energy is sufficiently high so that $k_o d \gg 1$. Then it is reasonable to expect that $\chi'(\vec{r})\cdot U$ varies very little in d. We shall drop the terms of the order $(\frac{1}{k_o d})$.

From (3.3) and (3.2), one gets

$$\chi'(\vec{r}) = 1 - \frac{2\rho}{4\pi}\int \frac{e^{iK_0|\vec{r}-\vec{r}'|}}{|\vec{r}-\vec{r}'|} e^{-i\vec{K}_0\cdot\vec{r}}\left[U_c(r') + U_s(r')\vec{\sigma}\cdot\vec{L}\right] e^{i\vec{K}_0\cdot\vec{r}'}\chi_k'(\vec{r}')\, d\vec{r}' \tag{3.4}$$

One gets from (3.4)

$$\chi'(\vec{r}) = 1 - \frac{2\rho}{4\pi}\int \frac{e^{iK_0|\vec{r}-\vec{r}'|}}{|\vec{r}-\vec{r}'|} e^{-i\vec{K}_0\cdot(\vec{r}-\vec{r}')} U_c(r')\chi'(\vec{r}')\, d\vec{r}'$$

$$- \frac{2\rho}{4\pi}\int \frac{e^{iK_0|\vec{r}-\vec{r}'|}}{|\vec{r}-\vec{r}'|} e^{-i\vec{K}_0\cdot(\vec{r}-\vec{r}')} U_s(r')\vec{\sigma}\cdot(\vec{r}'\times K_0)\chi'(\vec{r}')\, d\vec{r}' \tag{3.5}$$

Changing the variable $\vec{r}'' = \vec{r}-\vec{r}'$ in the right-hand side of (3.5) and using $d\vec{r} = r^2\, dr\, d\eta\, d\phi$

$$\chi'(\vec{r}) = 1 - \frac{2\rho}{4\pi}\int_0^\infty\int_{-1}^1\int_0^{2\pi} \frac{e^{iK_0 r''(1-\eta)}}{r''} U_c(|\vec{r}-\vec{r}''|)\chi'(\vec{r}-\vec{r}'') r''^2\, d\eta\, d\phi\, dr''$$

$$- \frac{2\rho}{4\pi}\int_0^\infty\int_{-1}^1\int_0^{2\pi} \frac{e^{iK_0 r''(1-\eta)}}{r''} U_s(|\vec{r}-\vec{r}''|)\, \sigma\cdot(\vec{r}-\vec{r}'')\times\vec{K}_0\, \chi'(\vec{r}-\vec{r}'')\, r''^2\, dr''\, d\eta\, d\phi \tag{3.6}$$

Consider the second term of (3.6). Integration by parts in η yields

$$-\rho\int_0^\infty \frac{U_c(|\vec{r}-\vec{r}''|)}{iK_0}\chi'(\vec{r}-\vec{r}'')\,dr''\Big]_{\eta=1} + \frac{\rho}{iK_0}\int e^{2iKr''}U_c(|\vec{r}-\vec{r}''|)\chi'\,dr''\Big]_{\eta=-1}$$

$$+\frac{\rho}{iK_0}\int e^{iK_0r''(1-\eta)}\frac{d}{d\eta}(U_c\chi')\,d\eta\,dr''$$

(3.7)

Because of the rapidly varying phase, the second and third terms are $O(\frac{1}{K_0 d})$ compared to the first. (13) Hence they are dropped.

One could apply the same argument to the second term of (3.6). One gets

$$\chi'(\vec{r}) = 1 + \frac{i\rho}{K_0}\int U_c(|\vec{r}-\vec{r}''|)\chi'(\vec{r}-\vec{r}'')\,dr''\Big]_{\eta=1}$$

$$+\frac{i\rho}{K_0}\int U_s(|\vec{r}-\vec{r}''|)\chi'(\vec{r}-\vec{r}'')\,\sigma\cdot(\vec{r}-\vec{r}'')\times\vec{K}_0\,dr''\Big]_{\eta=1}$$

(3.8)

Now taking our coordinate system such that k_o is along the z direction, $\eta = \cos\theta$ is measured from the z direction.

$$\chi'(b,z) = 1 + \frac{i\rho}{K_0}\int_0^\infty U_c(b,z-z'')\chi'(\vec{b},z-z'')\,dz''$$

$$+\frac{i\rho}{K_0}\int_0^\infty U_s(b,z-z'')\vec{\sigma}\cdot(\vec{b}\times\vec{K}_0)\chi'(\vec{b},z-z'')\,dz''$$

(3.9)

where $b = \sqrt{x^2+y^2}$. Hereafter, whenever convenient, we shall use the cylindrical coordinate system as defined by $\vec{r} = (x,y,z) = (\vec{b},z)$. If the particle is incident along z, then b is the impact parameter.

$$\chi' = 1 - \frac{i\rho}{K_0}\int_{-\infty}^{z}\left[U_c(b,z') + U_s(b,z')\,\vec{\sigma}\cdot\vec{b}\times\vec{K_0}\right]\chi'(b,z')\,dz' \tag{3.10}$$

One can rewrite (3.10) as

$$\chi'(b,z) = e^{-\frac{i\rho}{K_0}\int_{-\infty}^{z}\left[U_c(b,z') + U_s(b,z')\,\vec{\sigma}\cdot\vec{b}\times\vec{K_0}\right] dz'} \tag{3.11}$$

Combining (3.11) and (3.3), one finds the solution to (3.1)

$$\chi_{K_0}^{(+)} = \frac{e^{i\vec{K_0}\cdot\vec{r} - \frac{i\rho}{K_0}\int_{-\infty}^{z}\left[U_c(b,z') + U_s(b,z')\,\vec{\sigma}\cdot\vec{b}\times\vec{K_0}\right] dz'}}{(2\pi)^{3/2}} \tag{3.12}$$

To calculate $X_k^{(-)}$, one must solve

$$\left[-\frac{\nabla^2}{2\rho} + U_c^*(r) + U_s^*(r)\,\vec{\sigma}\cdot\vec{L}\right]\chi_k^{(-)} = E\,\chi_k^{(-)} \tag{3.13}$$

with the incoming plane wave of the wave number k and the incoming spherical wave. The procedure is exactly the same as before except this time $\eta = -1$ term survives.

$$\chi_K^{(-)} = \frac{e^{i\vec{K}\cdot\vec{r}}}{(2\pi)^{3/2}} + \frac{i\rho}{K} \int_z^\infty \left[U_c^*(b,z') + U_s^*(b,z')\, \vec{\sigma}\cdot\vec{b}\times\vec{K} \right] dz'$$

(3.14)

The scattering matrix (2.5) is now, with (2.37), (3.12) and (3.14),

$$S(\mu) = 2\sqrt{\frac{K}{K_0}}\left(\frac{\mathcal{N}}{1+\mathcal{N}}\right) \int \phi_f^*(\xi, r_i)\, \chi_K^{(-)*}(r) \left[\sum_i t_i(g)\, \delta(\vec{r}-\vec{r}_i) \right]$$

$$\chi_{K_0}^{(+)}(r)\, \phi_0(\xi, \vec{r}_i)\, d\vec{r}\, d\vec{r}_i\, d\xi$$

(3.15)

CHAPTER IV

FORM FACTORS

Nuclear States

The nuclear wave functions ϕ_f and ϕ_o that appear in (3.15) will be described in the language of the second quantization. Let $a^\dagger$ and a be the creation and annihilation operators of the fermions, i.e. the nucleons. a is the adjoint of $a^\dagger$.

$$a_s^\dagger\, a_t + a_t\, a_s^\dagger = \quad {}_{s,\,t}$$
$$a_s\, a_t + a_t\, a_s = 0$$
$$a_s^\dagger\, a_t^\dagger + a_t^\dagger\, a_s^\dagger = 0 \tag{4.1}$$

Let $|o\rangle$ be the "vacuum" state (closed shell state). Then $a_{jm}^\dagger|o\rangle$ represents a state of the closed shell plus a particle with the angular momentum j and its projection m. $(-1)^{j+m}a_{j-m}|o\rangle$ is a closed shell state minus a particle with the angular momentum j and the magnetic quantum -m. The effect of this missing particle on the shell is that as a whole the shell now has quantum numbers (j, m), which we call the "hole" state. The phase $(-1)^{j+m}$ is necessary to give the hole state the same rotational transformation property as the particle state. (16, 17)

We confine ourselves to nuclear reactions in which a particle makes the transition from a closed shell state to a higher state. The particle-hole states were used as the basis to calculate the nuclear wave function by the perturbation technique, the perturbation being the interaction between the particle and the hole. Then the nuclear state is a linear combination of the particle-hole states.

A particle-hole state φ_N with a total angular momentum J, its projection μ and the total isotopic spin T is given below. (5)

$$\varphi_N = \sum_{L,S,M_1,M_2} \hat{j}_N, \hat{j}'_N \hat{L} \hat{S} \begin{Bmatrix} \ell_N & s_N & j_N \\ \ell'_N & s'_N & j'_N \\ L & S & J \end{Bmatrix} \langle L, S, M_1, M_2 | J, \mu \rangle$$

$$\times \sum_{\lambda_N \lambda'_N} \langle \ell_N, \ell'_N, \lambda_N, \lambda'_N | L, M_1 \rangle (-1)^{\ell'_N + \lambda'_N} a^{+}_{\ell_N, \lambda_N, n_N} a_{\ell'_N, -\lambda'_N, n'_N} |0\rangle$$

$$\times \sum_{m_N, m'_N} \langle s_N, s'_N, m_N, m'_N | S, M_2 \rangle (-1)^{s'_N + m'_N} a^{+}_{s_N, m_N} a_{s'_N, -m'_N} |0\rangle$$

$$\times \sum_{\tau_{N_2}, \tau'_{N_2}} \langle \tau_N, \tau'_N, \tau_{N_2}, \tau'_{N_2} | T, 0 \rangle (-1)^{\tau'_N + \tau'_{N_2}} a^{+}_{\tau_N, \tau_{N_2}} a_{\tau'_N, -\tau'_{N_2}} |0\rangle \tag{4.2}$$

where primed and unprimed variables refer to the hole and the particle respectively and $\hat{L} = \sqrt{2L+1}$ $\cdot$ j_N, ℓ_N, s_N and τ_N are the total angular momentum, the orbital angular momentum, the spin and the isotopic spin of the particle respectively. n_N is the radial quantum number. The corresponding primed quantities have the similar meanings for the hole.

L and M_1 are the sum of the orbital angular momenta and its projection of the particle-hole state, while S and M_2 refer to the total spin and its projection. The quantity $\{ \}$ is Wigner's $9j$ symbol and $\langle | \rangle$ is the Clebsh-Gordan coefficient. (18)

The nuclear wave functions ϕ_0 and ϕ_f are given as

$$\phi_0 = |0\rangle$$

$$\phi_f = \sum_N (X+Y)_N \varphi_N \tag{4.3}$$

For the meaning of X and Y, see the last paragraph of this chapter.

The factor $\chi_k^{(-)*} \sum_i t_i \chi_{k_0}^{(+)}$ is to be replaced by

$$\sum_{\lambda,\lambda'} \left(\int \Phi_\lambda^* \chi_k^{(-)*} t \, \chi_{k_0}^{(+)} \Phi_{\lambda'} \, d\tau \right) a_\lambda^\dagger a_{\lambda'} \tag{4.4}$$

where t is any one of t_i's and Φ_λ and $\Phi_{\lambda'}$ are the eigenfunctions of a single particle in the harmonic oscillator well.

The scattering matrix (3.15) now becomes

$$S(\mu) = 2\sqrt{\frac{K}{K_0}} \left(\frac{\mathcal{N}}{1+\mathcal{N}} \right) \sum_N (X+Y)_N \langle \tau_f | \langle \phi_f | \sum_{\lambda,\lambda'} \left(\int \Phi_\lambda^* \chi_k^{(-)*} t \, \chi_{k_0}^{(+)} \Phi_{\lambda'} \, d\tau \right)$$
$$a_\lambda^\dagger a_{\lambda'} |0\rangle | \tau_0 \rangle \tag{4.5}$$

where $|\tau_0\rangle$ and $|\tau_f\rangle$ are the initial and final isotopic spin states of the beam particle.

Isotopic Spin Dependence

The two-body scattering amplitude has the most general expression in the isotopic spin space,

$$t = t_s + t_v\, \tau \cdot \tau_1 \tag{4.6}$$

τ, τ_i, t_s and t_v are defined in (2.35). As we exclude the charge exchange scattering from our considerations and our targets have T = 0 before the scattering, the projection of the isospin after the scattering again will be zero. Surviving terms will either be t_s or t_v depending on the final states of the nucleus.

When T = 0, the operator t becomes $\sqrt{2}t_s$.

When T = 1, " " t " $\sqrt{2}t_v$. (4.7)

Form Factors

Carrying out the algebra involving the creation and annihilation operators, (4.5) becomes

$$S(\mu) = 2\sqrt{\frac{K}{K_0}}\left(\frac{\mathcal{N}}{1+\mathcal{N}}\right) \sum_N (X+Y)_N T_N \tag{4.8}$$

where

$$T_N = \sqrt{2} \sum_{L,S} \hat{j}_N \hat{j}_N' \hat{L} \hat{S} \begin{Bmatrix} \ell_N, & s_N, & j_N \\ \ell_N', & s_N', & j_N' \\ L, & S, & T \end{Bmatrix} \sum_{M_1,M_2} \langle L, S, M_1, M_2 | T, \mu \rangle$$

$$\times \sum_{\lambda_N,\lambda_N'} (-1)^{\ell_N'+\lambda_N'} \langle \ell_N, \ell_N', \lambda_N, \lambda_N' | L, M_1 \rangle \sum_{m_N,m_N'} (-1)^{s_N'+m_N'} \langle s_N, s_N', m_N, m_N' | S, M_2 \rangle$$

$$\times \langle n_N, \ell_N, \lambda_N | \langle s_N, m_N | \chi_K^{(-)*}\, t\, \chi_{K_0}^{(+)} | s_N', -m_N' \rangle | n_N', \ell_N', -\lambda_N' \rangle \tag{4.9}$$

where $|n_N, l_N, \lambda_N\rangle$ and $|n_N', l_N', -\lambda_N'\rangle$ are now the eigenfunctions in the harmonic oscillator well.

Final state S = 0, L = J

With (2.33), one may write

$$T_N = 2\sum_L \hat{j}_N \hat{j}_N' \hat{L} \begin{Bmatrix} l_N & \frac{1}{2} & j_N \\ l_N' & \frac{1}{2} & j_N' \\ L & 0 & J \end{Bmatrix} \sum_{M_1} \langle L, 0, M_1, 0 | J, \mu\rangle \sum_{\lambda_N, \lambda_N'} (-1)^{l_N' + \lambda_N'} \langle l_N, l_N', \lambda_N, \lambda_N' | L, M_1\rangle$$

$$\times \langle n_N, l_N, \lambda_N | \chi_K^{(-)*} [A + C\sigma_y] \chi_{K_0}^{(+)} | n_N', l_N', -\lambda_N'\rangle$$

(4.10)

$$= 2\hat{j}_N \hat{j}_N' \hat{L} \begin{Bmatrix} l_N & \frac{1}{2} & j_N \\ l_N' & \frac{1}{2} & j_N' \\ J & 0 & J \end{Bmatrix} \sum_{\lambda_N, \lambda_N'} (-1)^{\lambda_N' + l_N'} \langle l_N, l_N', \lambda_N \lambda_N' | L, \mu\rangle$$

$$\times \int R^*_{n_N, l_N} Y^*_{l_N, \lambda_N}(\theta,\varphi) \chi_K^{(-)*} [A + C\sigma_y] \chi_{K_0}^{(+)} R_{n_N', l_N'} Y_{l_N', -\lambda_N'}(\theta,\varphi)\, d\vec{r}$$

(4.11)

where R's are the radial eigenfunctions.

Making use of the identities,

$$Y_{l,-m}(\theta,\varphi) = (-1)^m Y^*_{l,m}(\theta,\varphi)$$

(4.12)

$$\sum_L \frac{\hat{l}_1 \hat{l}_2}{\sqrt{4\pi}\,\hat{L}} \langle l_1, l_2, m_1, m_2 | L, M\rangle \langle l_1, l_2, 0, 0 | L, 0\rangle Y^*_{LM} = Y^*_{l_1 m_1} Y^*_{l_2, m_2}$$

(4.13)

and the formal properties of the Clebsh-Gordan coefficients, one can deduce from (4.11)

$$T_N = \frac{2\,\hat{j}_N\,\hat{j}'_N\,\hat{l}_N\,\hat{l}'_N}{\sqrt{4\pi}} \begin{Bmatrix} l_N & \frac{1}{2} & j_N \\ l'_N & \frac{1}{2} & j'_N \\ J & 0 & J \end{Bmatrix} \langle l_N, l'_N, 0, 0 \mid L, 0 \rangle (-1)^{l'_N}$$

$$\times \int R^*_{n_N, l_N} Y^*_{L,\mu} \chi^{(-)*}_{K} [A + c\sigma_y] \chi^{(+)}_{K_0} R_{n'_N, l'_N} r^2 dr d\Omega$$

(4.14)

Define the form factor F^{JOJ} as

$$F^{JOJ} = 2 \sum_N (X+Y)_N \frac{\hat{j}_N\,\hat{j}'_N\,\hat{l}_N\,\hat{l}'_N (-1)^{l'_N}}{\sqrt{4\pi}} \begin{Bmatrix} l_N & j_N & j_N \\ l'_N & \frac{1}{2} & j'_N \\ J & 0 & J \end{Bmatrix}$$

$$\times \langle l_N, l'_N, 0, 0 \mid J, 0 \rangle R^*_{n_N, l_N} R_{n'_N, l'_N}$$

(4.15)

$$\langle l_N, l'_N, 0, 0 \mid J, 0 \rangle \begin{Bmatrix} l_N & \frac{1}{2} & j_N \\ l'_N & \frac{1}{2} & j'_N \\ J & 0 & J \end{Bmatrix}$$

$$= (-1)^{L - l'_N + j'_N - \frac{1}{2}} \frac{1}{[2(2L+1)(2l_N+1)(2l'_N+1)]^{1/2}}$$

$$\times \begin{pmatrix} j_N & j'_N & L \\ \frac{1}{2} & -\frac{1}{2} & 0 \end{pmatrix}$$

(4.16)

where quantity $\begin{pmatrix} & \end{pmatrix}$ is called Wigner's 3-j symbol as given in reference 18. (4.15) becomes

$$T_N = \frac{2\,\hat{j}_N\,\hat{j}'_N\,\hat{\ell}_N\,\hat{\ell}'_N}{\sqrt{4\pi}} \begin{Bmatrix} \ell_N & \frac{1}{2} & j_N \\ \ell'_N & \frac{1}{2} & j'_N \\ J & 0 & J \end{Bmatrix} \langle \ell_N, \ell'_N, 0, 0 \mid L, 0 \rangle (-1)^{\ell'_N}$$

$$\times \int R^*_{n_N,\ell_N} Y^*_{L,\mu} \chi_K^{(-)*} [A + C\sigma_y] \chi_{K_0}^{(+)} R_{n'_N,\ell'_N} r^2 dr\, d\Omega$$

(4.14)

Define the form factor F^{JoJ} as

$$F^{JoJ} = 2 \sum_N (X+Y)_N \frac{\hat{j}_N\,\hat{j}'_N\,\hat{\ell}_N\,\hat{\ell}'_N (-1)^{\ell'_N}}{\sqrt{4\pi}} \begin{Bmatrix} \ell_N & j_N & j_N \\ \ell'_N & \frac{1}{2} & j'_N \\ J & 0 & J \end{Bmatrix}$$

$$\times \langle \ell_N, \ell'_N, 0, 0 \mid J, 0 \rangle R^*_{n_N,\ell_N} R_{n'_N,\ell'_N}$$

(4.15)

$$\langle \ell_N, \ell'_N, 0, 0 \mid J, 0 \rangle \begin{Bmatrix} \ell_N & \frac{1}{2} & j_N \\ \ell'_N & \frac{1}{2} & j'_N \\ J & 0 & J \end{Bmatrix}$$

$$= (-1)^{L-\ell'_N+j'_N-\frac{1}{2}} \frac{1}{[2(2L+1)(2\ell_N+1)(2\ell'_N+1)]^{1/2}}$$

$$\times \begin{pmatrix} j_N & j'_N & L \\ \frac{1}{2} & -\frac{1}{2} & 0 \end{pmatrix}$$

(4.16)

where quantity $\left(\quad \right)$ is called Wigner's 3-j symbol as given in reference 18. (4.15) becomes

$$F^{J0J} = \sqrt{2}\sum_N (X+Y)_N (-1)^{J+j_N'-\frac{1}{2}} \frac{\hat{j}_N \hat{j}_{N'}}{\sqrt{4\pi}} \begin{pmatrix} j_N & j_N' & J \\ \frac{1}{2} & -\frac{1}{2} & 0 \end{pmatrix} R^*_{n_N, l_N} R_{n_N', l_N'}$$

(4.17)

(4.8) is simplified as

$$S(\mu, S=0) = 2\sqrt{\frac{K}{K_0}}\left(\frac{N}{1+N}\right)\int F^{J0J} Y^*_{J\mu} \chi^{(-)*}_K [A + C\sigma_y] \chi^{(+)}_{K_0} r^2 dr d\Omega$$

(4.18)

<u>Final State S = 1, J = L</u>

Algebras involving the spins of the particle-hole states are more tedious than the S = 0 case. Writing out explicitly the spin operators of t,

$$t = t^0 1 + t^x \sigma_x + t^y \sigma_y + t^z \sigma_z \qquad (4.19)$$

with $t^0 = A + \sigma_{1y}$

$t^x = B\sigma_{1}x$

$t^y = C + B\sigma_1 y$

$t = F\sigma_1 z$

where σ_1's are the spin operators for the particle-hole and σ's for the incident nucleons. The coordinate system is defined in Chapter II.

A typical calculation goes as follows:

$$\sum_{m_N, m_N'} (-1)^{s_N'+m_N'} \langle s_N, s_N', m_N, m_N' | S, M_2\rangle \langle s_N, m_N | \sigma_{iy} | s_N', -m_N'\rangle$$

$$= \sum_{m_N, m_N'} (-1)^{s_N'+m_N'} \langle s_N, s_N', m_N, m_N' | S, M_2\rangle \langle s_N, m_N | \frac{\sigma_{i+} - \sigma_{i-}}{i} | s_N', -m_N'\rangle$$

$$= i\,[\delta_{M_2,1} + \delta_{M_2,-1}]$$

(4.20)

where $i = \sqrt{-1}$, $\sigma_{i+} = \frac{\sigma_{ix} + i\sigma_{iy}}{2}$ $\sigma_{i-} = \frac{\sigma_{ix} - i\sigma_{iy}}{2}$

Using (4.20) and the like, (4.9) becomes

$$T_N(\mu) = \sqrt{2}\,\hat{j}_N \hat{j}'_N \hat{L}\,\hat{S} \begin{Bmatrix} l_N & s_N & j_N \\ l'_N & s'_N & j'_N \\ L & S & J \end{Bmatrix} \sum_{M_1, M_2} \langle L, S, M_1, M_2 | J, \mu \rangle$$

$$\times \sum_{\lambda_N, \lambda'_N} (-1)^{l'_N + \lambda'_N} \langle l_N, l'_N, \lambda_N, \lambda'_N | L, M_1 \rangle$$

$$\times \int R^*_{n_N, l_N} Y^*_{l_N, \lambda_N} \chi^{(-)*}_K \langle t \rangle R_{n'_N, l'_N} Y_{l'_N, -\lambda'_N} \chi^{(+)}_{K_0} \, d\vec{r}$$

(4.21)

where

$$\langle t \rangle = i C (\delta_{M_2,-1} + \delta_{M_2,1}) + E (\delta_{M_2,-1} - \delta_{M_2,1}) \sigma_x$$

$$+ i B \sigma_y (\delta_{M_2,-1} + \delta_{M_2,1}) + \sqrt{2} F \delta_{M_2,0} \sigma_z$$

(4.22)

Remembering the identities (4.12) and (4.13), (4.21) can be simplified as

$$T_N(\mu) = \sqrt{2}\,\hat{j}_N \hat{j}'_N \hat{S}\,\hat{l}_N \hat{l}'_N (-1)^{l'_N} \begin{Bmatrix} l_N & s_N & j_N \\ l'_N & s'_N & j'_N \\ L & S & J \end{Bmatrix} \sum_{M_1, M_2} \langle L, 1, M_1, M_2 | J, \mu \rangle$$

$$\times \langle l_N, l'_N, 0, 0 | L, 0 \rangle \times \int R^*_{n_N, l_N} Y^*_{L, M_1} \chi^{(-)*}_K \langle t \rangle \chi^{(+)}_{K_0} R_{n'_N, l'_N} \, d\vec{r}$$

(4.23)

F^{iij} =

Makin

the a

F^{iij}

With

S(

<u>Final</u>

and s

J.

F^{isj}

Define the form factor

$$F^{J1J} = \frac{\sqrt{2}}{\sqrt{4\pi}} \sum_N (X+Y)_N \hat{j}_N \hat{j}'_N \hat{S} \hat{l}_N \hat{l}'_N (-1)^{l'_N} \begin{Bmatrix} l_N & S_N & j_N \\ l'_N & S'_N & j'_N \\ J & S & J \end{Bmatrix}$$

$$\times \langle l_N, l'_N, 0, 0 \mid L, 0 \rangle R^*_{n_N, l_N} R_{n_N, l_N}$$

(4.24)

Making use of the properties of 3-j and 9-j symbols listed in the appendix of Reference 18, one can reduce (4.24) to

$$F^{J1J} = \sum_N \frac{(X+Y)_N}{\sqrt{4\pi}} (-1)^{l_N} \hat{j}'_N \hat{j}_N \begin{pmatrix} j_N & j'_N & J \\ \frac{1}{2} & \frac{1}{2} & -1 \end{pmatrix} R^*_{n_N, l_N} R_{n'_N, l'_N}$$

(4.25)

With (4.23) and (4.25), (4.8) can be written

$$S(L=J, S=1, \mu) = 2\sqrt{\frac{K}{K_0}} \left(\frac{\mathcal{N}}{1+\mathcal{N}}\right) \sum_{M_1, M_2} \langle L, 1, M_1, M_2 \mid J, \mu \rangle$$

$$\times \int F^{J1J} Y^*_{LM_1} \chi^{(-)*}_K \langle t \rangle \chi^{(+)}_{K_0} \; r^2 dr \, d\Omega$$

(4.26)

<u>Final State $S = 1$, $J = L\pm 1$</u>

All the calculations are exactly the same as $J = L$ and $S = 1$ except that we have two values of L for a given J.

Define the form factors by

$$F^{LSJ} = \frac{\sqrt{2}}{\sqrt{4\pi}} \sum_N \frac{(X+Y)_N}{\Sigma} \cdot$$

$$\times \hat{j}_N \hat{j}_N' \hat{S} \hat{l}_N \hat{l}_N' (-1)^{l_N'} \langle l_N, l_N', 0, 0 | L, 0 \rangle \hat{L}$$

$$\times \begin{Bmatrix} l_N & s_N & j_N \\ l_N' & s_N' & j_N' \\ L & S & J \end{Bmatrix} R^*_{n_N, l_N} R_{n_N', l_N'} \tag{4.27}$$

For L = J-1, one gets

$$F^{J-1,1,J} = \frac{1}{\sqrt{4\pi}} \sum_N \frac{\hat{L} \hat{j}_N \hat{j}_N' (-1)^{j_N' + l_N' + l_N + \frac{1}{2}} (X+Y)_N \left[(l_N - j_N)(2j_N+1) + (l_N' - j_N')(2j_N'+1) - J \right]}{\left[J (2J+1)(2J-1) \right]^{1/2}}$$

$$\times \begin{pmatrix} j_N & j_N' & J \\ \frac{1}{2} & -\frac{1}{2} & 0 \end{pmatrix} R^*_{n_N, l_N} R_{n_N', l_N'} \tag{4.28}$$

For L = J+1,

$$F^{J+1,1,J} = \frac{1}{\sqrt{4\pi}} \sum_N (X+Y)_N (-1)^{j_N' + l_N' + l_N + \frac{1}{2}} \frac{\hat{j}_N \hat{j}_N' \hat{L} \left[(l_N - j_N)(2j_N+1) + (l_N' - j_N')(2j_N'+1) + J + 1 \right]}{\left[(J+1)(2J+1)(2J+3) \right]^{1/2}}$$

$$\times \begin{pmatrix} j_N & j_N' & J \\ \frac{1}{2} & -\frac{1}{2} & 0 \end{pmatrix} \cdot R_{n_N', l_N'} R^*_{n_N, l_N} \tag{4.29}$$

$$S(L, \mu, S=1) = 2\sqrt{\frac{K}{K_0}} \left(\frac{\mathcal{N}}{1+\mathcal{N}} \right) \sum_{L, M_1, M_2} \langle L, S, M_1, M_2 | J, \mu \rangle$$

$$\times \int F^{LSJ} Y^*_{LM_1} \chi^{(-)*}_K \langle t \rangle \chi^{(+)}_{K_0} \, d^3r \tag{4.30}$$

Although we have assumed that the ground state of the nucleus as the Hartree-Fock ground state, in (4.3) allowances for the correlations in the ground states were made by the coefficients Y. Gillet et al. (11) have allowed the ground state of the nucleus to have the excitations of the particle-hole pairs. Then a nucleus can be excited in two ways: first, by creating a particle-hole pair and secondly, by destroying a particle-hole pair that is present in the ground state. X is the amplitude of the first mechanism and Y is the amplitude of the second mechanism. These are given in References 11 and 12. X and Y satisfy the normalization condition

$$\sum_N (X^2 - Y^2)_N = 1$$

where summation is over all the particle-hole states that contribute to our nuclear state function. In evaluating the form factors, the corrections to the phase of (X+Y) should be made by multiplying $(-1)^{j'_N+\frac{1}{2}}$. (19) All the relevant form factors are evaluated and listed in Appendix I along with the radial wave functions.

CHAPTER V

DETAILED CALCULATIONS

Reduction of the Scattering Amplitudes

Scattering Amplitude for $S = 0$

For the final state of the nucleus with $L = J$, the total scattering amplitude will be the sum of (4.18) and (4.26). First let us consider (4.18).

With (3.12) and (3.14)

$$S(L=J,\ S=0,\mu) = 2\sqrt{\frac{K}{K_0}}\left(\frac{\mathcal{N}}{1+\mathcal{N}}\right)\int F^{J0J}\, Y^{*}_{LM}\, e^{-i(\vec{K}-\vec{K}_0)\cdot\vec{r}}$$

$$e^{-\frac{iK}{2E}\int_z^{\infty}[U_c + U_s\,\sigma\cdot(\vec{r}\times\vec{K})]\,dz'}\,[A + C\sigma_y]\,e^{-\frac{iK_0}{2E_0}\int_{-\infty}^{z}[U_c + U_s\,\sigma\cdot(\vec{r}\times\vec{K}_0)]\,dz'} \tag{5.1}$$

To evaluate the exponents with the optical potential, we use the coordinate system defined in Chapter II in which $\vec{k}_0$ is along the z component of vector $\vec{r}$. We further make the following approximations:

$$\vec{k} \simeq \vec{k}_0 \text{ and } \frac{k}{2E} = \frac{k_0}{2E_0} \tag{5.2}$$

The basis of the first part of (5.2) is that the deflection of the particle after scattering is roughly approximated by $e^{-i(\vec{K}-\vec{K}_0)\cdot\vec{r}}$ and $t(q)$. The second approximation of (5.2) is based on the fact that the energy loss of the beam is small compared to its incident energy.

Let

$$Q_1 = \frac{bK_0^2}{2E_0}\int_{-\infty}^{z} U_s(b,z')\,dz'$$

$$Q_2 = \frac{bK_0^2}{2E_0}\int_{z}^{\infty} U_s(b,z')\,dz'$$

$$\Gamma = e^{-\frac{iK_0}{2E_0}\int_{-\infty}^{\infty} U_c(b,z')\,dz'}$$

$$Q = Q_1 + Q_2 = \frac{bK_0^2}{2E_0}\int_{-\infty}^{\infty} U_s(b,z')\,dz'$$

(5.3)

Then (5.1) reduced to

$$S(L=J,\ S=0,\mu) = 2\sqrt{\frac{E}{K_0}}\left(\frac{\mathcal{N}}{1+\mathcal{N}}\right)\int Y_{LM}^{*}\ F^{JOJ}\ e^{-i\vec{q}\cdot\vec{r}}\ \Gamma(b)$$

$$e^{-iQ_2\sigma\cdot(\hat{b}\times\hat{k}_0)}\,[A + C\sigma_y]\,e^{-iQ_1\sigma\cdot(\hat{b}\times\hat{k}_0)}\quad d\vec{r} \qquad (5.4)$$

where $\hat{b}$, $\hat{k}_0$ are the unit vectors of $\vec{b}$, $\vec{k}_0$, and $\vec{q} = \vec{k}-\vec{k}_0$.

Let

$$e^{-iQ_2\sigma_m}\,\sigma_n\,e^{-iQ_1\sigma_n} = \sigma_n\cos(Q_1+Q_2) - i\,\sigma_n.\sigma_m \sin(Q_1+Q_2)$$

$$+\frac{i}{2}\left[\sin(Q_1+Q_2) - \sin(Q_1-Q_2)\right][\sigma_n,\sigma_m]$$

$$+\frac{i}{2}\left[-\cos(Q_1+Q_2) + \cos(Q_1-Q_2)\right]\sigma_m[\sigma_m,\sigma_n]$$

(5.5)

Considering Q_1, Q_2, and $Q_1 + Q_2$ to be small, (5.5) becomes

$$e^{-iQ_2\sigma_m}\sigma_n e^{-iQ_1\sigma_m} = \sigma_n - i\sigma_n\sigma_m(Q_1+Q_2) + \frac{i}{2}\left[(Q_1+Q_2)-(Q_1-Q_2)\right][\sigma_n,\sigma_m]$$

$$= \sigma_n - i\sigma_n\sigma_m Q \quad + \frac{i}{2} Q\,[\sigma_n,\sigma_m]$$

(5.7)

where $Q_1 - Q_2 = \frac{k_o b^2}{2E_o}\int_{-z}^{z} U_s dz'$ is dropped for convenience. (See Appendix II)

With (5.7), (5.4) becomes

$$S(L=J,\ S=0,\ ) = 2\sqrt{\frac{k}{k_o}\left(\frac{\mathcal{N}}{1+\mathcal{N}}\right)}\int e^{-i\vec{q}\cdot\vec{r}}\,\Gamma\ Y^{*}_{J,\mu}(\theta,\phi)\ F^{JoJ}[A+C\sigma_y]\,d\vec{r}$$

$$-2\sqrt{\frac{k}{k_o}\left(\frac{\mathcal{N}}{1+\mathcal{N}}\right)}\frac{i}{2}\int e^{-i\vec{q}\cdot\vec{r}}\,\Gamma(b)\ F^{JoJ}\,Q(b)\,Y^{*}_{J,\mu}(\theta,\phi)\,C\,[\sigma_y,\sigma_m]\ d\vec{r}$$

$$-2\sqrt{\frac{k}{k_o}\left(\frac{\mathcal{N}}{1+\mathcal{N}}\right)}\,i\int e^{-i\vec{q}\cdot\vec{r}}\,\Gamma(b)F^{JoJ}\ Q(b)\ Y^{*}_{J,\mu}\ \sigma_m[A+C\sigma_y]\ d\vec{r}$$

(5.8)

where $\sigma_m = \sigma_x \sin\phi - \sigma_y \cos\phi$

Expanding $S(L=J,\ S=0,\mu)$ in the spin space, as $S(L=J,\ S=0,\mu) = S^{o}(L=J,\ S=0,\mu)\ 1 + S^{x}(L=J,\ S=0,\mu)\sigma_x + S^{y}(L=\ ,\ S=0,\mu)\sigma_y + S^{z}(L=J,\ S=0,\mu)\sigma_z$

(5.9)

We get

$$S^{o}(L=J,\ S=0,\mu) = 2\sqrt{\frac{k}{k_o}\left(\frac{\mathcal{N}}{1+\mathcal{N}}\right)}A\int e^{-i\vec{q}\cdot\vec{r}}\,\Gamma(b)\,Y^{*}_{J,\mu}(\theta,\phi)\ F^{JoJ}\ d\vec{r}$$

$$+ 2i\sqrt{\frac{k}{k_o}\left(\frac{\mathcal{N}}{1+\mathcal{N}}\right)}C\int e^{-i\vec{q}\cdot\vec{r}}\ \Gamma(b)\ F^{JoJ}\,Q(b)\ Y^{*}_{J,\mu}(\theta,\phi)\ \cos\phi\ dr$$

$$S^{x}(L=J,\ S=0,\mu) = -2\sqrt{\frac{k}{k_o}\left(\frac{\mathcal{N}}{1+\mathcal{N}}\right)}A\int e^{-i\vec{q}\cdot\vec{r}}\,\Gamma\ F^{JoJ}\ Q(b)\,Y^{*}_{J,\mu}(\theta,\phi)\sin\phi\ d\vec{r}$$

$$S^{y}(L=J,\ S=0,\mu) = 2\sqrt{\frac{k}{k_o}\left(\frac{\mathcal{N}}{1+\mathcal{N}}\right)}C\int e^{-i\vec{q}\cdot\vec{r}}\,\Gamma\ F^{JoJ}\ Y^{*}_{J,\mu}\ (\theta,\phi)\qquad d\vec{r}$$

$$+ 2\sqrt{\frac{K}{K_0}}\, iA \left(\frac{N}{1+N}\right) \int e^{-i\vec{q}\cdot\vec{r}}\, \Gamma(b) \quad F^{JOJ} Q\; Y^*_{J,\mu}(\theta,\phi) \;\cos\phi \, d\vec{r}$$

$$S^Z(L=J,\; S=0, \mu) = 0 \tag{5.10}$$

The integral over ϕ is carried out below:

$$Y^*_{J,\mu}(\theta,\phi) = Y^*_{J,\mu}(\theta, 0)\; e^{-\mu\phi}$$

$$\vec{q}\cdot\vec{r} = qr\sin\theta\cos\phi$$

Using the formula (20)

$$\frac{1}{2\pi i^m}\int_0^{2\pi} e^{iz\cos\mu}\cos(m\mu)\,d\mu = J_m(z) \tag{5.11}$$

$J_m(z)$ being the Bessel function of order m, we have

$$\int_0^{2\pi} e^{-i\vec{q}\cdot\vec{r}}\, e^{i\mu\phi}\, d\phi = 2\pi\, i^{|\mu|}\, J_{|\mu|}(-qr\sin\theta)$$

$$\int_0^{2\pi} e^{-i\vec{q}\cdot\vec{r}}\, e^{-i\mu\phi}\cos\phi\, d\phi = \pi\left(i^{|\mu+1|}J_{|\mu+1|}(-qr\sin\theta) + i^{|\mu-1|}J_{|\mu-1|}(-qr\sin\theta)\right) \tag{5.12}$$

$$\int_0^{2\pi} e^{-i\vec{q}\cdot\vec{r}}\, e^{-i\mu\phi}\sin\phi\, d\phi = i\pi\left[i^{|\mu+1|}J_{|\mu+1|}(-qr\sin\theta) - i^{|\mu-1|}J_{|\mu-1|}(-qr\sin\theta)\right] \tag{5.13}$$

(5.14)

Let us look at the integrand of (5.8). F^{JOJ} is $e^{-\alpha r^2}$ multiplied by a polynomial in r of even or odd parity as given in Appendix I. We shall approximate Γ and Q by the functions of the following type. (See next section)

$$\Gamma(b) = 1.0 - (CM + CNb^2)e^{-Ab^2} - (DM + DNb^2)e^{-Bb^2} \tag{5.15}$$

$$Q(b) = \text{Const.} \times \left[(CFb + CSb^3)\,{}^{-Rb^2} + (DFb + DSb^3)\,e^{-Sb^2} \right] \tag{5.16}$$

Then all the integral can be carried out analytically. The integral of (5.8) along Z is the following type: (21)

$$\int_0^\infty z^n e^{-az^2} dz = \frac{1\cdot 3 \cdots (2n-1)}{2^{n+1} \quad a^n} \sqrt{\frac{\pi}{a}} \tag{5.17}$$

A typical integral in (5.8) along b is given below: (22)

$$\int_0^\infty e^{-(\alpha+\beta)b^2} J_\nu(\gamma b)\, b^{\mu-1}\, db$$

$$= \frac{\Gamma\left(\frac{\nu}{2}+\frac{\mu}{2}\right)\left(\frac{1}{2}\frac{\gamma}{(\alpha+\beta)^{1/2}}\right)^{\nu}}{2(\alpha+\beta)^{\mu/2}\,\Gamma(1+\nu)}\, e^{-\frac{\gamma^2}{4(\alpha+\beta)}}\; {}_1F_1\left(\frac{\nu}{2}-\frac{\mu}{2}+1\,;\, 1+\nu\,;\, \frac{\gamma^2}{4(\alpha+\beta)}\right) \tag{5.18}$$

where

$${}_1F_1(\lambda, \rho, z) = \sum_{n=0}^{\infty} \frac{(\lambda)_n \, z^n}{n! \;\, (\rho)_n}$$

$$(\lambda)_0 = 1 \qquad (\lambda)_n = \lambda(1+\lambda) \cdots (\lambda+n-1)$$

$$(\rho)_0 = 1 \qquad (\rho)_n = \rho(1+\rho) \cdots (\rho+n-1) \tag{5.19}$$

and $\Gamma(1+n) = n!$

${}_1F_1$ is called the generalized hypergeometric function and in our case always a polynomial of the finite degrees.

Scattering Amplitude for S = 1

Following exactly the same procedure as before, we have, using $\sigma_m = (\sigma_x \sin\phi - \sigma_y \cos\phi)$,

$$e^{-iQ_2\sigma_m}\,\sigma_x\,e^{-iQ_1\sigma_m} = [\sigma_x - iQ\sin\phi]$$

$$e^{-iQ_2\sigma_m}\,\sigma_y\,e^{-iQ_1\sigma_m} = [\sigma_y + iQ\cos\phi]$$

$$e^{-iQ_2\sigma_m}\,\sigma_z\,e^{-iQ_1\sigma_m} = \sigma_z$$

(5.20)

Substituting (5.20) into (4.26), we have after integrating over ϕ,

$$S^0(L,S=1,\mu)\cdot\frac{1}{2}\sqrt{\frac{K_0}{K}}\left(\frac{1+\mathcal{N}}{\mathcal{N}}\right) = iC\sum_{M_1,M_2}(\delta_{M_2,-1}+\delta_{M_2,1})\langle L,1,M_1,M_2|J,\mu\rangle\, 2\pi i^{|M_1|}$$

$$\int Y^*_{LM_1}(\theta,0)\,F^{L1J}\,J_{|M_1|}(-qb)\,\Gamma(b)\,r^2dr\sin\theta\,d\theta + E\cdot\pi\sum_{M_1,M_2}(\delta_{M_2,-1}-\delta_{M_2,1})\langle L,1,M_1,M_2|J,\mu\rangle$$

$$\times\int Y^*_{LM_1}(\theta,0)\,F^{L1J}\,\Gamma(b)\,Q(b)\left[i^{|M_1+1|}J_{|M_1+1|}(-qb) - i^{|M_1-1|}J_{|M_1-1|}(-qb)\right]r^2dr\sin\theta\,d\theta$$

$$-B\pi\sum_{M_1,M_2}(\delta_{M_2,-1}+\delta_{M_2,1})\langle L,1,M_1,M_2|J,\mu\rangle\int_0^\infty Y^*_{LM_1}(\theta,\phi)\,F^{L1J}\,\Gamma(b)\,Q(b)$$

$$\left[i^{|M_1+1|}J_{|M_1+1|}(-qb) + i^{|M_1-1|}J_{|M_1-1|}(-qb)\right]r^2dr\sin\theta\,d\theta$$

(5.21)

$$S^{x}(L,S=1,\mu)\,\frac{1}{2}\sqrt{\frac{K_0}{K}}\left(\frac{1+\mathcal{N}}{\mathcal{N}}\right)=2\pi E\sum_{M_1,M_2}\left(\delta_{M_2,-1}-\delta_{M_2,1}\right)\langle L,1,M_1,M_2|J,\mu\rangle\, i^{|M_1|}$$

$$\times\int Y^{*}_{LM_1}(\theta,0)\,F^{L1J}\,\Gamma(b)\,J_{|M_1|}(-gb)\,r^2dr\sin\theta\,d\theta$$

$$+iC\pi\sum\left(\delta_{M_2,-1}+\delta_{M_2,1}\right)\langle L,1,M_1,M_2|J,\mu\rangle\int F^{L1J}\,Y^{*}_{L,M_1}(\theta,0)\,\Gamma(b)$$

$$Q(b)\left[i^{|M_1+1|}J_{|M_1+1|}(-gb)-i^{|M_1-1|}J_{|M_1-1|}(-gb)\right]r^2dr\sin\theta\,d\theta$$

(5.22)

$$S^{y}(L,S=1,\mu)\,\frac{1}{2}\sqrt{\frac{K_0}{K}}\left(\frac{1+\mathcal{N}}{\mathcal{N}}\right)=2\pi i\,B\sum_{M_1,M_2}\left(\delta_{M_2,-1}+\delta_{M_2,1}\right)\langle L,1,M_1,M_2|J,\mu\rangle$$

$$\times\int F^{L1J}\,Y^{*}_{LM}(\theta,0)\,\Gamma(b)\,J_{|M_1|}(-gb)\,i^{|M_1|}\,r^2dr\sin\theta\,d\theta$$

$$-\pi C\sum_{M_1,M_2}\left(\delta_{M_2,-1}+\delta_{M_2,1}\right)\langle L,1,M_1,M_2|J,\mu\rangle\int F^{L1J}\,Y^{*}_{L,M_1}(\theta,0)$$

$$\Gamma(b)\,Q(b)\left[i^{|M_1+1|}J_{|M_1+1|}(-gb)+i^{|M_1-1|}J_{|M_1-1|}(-gb)\right]r^2dr\sin\theta\,d\theta$$

(5.23)

$$S^{z}(L,S=1,\mu)\,\frac{1}{2}\sqrt{\frac{K_0}{K}}\left(\frac{1+\mathcal{N}}{\mathcal{N}}\right)=\sqrt{2}\,F\,2\pi\sum_{M_1,M_2}{}'\, i^{|M_1|}\,\delta_{M_2,0}\,\langle L,1,M_1,M_2|J,\mu\rangle$$

$$\times\int F^{L1J}\,Y^{*}_{LM_1}(\theta,0)\,\Gamma(b)\,J_{|M_1|}(-gb)\,r^2dr\sin\theta\,d\theta$$

(5.24)

All the integrals involved in (5.21) --- (5.24) may be carried out with (5.17) and (5.18).

The total scattering amplitude for a normal parity ($L = J$) state with any spin (0 and 1) is given by the sum of $S(L = J,\ S = 0, \mu)$ and $S(L = J,\ S = 1, \mu)$.

$$S(L{=}J,\mu) = S^{o}(L{=}J,\mu)\cdot 1 + S^{x}(L{=}J,\mu)\sigma_x + S^{y}(L{=}J,\mu)\sigma_y + S^{z}(L{=}J,\mu)\sigma_z \tag{5.25}$$

where

$$\begin{aligned}
S^{o}(L{=}J,\mu) &= S^{o}(L{=}J,\ S{=}0,\mu) + S^{o}(L{=}J,\ S{=}1,\mu)\\
S^{x}(L{=}J,\mu) &= S^{x}(L{=}J,\ S{=}0,\mu) + S^{x}(L{=}J,\ S{=}1,\mu)\\
S^{y}(L{=}J,\mu) &= S^{y}(L{=}J,\ S{=}0,\mu) + S^{y}(L{=}J,\ S{=}1,\mu)\\
S^{z}(L{=}J,\mu) &= S^{z}(L{=}J,\ S{=}1,\mu)
\end{aligned} \tag{5.26}$$

The total scattering amplitude for the abnormal parity states ($J \neq L$, $S=1$) is the sum of amplitudes for $J = L-1$ and $J = L+1$. One may expand this scattering amplitude as in (5.25):

$$\begin{aligned}
S^{o}(\mu) &= S^{o}\ (L{=}J-1,\ S{=}1,\mu) + S^{o}(L{=}J+1,\ S{=}1,\mu)\\
S^{x}(\mu) &= S^{x}\ (L{=}J-1,\ S{=}1,\mu) + S^{x}(L{=}J+1,\ S{=}1,\mu)\\
S^{y}(\mu) &= S^{y}\ (L{=}J-1,\ S{=}1,\mu) + S^{y}(L{=}J+1,\ S{=}1,\mu)\\
S^{z}(\mu) &= S^{z}\ (L{=}J-1,\ S{=}1,\ ) + S^{z}(L{=}J+1,\ S{=}1,\mu)
\end{aligned} \tag{5.27}$$

where the terms on the right-hand sides are exactly the same as the corresponding terms (5.21) --- (5.24) except that $L \neq J$ and the form factors are different.

Numerical Calculations

The optical potentials used in this investigation are of the form, (10)

$$U(r) = V_c(r) - V(1+e^x)^{-1} - i\left(W - 4iW_D \frac{d}{dx'}\right)(1+e^{x'})^{-1}$$

$$+ \frac{\hbar^2}{m_\pi^2 c^2}(WR + iWI)\frac{1}{r}\frac{d}{dr}(1+e^x)^{-1}\,\vec{\sigma}\cdot\vec{L} \tag{5.28}$$

where $x = (r - r_o A^{1/3})/a$, $x' = (r - r_o' A^{1/3})/a'$.
We shall ignore $V_c(r)$, the Coulomb interactions, and $-V(e^x+1)^{-1}$, the real part of the central interaction. The effect of the Coulomb scattering is significant only at the forward angles in the elastic scattering. Furthermore, in the inelastic scattering, the momentum transfer is never zero and hence the effect of Coulomb interaction is still smaller where the inelastic scattering is important, i.e. at the angles $\gtrsim 10^\circ$. The real central part contributes to the phase of the distorted wave. As we will be squaring the amplitudes for any observable quantity, this is not going to be important at the high energy. This was borne out in References 4 and 23.

The relevant parameters for the optical potentials at the incident energy of 182 MeV are given below for C^{12} and Ca^{40}. The parameters for O^{16} are assumed to be the same as those of C^{12} except the atomic number A. M is the mass of π meson. (10)

TABLE 1.--Optical Parameters

	r_o	a	W	W_D	r_o	a'	W_R	W_I
C^{12}	.902f.	0.452	15.6	0	1.186	0.556	4.12	- .10
Ca^{40}	1.012	0.548	16.4	0	1.364	0.542	4.06	-2.0

The unit for the length is fermi and the energy is in MeV.

From (5.3), (5.15) and (5.16), we have

$$\Gamma(b) = e^{-\frac{K_0}{2E_0}\int_{-\infty}^{\infty}\frac{W}{e^{x}+1}\,dz'} = 1-(CM+CN\,b^2)e^{-Ab^2}-(DM+DN\,b^2)e^{-Bb^2}$$

(5.29)

$$Q(b) = \frac{bK_0^2}{2E_0}\left(\frac{\hbar}{m_\pi c}\right)^2(WR+iWI)\int_{-\infty}^{\infty}\frac{1}{r}\frac{d}{dr}(1+e^{x})^{-1}\,dz'$$

$$= PEK\cdot(WR+iWI)\cdot\left[(CF\,b+CS\,b^3)e^{-Rb^2}+(DF\,b+DS\,b^3)e^{-Sb^2}\right]$$

(5.30)

The integration along Z' was carried out numerically with Simpson's rule. A typical program for the numerical integration is listed in Appendix III. The results were fitted to the function on the right-hand side of (5.29). Take $\Gamma(bn)$ for N different points of b. Then adjust the parameters CM, CN, A, B, DM and DN such that

$$\sigma = \sum_{n=1}^{N}\left[\Gamma(b_n)-1+(CM+CN\,b^2)e^{-Ab^2}+(DM+DN\,b^2)e^{-Bb^2}\right]^2$$

becomes very small. This was done again with the computer and a typical program is listed in Appendix IV.

The exact same procedure was repeated for Q(b). In the case of Ca^{40}, the curve for Q(b) was fitted by three different sets of the parameters on the right-hand side of

(5.30). The quality of each fitting is measured by σ . As we shall see, each fitting gives different polarizations for Ca^{40}, indicating that perhaps the polarization depends sensitively on the shape of the Q(b) (i.e., spin-orbit potential). Final values for the parameters in (5.29) and (5.30) are given below.

TABLE 2.---Central Absorption

$\Gamma(b^2)$									
	Interval	No. of pts.	σ	CM	CN	DM	DN	A	B
C^{12}	$0\sim8$	40	$.17\times10^{-3}$	1.613	-.046	-1.078	-.127	.17	.39
O^{16}	"	"	$.86\times10^{-4}$	3.154	-.035	-2.586	-.269	.2	.35
Ca^{40}	$0\sim10$	50	$.33\times10^{-2}$	34.49	-.517	-33.75	-.911	.0991	.143

TABLE 3.---Spin-Orbit Integration

Q(b)									
	Interval	No. of pts.	σ	CF	CS	DF	DS	R	S
C^{12}	$0\sim7$	35	$.76\times10^{-2}$	.783	-.1006	-.315	.520	.3	.39
O^{16}	"	"	$.33\times10^{-2}$	-348.7	-11.58	349.2	-5.64	.5	.45
Ca^{40}	"	"	$.39\times10^{-2}$	-152.5	6.89	152.8	7.02	.29	.38
I	"	"	$.79\times10^{-2}$	-1868	29.01	1869	27.11	.29	.32
II	"	"	$.20\times10^{-1}$	-978.7	28.38	978.9	30.69	.33	.39

Using the two-body scattering amplitudes given in References 1 and 35, we now are ready to evaluate the inelastic scattering amplitudes. All the integrations in Z and b can be carried out analytically with the aid of (5.17) and (5.18). In Appendix V, the outline of the actual calculations of the scattering amplitude for O^{16} 1^-, T = 1 state is followed by the computer program.

CHAPTER VI

DISCUSSION

$\underline{C^{12}}$

4.4 MeV

Figure 1 illustrates the comparison between the experiments at Orsay (7) and Uppsala (8), and the theoretical predictions for 2^+ T = 0 state at 4.8 MeV. The theoretical prediction reproduces in both shape and magnitude the data obtained by the Uppsala group. The agreement between theory and the Orsay experiment is equally good in shape, although not as good in magnitude. Also shown in Figure 1 is the result of the DWIA calculation. (19) The WKB and DWIA show good agreement.

The polarization predictions obtained by theory confirm the Uppsala results (27) and also the Orsay data (36) at large angles. (Figure 2) The discrepancy between theoretical prediction and the Orsay results at the small angles is serious as the addition of spin-orbit interaction makes the situation worse. Again, agreement between the WKB and DWIA is good.

9.7 MeV

Figure 3 shows the comparison between the cross sections measured by the Orsay (7) and Uppsala (8) groups and the theoretical calculations for 3^-, T = 0 state at 12.8 MeV. The WKB calculation shows good agreement with the Orsay result, but predicts larger cross sections than were obtained in the Uppsala experiment. Agreement between the WKB and DWIA results are reasonable although DWIA favors the Uppsala data.

The theoretical prediction of the polarizations matches the result of HJT (27) as shown in Figure 4. Although not shown in Figure 4, the DWIA calculation (19) gives practically the same polarizations as the WKB.

12.7 MeV

Figure 5 illustrates the comparison between the theoretical cross-sections (1^+, T = 0 at 14 MeV) and the experimental results. Although the angular dependence shows reasonable agreement, the experimental cross-sections are too small by a factor of 10. In Figure 6, the theoretical prediction of the polarizations is given.

15.2 MeV

The angular distribution predicted for the state 1^+, T = 1 at 16.6 MeV is in good agreement with the experiment, but the magnitude of the cross-sections is too large. (Figure 7) Electron scattering and β decay agree with the form factor given by the intermediate coupling. This gives a transition strength equal to one-third of the Gillet vector and would give fair agreement with the curve here. The polarization is too large when spin-orbit is taken into account but too small when it is ignored. Because of the paucity of the data and the large associated errors, we can only claim the consistency between the theory and the experiment. (Figure 8)

16.1 MeV

The theoretical curve of the cross-sections for the final state 2^+, $T = 1$ at 16.3 MeV matches the Orsay result (7) both in angular dependence and in magnitude, and is consistent with the Uppsala data (8) as shown in Figure 9. Also, the polarization curve is consistent with the Orsay measurements (6). (Figure 10) This conclusion is in disagreement with Reference 28 which stated that the observed polarization was a mixture of 2^+, $T = 1$ and 2^+, $T = 0$ at 16.7 MeV. The reason for such a disagreement is that the spin-orbit potential was ignored in the calculations contained in Reference 28.

18.2 MeV

Figure 11 gives the theoretical predictions of the cross-sections for 2^-, $T = 0$ at 16 MeV and the experimental points. Two sets of the data do not seem to agree with each other at the small angles. The agreement between the theoretical result and the Uppsala experiment is very good.

The polarization measurements are crude and the number of points measured few (Figure 12). Our calculation with the spin-orbit potential is consistent with the experiment.

19.3 MeV

Figures 13 and 14 show the theoretical calculations of the cross-sections and polarizations for 2^-, T = 1 at 19.3 MeV along with the experimental points. We note that the change in polarization due to the L•S term is significant. We can claim only the consistency of the theory with the experiment.

21.0 MeV

Figure 15 compares the Orsay data with the theoretical prediction for the state of 3^-, T = 1 at 23.5 MeV. Two results agree with each other in shape but not as well in magnitude. The polarization prediction is given in Figure 16. Variations of the polarization due to L•S are large.

22.3 MeV

The theoretical level of 1^-, T = 1 at 21.5 MeV is compared with the experimental results of the Orsay group in Figure 17. The agreement between the two results is very good. In Figure 18, the polarization prediction is shown along with the Orsay data. The Born approximation is consistent with the experiments but the introduction of the L•S term changes the curve a great deal.

Figures 19 and 20 represent the theoretical predictions of the cross-sections and polarization for the final state of 2^-, T = 0 at 21.2 MeV. We note that the L•S term changes the polarization curve extensively. The cross-sections and polarizations computed for the state 3^-, T = 0 at 19.5 MeV are given in Figures 21 and 22. The change in polarizations due to the L·S term is the "standard" type.

Figure 23 shows the calculations for 2^-, T = 1 at 23.2 MeV. In Figures 24 and 25, the predictions for the cross-sections and polarizations are given for the state 2^+, T = 0 at 19.2 MeV while Figure 26 shows the theoretical cross-sections of 1^-, T = 1 at 24.2 MeV.

O^{16}

6.15 MeV

The observed cross-section is larger than the theoretical prediction for 3^-, T = 0 at 6.25 MeV by 0.6 ~ 1.0 mb. (See Figure 27) Since the experiment did not resolve 0^+ level at 6.05 MeV, the discrepancy is certainly reasonable. The general shape and angular dependence of the predictions are in good agreement with the experiment. Also, our calculations compare favorably with the DWIA results. The polarization with L·S is shown. There is reasonable agreement between the theory and the experiment. (Figure 28)

11.5 MeV

Figure 29 compares the Uppsala experiment with the theoretical prediction for 2^-, T = 0 at 10.5 MeV. Although the theory predicts the cross-sections about 50% smaller than the observed values, the angular distribution matches the data. In view of the fact that T. Erickson gets slightly larger cross-sections by using different form factors, (5) we may obtain better agreement by using a better form factor.

Polarization prediction is given in Figure 30.

13.1 MeV

The prediction of the cross-sections for 2^-, T = 1 at 13.0 MeV and the experimental data show good agreement. (Figure 31) The effect of the L·S potential on the polarization is shown in Figure 32. No data are available for comparison.

15.3 MeV

The Uppsala results are compared with the level 2^-, T = 0 at 14.6 MeV in Figure 33. The theoretical curve is too low, but the angular distribution looks good. The predicted polarizations are small as seen in Figure 34.

18.7 MeV

The experimental data and the prediction of the cross-sections for the state 3^-, T = 0 at 15.1 MeV are given in Figure 35. Agreement between them is good in shape, but not in magnitude. Also shown is the result of the DWIA calculations. The WKB result gives a factor of 3 larger than that of DWIA. The polarization curve is practically the same as Figure 28.

20.2 MeV

Figure 36 compares the measurements of the Uppsala group with the prediction for 2^-, T = 1 at 19.1 MeV. Two results agree with each other in angular distributions including the plateau at 25°. The height of the predicted

curve is again too low. The polarization prediction is given in Figure 37.

Figures 38 through 48 show the cross-sections and polarizations for various final states. No data for these states are available to us. The results for 3^-, T = 1 states are not shown as the maximum cross-sections are around 0.2 mb at the angle of 25° for both states at 12.7 MeV and 24.1 MeV.

Ca^{40}

3.7 MeV

Figure 49 shows the results of the experiments (9, 30) and the theoretical predictions for 3^- at 3.84 MeV. Curve I is calculated on the assumption that the excited state is purely T = 0 while Curve II takes into account both the T = 0 and T = 1 states. Two sets of experimental points do not seem to agree with each other. Roos's results show the peak at a smaller angle than the results of the Harwell group. Our Curve I agrees reasonably well with the Harwell results and the DWIA calculations. However, Curve II overestimates the magnitudes of the cross sections. This is probably due to the fact that the addition of T = 1 changes the form factors.

We have varied the imaginary part of the spin-orbit potential in the calculation of the polarizations. The results are given in Figure 50. We conclude that the imaginary part of the spin-orbit potential is not necessary in our optical potential as it does not affect the cross-section either. In Figure 51, as we improve the fitting to Q(b) (see Chapter V for the definition $\Gamma(b)$ and $Q(b)$), the wild interference pattern disappears. Finally we get the curve in Figure 50 if we include $S = 1$ to our wave functions. Such interference was also noted in Reference 19. So we note that the polarizations are very sensitive to the changes in the shape of the spin-orbit potential.

4.4 MeV

The experimental cross-sections are lower than the theoretical calculations for 5^- at 4.38 MeV. (Figure 52) The angular dependence of the curve seems to be consistent with the experiment. In Figure 53, polarization predictions are illustrated.

Figures 54-59 show other excited states of 3^- and 5^-. No data are available to us for comparison.

CHAPTER VII

THE WKB METHOD AT 40 MEV

We wish to apply the WKB method to a few nuclear reactions with the incident particle energy of 40 MeV. At this energy, we do not expect any good quantitative answer, as the validity of the WKB requires the incoming particle energy to be above 100 MeV. However, if we could reproduce the rough features of the experiments, the WKB method should help us gain insights into the nuclear reaction mechanism at this energy.

We shall make the drastic approximations. The spin-orbit part of the optical potential will be ignored as will be the Coulomb part. However, unlike the situation at 156 MeV, the real central part of the optical potential will be retained. The two-nucleon potential will be assumed to be independent of the spins and isotopic spins, which amounts to making B, C, E, and F of the two nucleon scattering amplitudes zero in the limit of the impulse approximations. Hence the final states have zero spin and zero isotopic spin. Furthermore, the two-nucleon interaction potential will be assumed to be of the Yukawa type. We shall examine the final states 2^+, $T = 0$ at 4.4 MeV and 3^-, $T = 0$ at 9.6 MeV of C^{12} and 3^-, $T = 0$ at 6.15 MeV of O^{16}.

Everything is the same as at 156 MeV except for the fact that since the two-body interaction potential is used, the two-body scattering amplitude cannot be used.

$$S(\mu) = 2\sqrt{\frac{k}{k_0}}\left(\frac{\mathcal{N}}{1+\mathcal{N}}\right)\int \chi_k^{(-)*}(\vec{r}) < \Phi_f(\vec{r}_j) \mid \sum_j V(\vec{r},\vec{r}_j) \mid \Phi_0(\vec{r}_j) > \chi_{k_0}^{(+)}(\vec{r})\, d\vec{r}\, d\vec{r}_j \tag{7.1}$$

where $\vec{r}$ refers to the position of the incoming nucleon and $\vec{r}_j$ to j^{th} nucleon in the target nucleus. $X_{k_0}^{(+)}$, and $X_k^{(-)}$ are distorted waves with outgoing and incoming boundary conditions in a central optical potential only. Φ_0 and Φ_f are the nuclear state functions of initial and final states. $V(\vec{r}, \vec{r}_j)$ is the two-body interaction potential of Yukawa type. In the following equation, symbols have the same meanings as in Chapter V:

$$S(\mu) = 4\sqrt{\frac{k}{k_0}}\left(\frac{\mathcal{N}}{1+\mathcal{N}}\right) \sum_N (X+Y)_N \sum_L \hat{j}_N \hat{j}_N' \hat{L} \begin{Bmatrix} l_N & s_N & j_N \\ l_N' & s_N' & j_N' \\ L & 0 & J \end{Bmatrix} \sum_{M_1} < L, 0, M_L 0 \mid L, \mu)$$

$$\times \sum_{\lambda_N, \lambda_N'} < l_N, l_N', \lambda_N, \lambda_N' \mid L, M > (-)^{l_N' + \lambda_N'}$$

$$\times \int \chi_k^{(-)*}(\vec{r}) R^*_{n_N, l_N}(\vec{r}') Y^*_{l_N, \lambda_N}(\vec{r}') V(\vec{r}, \vec{r}') Y_{l_N', -\lambda_N'}(\vec{r}') R_{n_N', l_N'}(\vec{r}') \chi_{k_0}^{(+)}(\vec{r})\, d\vec{r}\, d\vec{r}' \tag{7.2}$$

$V = V_R \dfrac{e^{-\rho|\vec{r}-\vec{r}'|}}{\rho|\vec{r}-\vec{r}'|} + i V_I \dfrac{e^{-\rho'|\vec{r}-\vec{r}'|}}{\rho'|\vec{r}-\vec{r}'|}$ may be expanded using

$$\frac{e^{-\rho|\vec{r}-\vec{r}'|}}{\rho|\vec{r}-\vec{r}'|} = i \sum_{l=0}^{\infty} (2l+1) j_l(i\rho r_<) h_l^{(+)}(i\rho r_>) P_l(\hat{r}\cdot\hat{r}')$$

$$= 4\pi i \sum_{l=0}^{\infty} j_l(i\rho r_<) h_l^{(+)}(i\rho r_>) \sum_{m=-l}^{l} Y^*_{l,m}(\hat{r}) Y_{l,m}(\hat{r}') \tag{7.3}$$

where $j(i\rho r_<)$ and $h^+(i\rho r_>)$ are the spherical Bessel function and Hankel function of the first kind, respectively, and are given by

$$j_\ell(r) = R_\ell \frac{\sin r}{r} + S_\ell \frac{\cos r}{r}$$

$$h_\ell^{(+)}(r) = (R_\ell + iS_\ell) \frac{e^{ir}}{r}$$

$$R_\ell + iS_\ell = \sum_{s=0}^{\ell} \frac{i^{s-\ell}}{2^s s!} \frac{(\ell+s)!}{(\ell-s)!} r^{-s}$$

(7.4)

The arguments of $j(i\rho r_<)$ and $h^+(i\rho r_>)$, $r_>$ and $r_<$, refer to larger and smaller of lengths (r, r'). (25)

Using the identities (4.12) and (4.13), the orthogonality of $Y_{\ell,m}$ and the definition of the form factors given in Chapter IV, we get

$$S(\mu) = 2\sqrt{\frac{K}{K_0}}\left(\frac{\mathcal{N}}{1+\mathcal{N}}\right) 4\pi i \int \chi_K^{(-)*} Y_{LM}^*(\hat{r}) \Big[V_R h_\ell^{(+)}(i\rho r) \int_0^r j_\ell(i\rho r') F^{J0J} r'^2 dr'$$

$$+ V_R j_\ell(i\rho r) \int_r^\infty h_\ell^{(+)}(i\rho r') F^{J0J}(r') r'^2 dr'$$

$$+ iV_I h_\ell^{(+)}(i\rho' r) \int_0^r j_\ell(i\rho' r') F^{J0J} r'^2 dr'$$

$$+ iV_I j_\ell(i\rho' r) \int_r^\infty h_\ell^{(+)}(i\rho' r') F^{J0J} r'^2 dr' \Big] \chi_{K_0}^{(+)}(r)\, d^3r$$

(7.6)

Distorted Wave

As before, we have

$$\chi_{K}^{(-)*}\chi_{K_0}^{(+)} = e^{-i\vec{q}\cdot\vec{r} - \frac{K_0}{2E_0}\int_{-\infty}^{\infty} U\,dz'} \tag{7.7}$$

where the real and imaginary parts of U for C^{12} are in the notation of (5.28), (24)

$$U_R = -V(1+e^{x})^{-1} \;;\; V = 34.5\text{ MeV. } r_o = 1.22f \quad a = 0.67f$$
$$U_I = -W(1+e^{x'})^{-1} \;;\; W = 4.9\text{ MeV. } r_o' = 1.4f \quad a' = 0.7f \tag{7.8}$$

Integral along Z is carried out numerically and the results are fitted to suitable functions of b, the impact parameter. The methods employed are exactly the same as in Chapter V.

$$\begin{aligned} \text{GAMCA}(b) &= e^{-\frac{K_0}{2E_0}\int_{-\infty}^{\infty} U_I dz'} \\ &= 1.0 - (CM + CNb^2)e^{-Ab^2} - (DM + DNb^2)e^{-Bb^2} \end{aligned} \tag{7.9}$$

$$\begin{aligned} \text{FRE}(b) &= \frac{K_0}{2E_0}\int_{-\infty}^{\infty} U_R dz' \\ &= 34.5\,(CM + CNb^2)e^{-Ab^2} + 34.5\,(DM + DNb^2)e^{-Bb^2} \end{aligned} \tag{7.10}$$

$$\chi_{k}^{(-)*}\chi_{k_o}^{(+)} = e^{-i\vec{q}\cdot\vec{r}}\,(\cos(\text{FRE}) - i\sin(\text{FRE})) \times \text{GAMCA} \tag{7.11}$$

where $b = r\sin\theta$.

Determination of V_R, V_I ρ and ρ'

A rough estimate for the constants of the Yukawa potential is made by calculating the free two-particle scattering amplitudes in the Born approximation in the two-body center of mass system and comparing the result with

the coefficient A of the two-body scattering amplitude. Remembering that the interaction is complex,

$$\begin{aligned} M(q) &= A_R + iA_I(q) \\ &= -\frac{(2\pi)^2}{2} m \left\langle k \right| V_R \frac{e^{-\rho r}}{r} + iV_I \frac{e^{-\rho' r}}{r} \left| k_0 \right\rangle \\ &= -\frac{m V_R}{\rho} \frac{1}{q^2+\rho^2} - \frac{imV_I}{\rho'} \frac{1}{q^2+\rho'^2} \end{aligned} \tag{7.12}$$

From KMT, we have values of A(q)

A_R		A_I	
$q = 0$	.78 fermi	$q = 0.0$	.86 fermi
$= 1.1$	.39 fermi	$= 1.87$	.43 fermi

Equating M(q) to A's for two values of q's, we get

$$V_R = -.217\ f^{-1} \qquad V_I = -.74$$

$$\rho = 1.1\ f \qquad \rho' = 1.67$$

Effective Form Factor

For a given state, one can evaluate numerically the quantities

$$\hat{F}_R^{JOJ} = h_\ell^{(+)}(i\rho r)\int_0^r j_\ell(i\rho r')F^{JOJ}r'^2dr' + j_\ell(i\rho r)\int_r^\infty h_\ell(i\rho r')F^{JOJ}r'^2dr' \tag{6.13}$$

$$\hat{F}_I^{JOJ} = h_\ell^{(+)}(i\rho' r)\int_0^r j_\ell(i\rho' r')F^{JOJ}r'^2dr' + j_\ell(i\rho' r)\int_r^\infty h_\ell(i\rho' r')F^{JOJ}r'^2dr' \tag{6.14}$$

as the functions of r and the results are fitted to the linear combinations of Gaussians multiplied by polynomials. Again the numerical methods are the same as those in Chapter V.

$$S(\mu) = 2\sqrt{\frac{K}{K_0}}\left(\frac{N}{1+N}\right)4\pi^2 i^{MH}\int\left[\cos(FRE) - i\sin(FRE)\right]\left[V_R\hat{F}_R^{JOJ} + iV_I\hat{F}_I^{JOJ}\right]$$

$$Y^*_{L,M}(\theta,0) J_{M1}{}^{(-qb)} \cdot \mathrm{GAMCA}(b) r^2 dr \sin\theta \, d\theta \qquad (6.15)$$

C^{12} 2^+, T = 0 at 4.8 MeV

$$J_2(i\rho r) = \tfrac{1}{2}\left[\frac{3}{\rho^3 r^3} + \frac{1}{\rho r}\right]\left[e^{-\rho r} - e^{\rho r}\right] + \frac{3}{2\rho^2 r}\left[e^{-\rho r} + e^{\rho r}\right] \qquad (6.16)$$

$$h_2^{(+)}(i\rho r) = i\left[\frac{1}{\rho r} + \frac{3}{\rho^2 r^2} + \frac{3}{\rho^3 r^3}\right] e^{-\rho r} \qquad (6.17)$$

$F^{JOJ}(r') = Al \cdot r'^2 \, e^{-\alpha r'^2}$ (See Appendix I)

The results of integrations over r' are fitted to the functions of the form

$$Al \cdot r^2 (CA \, e^{-AL \, r^2} + CB \, e^{-AM \, r^2}) \qquad (6.18)$$

The constants CA, CB, AL, and AM for $\hat{F}_R^{202}$ and $\hat{F}_I^{202}$ are given below:

TABLE 4.--Effective Form Factors for C^{12} 2^+, T = 0

	CA	CB	AL	AM
$\hat{F}_R^{202}$	-.116	-.057	.35	.20
$\hat{F}_I^{202}$	-.065	-.018	.35	.21

For FRE(b), and GAMCA(b), the coefficients are as follows:

TABLE 5.--Parameters for the Distorted Wave

	CM	CN	A	DM	DN	B
FRE(b)	.129	-.0031	.12	-.032	-.0048	.54
GAMCA(b)	1.000	-.0153	.12	-.0580	-.0504	.29

$J_2(r)$ is evaluated using the polynomial approximations to J_0 and J_1 (see Appendix 6) and the relation

$$J_{N+1}(r) = \frac{J_N(r)\ 2N}{r} - J_{N-1}(r) \tag{6.19}$$

The Fortran program for IBM 1620 is given in Appendix 7. The result is plotted in Figure 60 along with the experimental points. (29) It is gratifying to note that, despite drastic approximations and validity of the WKB in doubt at this energy region, the curve shows a qualitative agreement with the experiments. The dotted line is the result of local, impulse, spin-independent approximation, i.e., exactly the same as at 156 MeV except that B, C, E, F of t(q) were set to zero.

<u>C^{12} 3^-, T = 0 at 9.7 MeV</u>

All the necessary informations are contained in C^{12} 2^-, T = 0 case except $j_3(i\rho r)$ and $h_3^{(+)}(i\rho r)$ and the effective form factors:

$$j_3(i\rho r) = i\left[\left(-\frac{6}{\rho r} - \frac{15}{(\rho r)^3}\right)\frac{e^{-\rho r}-e^{\rho r}}{2\rho r} - \left(1+\frac{15}{(\rho r)^2}\right)\left(\frac{e^{-\rho r}+e^{\rho r}}{2\rho r}\right)\right]$$

$$h_3^{(+)}(i\rho r) = \left[\frac{6}{\rho r} + \frac{15}{(\rho r)^3} + 1 + \frac{15}{(\rho r)^2}\right]\frac{e^{-\rho r}}{\rho r}$$

$\hat{F}_R^{303}$ and $\hat{F}_I^{303}$ are fitted to

$$(CA\ r^3\ e^{-ALr^2} + CB\ r^3\ e^{-AMr^2}).$$

The constants are listed in the following table.

TABLE 6.--Effective Form Factors for C^{12} 3^-, T = 0

	CA	CB	AL	AM
$\hat{F}_R^{303}$	-.110	-.031	.35	.2
$\hat{F}_I^{303}$	-.063	-.0046	.32	.2

With J_3 from equation (6.19), one can integrate along Z analytically but along b, the numerical integration is performed. The result is shown in Figure 61 along with the data. (29) Again the results look reasonable.

<u>O^{16} 3^-, T = 0 at 6.15 MeV</u>

Calculation is identical with C^{12} 3^-, T = 0 except that the effective form factors have different constants.

TABLE 7.--Effective Form Factors for O^{16} 3^-, T = 0

	CA	CB	AL	AM
$\hat{F}_R^{303}$	-.0888	-.0694	.32	.20
$\hat{F}_I^{303}$	-.0595	-.0182	.30	.20

The results are shown in Figure 62. There are no experimental data available to us.

CHAPTER VIII

CONCLUSION

156 MeV

The predictions of the cross-sections by the WKB method show reasonable agreement with the experiments. Our predictions of the cross-sections also compare very favorably with the DWIA results. The effects of the spin-orbit terms on the cross-sections are found to be small. Also, we have found that the Born approximations give essentially the same angular distributions as the distorted wave predictions except that the former gives cross-sections which are a few times larger than those given by the distorted wave predictions, a conclusion reached by the DWIA. (19) The WKB appears to predict consistently larger values of the cross-sections than the DWIA does. The reason for this is not evident as the precise comparison between the WKB and the DWIA is not possible because of different approximations made in algebraic work. We may change our magnitude a little by correcting for the motion of the center of the mass of the nucleus as in our calculations we have assumed that each nucleon is in an orbit of a central potential. Also, we believe that better nuclear wave functions would also change the magnitudes. On the whole, the WKB method as a theoretical tool for the prediction of the nuclear cross-sections is comparable to the DWIA.

For the final states in which the contributions of the S = 1 states to the cross sections are small, the polarizations predicted by the WKB agree with the results of the DWIA. The predictions by both the WKB and the DWIA agree with the experiments except at the small angles where the theoretical values are too large. (Figure 2) This feature seems to be common among the calculations that use the impulse approximations. Addition of the L·S term in the optical potential makes the situation worse.

For the final states where the S = 1 contributions to the cross-sections are important, our predictions of the polarizations are quite irregular.

In some cases like 1^+, T = 1 of C^{12} at 15.1 MeV (Figure 8) the L·S term merely enhances the Born approximations. The spin-orbit term changes the curve in the right direction. In other cases like 2^-, T = 0 of C^{12} at 18.2 MeV (Figure 12) the changes brought about by the L·S term are quite radical. We cannot say that the L·S term improves our prediction over the Born approximations, but we can say that the L·S term should not be ignored in the calculations of the polarizations as Perrain and Vinh-Mau did. Also we have found that, at least for 3^- of Ca^{40}, the contributions of the imaginary part of the spin-orbit potential to the polarizations are negligible. Also for 3^- of Ca^{40}, we have found that the wild interference pattern observed in the DWIA calculations (19) disappear as we improve the fitting of the numerical integral along Z of $U_s(L \cdot S)$ to a Gaussian function multiplied by the polynomials. This is another indication that the polarizations are sensitive to the spin-orbit potential.

As much as the polarizations are very sensitive to the L•S term, the sensible thing to do is to take the polarization data of the inelastic scattering and adjust the L•S part of the optical potential to fit the data.

On the basis of our calculations, we have made an attempt to identify some of the states observed in the experiments. The results are given in Table 8. However, it should be remarked that as many as six peaks are observed near the excitation energy of 20 MeV of C^{12}, our identifications may change when further studies are done on these peaks.

40 MeV

Despite the drastic approximations involved, we reproduced roughly the experimental situations. When we used the Yukawa two-body potential in place of the impulse approximations, we improved the predictions considerably. Our calculations show that although the WKB in its present form is inadequate at 40 MeV, it may be possible to improve on the WKB at this energy.

TABLE 8.--Identification of the Final States

Exp. State		Theoret. State (Gillet et al.)	Comment
		C^{12}	
4.4 Mev	. . .	2^+, T = 0 at 4.8 Mev	
9.7 "	. . .	3^-, T = 0 " 12.8 "	
12.7 "	. . .	1^+, T = 0 " 14.0 "	. . . Poor
15.1 "	. . .	1^+, T = 1 " 16.6 "	
16.1 "	. . .	2^+, T = 1 " 16.3 "	
18.2 "	. . .	2^-, T = 0 " 16.0 "	
19.3 "	. . .	2^-, T = 1 " 19.3 "	. . . Poor
21.0 "	. . .	3^-, T = 1 " 23.5 "	
22.3 "	. . .	1^-, T = 1 " 21.5 "	
		O^{16}	
6.15 "	. . .	3^-, T = 0 " 6.25 "	
11.5 "	. . .	2^-, T = 0 " 10.5 "	
13.1 "	. . .	2^-, T = 1 " 13.0 "	
15.3 "	. . .	2^-, T = 0 " 14.6 "	
18.7 "	. . .	3^-, T = 0 " 15.1 "	
20.2 "	. . .	2^-, T = 0 " 19.1 "	
		Ca^{40}	
3.7 "		3^- at 3.84 "	
4.4 "		5^- " 4.38 "	

APPENDIX I

The radial wave functions used in evaluating the form factors are: (33)

$$R_{1,\ell} = \pi^{-1/4}\,\alpha^{3/4}\sqrt{\frac{2^{\ell+2}}{(2\ell+1)!!}}\;\alpha^{\frac{\ell}{2}}\,r^{\ell}\,e^{-\frac{\alpha r^2}{2}}$$

$$R_{2,\ell} = \pi^{-1/4}\,\alpha^{3/4}\sqrt{\frac{2^{\ell+3}}{(2\ell+3)!!}}\;\alpha^{\frac{\ell}{2}}\,r^{\ell}\left[\frac{2\ell+3}{2}-\alpha r^2\right]e^{-\frac{\alpha r^2}{2}}$$

$$R_{3,\ell} = \pi^{-1/4}\,\alpha^{3/4}\sqrt{\frac{2^{\ell+3}}{(2\ell+5)!!}}\;\alpha^{\frac{\ell}{2}}\,r^{\ell}\left[\frac{(2\ell+3)(2\ell+5)}{4}-(2\ell+5)\alpha r^2+\alpha^2 r^4\right]e^{-\frac{\alpha r^2}{2}}$$

The values of α for C^{12}, O^{16} and Ca^{40} are taken from the analysis of the electron scattering experiments: (34)

C^{12} ----- .37 fm^{-2}

O^{16} ----- .311

Ca^{40} ----- .22

Using the definitions of the form factors (4.17), (4.24), and (4.29), we get the following results:

C^{12} 1^-, T = 1

$$p101 = -0.225\alpha^2\,e^{-\alpha r^2}\left[Y1\ r + Y2\ \alpha r^3\right]$$

$$p111 = .159\alpha^2\,e^{-\alpha r^2}\left[R1\ r + R2\ \alpha r^3\right]$$

E	Y1	Y2	R1	R2
17.7 MeV	4.59	-2.7	3.24	-2.17
21.5	.674	-2.77	.682	1.34

$C^{12}\ 1^+$

$$F^{011} = 0.159\, \alpha^{(3/2)} e^{-\alpha r^2} [YL + YM\, \alpha r^2 \quad + YN\, \alpha^2 r^4$$

$$F^{211} = 0.159\, \alpha^{(5/2)} e^{-\alpha r^2} [YA\ r^2 + YB\, \alpha r^4]$$

T = 0

E	YL	YM	YN	YA	YB
14.0 MeV	-0.485	2.34	0.53	-1.54	0.167
T = 1					
16.6 MeV	-0.137	2.6	0.336	-1.064	0.043

$C^{12}\ 2^-$

$$F^{112} = 0.159\, \alpha^2\ e^{-\alpha r^2} [Y1\ r + Y2\, \alpha r^3]$$

$$F^{312} = 0.159\, \alpha^3\ r^3 e^{-\alpha r^2}\ Y3$$

T = 1

E	Y1	Y2	Y3
18.2 MeV	-5.0	2.36	-0.256
19.3	-2.49	3.29	0.645
23.2	-0.312	1.51	-1.045
T = 0			
15.6 MeV	2.46	0	0.78
16	-5.04	4.09	0.398
21.2	-0.148	1.57	-0.97

C^{12} 2^+

$$F^{202} = -0.225\,\alpha(5/2)e^{-\alpha r^2}[Y1\ r^2 + Y2\,\alpha\, r^4]$$
$$F^{212} = 0.159\,\alpha(5/2)e^{-\alpha r^2}[R1\ r^2 + R2\,\alpha\, r^4]$$

T = 0

E	Y1	Y2	R1	R2
4.8 MeV	5.52	-0.183	-3.536	0.665
19.2	-2.011	1.60	0.195	0.535

T = 1

E	Y1	Y2	R1	R2
16.3 MeV	1.98	-0.027	-2.64	-0.083

C^{12} 3^-

$$F^{303} = \text{FORM}\,\alpha^3\ r^3 e^{-\alpha r^2}$$
$$F^{313} = \text{FACTOR}\,\alpha^3\ r^3\ e^{-\alpha r^2}$$

T = 0

E	FORM	FACTOR
12.8 MeV	-0.545	0.126
19.5	0.2	-0.314

T = 1

E	FORM	FACTOR
18.4 MeV	-0.306	-0.067
23.5	0.39	-0.314

O^{16} 1^-, T = 1

$$F^{101} = -0.225\,\alpha^2\ e^{-\alpha r^2}\ [Y1\ r + r^3\alpha\, Y2]$$
$$F^{111} = 0.159\,\alpha^2\ e^{-\alpha r^2}\ [R1\ r + R2\,\alpha\, r^3]$$

E	Y1	Y2	R1	R2
13.5 MeV	-3.32	2.175	4.56	-2.85

O^{16} 2^-

$$F^{112} = 0.159\alpha^2 e^{-\alpha r^2}[Y1 \; r + Y2\alpha r^3]$$

$$F^{312} = 0.159\alpha^3 r^3 e^{-\alpha r^2} \; Y3$$

T = 0

E	Y1	Y2	Y3
10.5 MeV	0.0056	1.72	-0.369
14.6	0.0056	-0.949	1.78
16.6	-0.068	2.225	1.74
17.3	-5.64	3.72	-0.0219

T = 1

E	Y1	Y2	Y3
13.0 MeV	0.34	1.72	-0.475
17.6	-1.19	0.574	1.96
19.1	2.88	0.08	1.04
20.2	-4.84	4.38	0.62

O^{16} 3^-

$$F^{303} = -0.387\alpha^3 \, r^3 \, e^{-\alpha r^2} \quad Y1$$

$$F^{313} = +0.268\alpha^3 \, r^3 \, e^{-\alpha r^2} \quad Y2$$

T = 0

E	Y1	Y2
6.25 MeV	-1.93	.839
15.1	1.415	.519
20.1	- .621	-1.268

T = 1

E	Y1	Y2
12.7 MeV	-0.854	1.14
18.5	0.822	-0.226
24.1	-1.06	-1.14

Ca^{40} 3^-

$$F^{303} = -\frac{\alpha^3}{\sqrt{2}\,\pi} e^{-\alpha r^2} \left[Y1\, r^3 + Y2\, \alpha r^5 \right]$$

$$F^{313} = \frac{\alpha^3}{4\pi} e^{-\alpha r^2} \left[R1\, r^3 + R2\, \alpha r^5 \right]$$

T = 0

E	Y1	Y2	R1	R2
3.84 MeV	4.95	-3.43	-1.775	1.309
7.15	-2.795	1.123	2.824	-0.466
7.73	1.59	-0.472	-2.19	0.44
8.34	-0.1	-0.385	1.81	-0.85

T = 1

E	Y1	Y2	R1	R2
3.84 MeV	-0.07	0.044	-0.1	0.025
7.15	0.399	-0.054	-0.485	-0.505
7.73	0.223	0.098	-0.118	-0.857
8.34	0.374	-0.074	-0.92	0.1

Ca^{40} 5^-

$$F^{505} = -\frac{0.569}{\sqrt{2}\,\pi} \alpha^4 r^5 e^{-\alpha r^2}\, Y1$$

$$F^{515} = \frac{0.569}{4\pi} \alpha^4 r^5 e^{-\alpha r^2}\, Y2$$

	T = 0		T = 1	
E	Y1	Y2	Y1	Y2
4.38 MeV	2.163	-1.92	-0.054	-0.118
8.0	-0.232	-0.284	-0.822	2.657
12.2	0.787	0.212	-0.19	0.303
13.4	0.22	0.0728	0.624	-0.989
18.2	0.98	2.888	-0.161	-0.253
20.5	-0.13	-0.355	-1.138	-2.42

APPENDIX II

The basis of this approximation is the experimental observation that the polarization of an initially unpolarized nucleon and the asymmetry (to be defined below) of a 100% polarized nucleon are very nearly the same. (31,32) We shall take the xz plane as the scattering plane.

Asymmetry is defined as follows:

Assume that the incident nucleon has a polarization vector $\vec{P}_i$ and the target has zero spin.

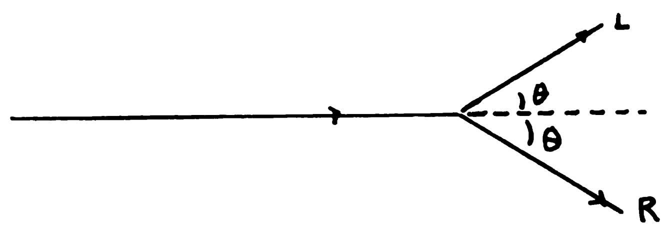

The cross-section at an angle θ is (15)

$$\frac{d\sigma}{d\Omega}(L,R) = \frac{1}{2}\left\{ \sum_{\mu} T_r\left(S^{+}(\mu)\, S(\mu)\right) + \sum_{\mu} T_r\left(S(\mu)\,\vec{\sigma}\, S^{+}(\mu)\,\vec{P}_i\right) \right\}$$

(AII.1)

If the incoming nucleon is 100% polarized along the y direction

$\vec{\sigma}\cdot\vec{P}_i = \sigma_y$ when scattered to the left (L),

$\vec{\sigma}\cdot\vec{P}_i = -\sigma_y$ when scattered to the right (R).

Then asymmetry A is defined as

$$A = \frac{\frac{d\sigma}{d\Omega}(L) - \frac{d\sigma}{d\Omega}(R)}{\frac{d\sigma}{d\Omega}(L) + \frac{d\sigma}{d\Omega}(R)} = \frac{\sum_\mu T_r[S(\mu)\sigma_y S(\mu)^\dagger]}{\sum_\mu T_r[S(\mu)S^\dagger(\mu)]} \tag{AII.2}$$

With the definition of P in Chapter II, we have

$$[A-P]\sum_\mu T_r[S(\mu)S^\dagger(\mu)] = \sum_\mu T_r[S(\mu)\sigma_y S^\dagger(\mu)] - \sum_\mu T_r[S^\dagger(\mu)\sigma_y S(\mu)] \tag{AII.3}$$

Using $S(\mu) = S^0(\mu) + S^x(\mu)\sigma_x + S^y(\mu)\sigma_y + S^z(\mu)\sigma_z$

we have

$$[A-P]\sum_\mu T_r[S(\mu)S(\mu)^\dagger] = 8\, \mathrm{Im}\,(S^x(\mu)\, S^{z*}(\mu)) \tag{AII.4}$$

If we rewrite (5.6), following Reference 37

$$e^{-iQ_2\sigma_m}\sigma_n e^{-iQ_1\sigma_m} = \sigma_n - i\sigma_m\sigma_n Q - \frac{i}{2}[Q+\mathcal{P}][\sigma_n,\sigma_m] \tag{AII.5}$$

where

$$Q = \frac{K_0^2 b}{2E_0}\int_{-\infty}^{\infty} U_s\, dz'$$

$$\mathcal{P} = \frac{K_0^2 b}{2E_0}\int_{-z}^{z} U_s\, dz'$$

It can be shown that $\mathcal{P} = 0$ makes the right-hand side of (AII.4) either very small or zero.

APPENDIX III

Read the integrand γ (the optical potential) into the memory as a subfunction. First fix the value of b. For a given interval in Z, do the integration twice: first, by dividing the interval into two sub-intervals we have the result F1; secondly, by dividing the interval into 4 sub-intervals we get F2. Compare the results F1 and F2. If $|F1-F2| < 0.01$, go to the next interval. Repeat the procedure until Z = 16.0. The program evaluates the integral for $0 \leq b \leq 16.0$ with an increment of 0.2

This program is written for CDC-3600 at Michigan State University.

```
* 151238  LEE,H
      PROGRAM INELAS
      B=0.0
 105  Z=0.0
      SUM=0.0
 107  DH=0.01
 108  X1=Z+DH/2.0
      X2=Z+DH
      X3=Z+3.0*DH/2.0
      X4=Z+2.0*DH
 110  F1=DH*(Y(B,Z)+4.0*Y(B,X2)+Y(B,X4))/3.0
      F2=DH*(Y(B,Z)+4.0*(Y(B,X1)+Y(B,X3))+2.0*Y(B,X2)+Y(B,X4))/6.0
 120  IF(ABSF(F1-F2)-0.01  ) 130, 130, 125
 125  DH=DH/2.0
      GO TO 108
 130  SUM=SUM+F2
      Z=X4
      IF(Z-16.0) 107,140,140
 140  PRINT 145, B,F1, F2, SUM
 145  FORMAT(/4F20.6
      B=B+0.2
      IF(B-16.0) 105,150,150
 150  CONTINUE
      END
      FUNCTION Y(B,Z)
      Y=15.9/(1.0+EXPF((SQRTF(B*B+Z*Z)-3.00)/0.556))
      RETURN
      END
      END
```

APPENDIX IV

Read the results of the integration performed by the program in Appendix III as the elements of the matrix E. Evaluate the exponential function Q using the elements of the E matrix as the exponents.

Consider

$$THF(N) = 1.0 - (x + \gamma b^2)_e{-A\ b^2} - (Z + V\ b^2)_e{-D\ b^2}$$

$$\sigma = \sum_N (Q(N) - THF(N))^2$$

Make σ as small as possible by varying x, γ, A, Z, V and D. First fix A and D. Then solve the equations:

$$\frac{\partial \sigma}{\partial x} = 0$$

$$\frac{\partial \sigma}{\partial \gamma} = 0$$

$$\frac{\partial \sigma}{\partial z} = 0$$

$$\frac{\partial \sigma}{\partial V} = 0$$

These four equations are solved to get X, γ, Z, and V. Then we evaluate σ. Repeat this procedure by giving different values of A and D. THF corresponds to $\Gamma(b)$ in the text while X, γ, Z, V, A, and D correspond to CM, CN, DM, DN, A and B. This program is written for CDC-3600 at Michigan State University.

```
*  151238 Lee H
        PROGRAM FITTIM
        DIMENSION Q(50),E(50),QI(50),B(50),FL(5),FM(5), FN(5),
       1AF(50),AT(50),BT(50),THF(50)
C       0 IMAGINARY PART CENTRAL FITTING
        DO 10 K=1,45
        U=K
        B(K)=0.2*(U-1.0)
   10   CONTINUE
        READ 11, (QI(N),N=1,40
   11   FORMAT(8F10.5)
        DO 15  N=1,40
   15   Q(N)=EXPF(-0.0176*QI(N))
        A=0.14
        DO 800 I=1,5
        A=A+0.02
        D=0.09
        DO 750  J=1,20
        DO 25 M=1,4
        FL(M)=0.0
        FM(M)=0.0
        FN(M)=0.0

   25   CONTINUE
        D=D+0.02
        DO 30 N=1,40
        AF(N)=EXPF(-A*B(N)**2)-EXPF(-D*B(N)**2)
        AT(N)=B(N)**2*EXPF(-A*B(N)**2)
        BT(N)=B(N)**2*EXPF(-D*B(N)**2)
        E(N)=Q(N)-1.0+(1.0-Q(1))*EXPF(-D*B(N)**2)
        FL(1)=FL(1)+E(N)*AF(N)
        FL(2)=FL(2)+AF(N)**2
        FL(3)=FL(3)+AF(N)*AT(N)
        FL(4)=FL(4)+AF(N)*BT(N)
        FM(1)=FM(1)+E(N)*AT(N)
        FM(2)=FM(2)+AF(N)*AT(N)
        FM(3)=FM(3)+AT(N)**2
        FM(4)=FM(4)+AT(N)*BT(N)
        FN(1)=FN(1)+E(N)*BT(N)
        FN(2)=FN(2)+AF(N)*BT(N)
        FN(3)=FN(3)+AT(N)*BT(N)
        FN(4)=FN(4)+BT(N)**2
   30   CONTINUE
        DET=FL(2)*FM(3)*FN(4)+FL(3)*FM(4)*FN(2)+FL(4)*FN(3)*FM(2)
       1-FL(4)*FM(3)*FN(2)-FM(4)*FN(3)*FL(2)-FN(4)*FM(2)*FL(3)
        DEX=FL(1)*FM(3)*FN(4)+FL(3)*FM(4)*FN(1)+FL(4)*FN(3)*FM(1)
       1-FL(4)*FM(3)*FN(1)-FM(4)*FN(3)*FL(1)-FN(4)*FM(1)*FL(3)
        DEY=FL(2)*FM(1)*FN(4)+FL(1)*FM(4)*FN(2)+FL(4)*FN(1)*FM(2)
       1-FL(4)*FM(1)*FN(2)-FM(4)*FN(1)*FL(2)-FN(4)*FM(2)*FL(1)
        DEV=FL(2)*FM(3)*FN(1)+FL(3)*FM(1)*FN(2)+FL(1)*FN(3)*FM(2)
       1-FL(1)*FM(3)*FN(2)-FM(1)*FN(3)*FL(2)-FN(1)*FM(2)*FL(3)
        X=-DEX/DET
        Y=-DEY/DET
        V=-DEV/DET
```

```
      Z=1.0-X-Q(1)
      EQA=FL(1)+X*FL(2)+Y*FL(3)+V*FL(4)
      EQB=FM(1)+X*FM(2)+Y*FM(3)+V*FM(4)
      EQC=FN(1)+X*FN(2)+Y*FN(3)+V*FN(4)
      PRINT 301,X,Y,Z,V,A,D
301   FORMAT(5X,1HX,E15.5 ,2X,1HY,E15.5,2X,1HZ,E15.5,
     12X,1HV,E15.5,2X,1HA,E15.5,2X,1HD,E15.5)
      PRINT 302,EQA,EQB,EQC
302   FORMAT(3E15.5)
      SIGMA=0.0
      DO 500 N=1,40
      THF)N)=1.0-(X+Y*B(N)**2)*EXPF(-A*B(N)**2)
     1-(Z+V*B(N)**2)*EXPF(-D*B(N)**2)
500   SIGMA=SIGMA+(Q(N)-THF(N))**2
      PRINT16,(Q(N),THF(N),N=1,40)
16    FORMAT(8F10.6)
      PRINT520,SIGMA
520   FORMAT(10X,5HSIGMA,E15.4)
750   CONTINUE
800   CONTINUE
      END
      END
```

47.74001	47.61321	47.23718	46.60842	45.71755	44.55089	43.09150	41.32066
39.22056	36.77877	33.99509	30.89058	27.51745	23.96597	20.36925	16.85940
13.60243	10.71003	8.25023	6.23781	4.64469	3.41680	2.49008	1.801833
1.29684	.92962	.66437	.47371	.33717	.23965	.17014	.12070
.08555	.06060	.04291	.03036	.02148	.01519	.01073	.00758

APPENDIX V

A brief outline of the calculations of the scattering amplitude for the final state 1^-, $T = 1$ of O^{16} is given below.

From the consideration of the parity, $L = 1$ and $S = 0$, or 1.

Let $\mathrm{CON} = 2\sqrt{\frac{K}{K_0}}\left(\frac{N}{1+N}\right)$

$$S(\mu=1, S=0) = \mathrm{CON} \int e^{-i\vec{q}\cdot\vec{r}}\,\Gamma(b^2)\,Y_{11}^{*}(\theta,\phi)\,F^{101}(r)\,[A + c\,\sigma_y]$$

$$- i\,\frac{\mathrm{CON}}{2}\cdot(-.098)\cdot W\cdot \int e^{-i\vec{q}\cdot\vec{r}}\,\Gamma(b^2)\,Y_{11}^{*}(\theta,0)\,F^{101}(r)\;Q(b)\,[\sigma_y,\sigma_m]\,c$$

$$- i\,\mathrm{CON}\cdot(-.098)\cdot W\cdot \int e^{-i\vec{q}\cdot\vec{r}}\,\Gamma(b^2)\,F^{101}\,Y_{11}^{*}\,Q(b)\,\sigma_m\,[A + c\,\sigma_y]$$

(AV-1)

Consider

$$SI = \mathrm{CON} \int e^{-i\vec{q}\cdot\vec{r}}\,\Gamma(b^2)\,Y_{11}^{*}\,[Y1\,r + Y2\,r^3]\,e^{-\alpha r^2}\,d^3r$$

$$= 2\pi i\ \mathrm{CON} \int \Gamma(b^2)\,Y_{11}^{*}(\theta,0)\,[Y1\,r + Y2\,r^3]\,e^{-\alpha r^2}\,J_1(-qb)\;r^2dr\,\sin\theta\,d\theta$$

(AV-2)

Integration over Z yields

$$= \mathrm{CON}\cdot 2\pi i\cdot\sqrt{\tfrac{3}{8}} \int \Gamma(b)\,e^{-\alpha b^2}\left[\frac{Y1\,b^2}{\sqrt{\alpha}} + \frac{Y2\,b^4}{\sqrt{\alpha}} + \frac{Y2\,b^2}{2\,\alpha^{3/2}}\right]J_1(qb)\,db$$

Defi

Like

repl

pla

Def

The

S

Define

$$\int_0^\infty e^{-(\alpha+A)b^2}\, b^2\, J_1(qb)\, db = FB2(A,U) \qquad \text{(AV-3)}$$

$$\int_0^\infty e^{-(\alpha+A)b^2}\, b^4\, J_1(qb)\, db = FB4(A,U) \qquad \text{(AV-4)}$$

$$\int_0^\infty e^{-(\alpha+A)b^2}\, b^6\, J_1(qb)\, db = FB6(A,U) \qquad \text{(AV-5)}$$

Likewise we define FB2(B,U) --- and FB2(Z,U) --- when A is replaced by B and zero respectively. The variable q is replaced by U.

Define also

$$CFB2 = FB2(Z,U) - CM\cdot FB2(A,U) - DM\cdot FB2(B,U) - CN\cdot FB4(A,U) - DN\cdot FB4(B,U) \qquad \text{(AV-6)}$$

$$CFB4 = FB4(Z,U) - CM\cdot FB4(A,U) - DM\cdot FB4(B,U) - CN\cdot FB6(A,U) - DN\cdot FB6(B,U) \qquad \text{(AV-7)}$$

Then making use of $\Gamma(b^2)$ from the text,

$$SI = CON\cdot 2\pi\sqrt{\tfrac{3}{8}}\; i\left\{\left[\frac{Y1}{\sqrt{\alpha}} + \frac{Y2}{2\alpha^{3/2}}\right] CFB2 + \frac{Y2}{\sqrt{\alpha}}\, CFB4\right\} = iSFA1 \qquad \text{(AV-8)}$$

The third term in (AV-1) is, after integrating over Z,

$$SII = -iCON\cdot\pi\cdot(0.098)\cdot\sqrt{\tfrac{3}{8}}\, W\int_0^\infty \Gamma(b^2)\left[\left(\frac{Y1}{\sqrt{\alpha}} + \frac{Y2}{2\alpha^{3/2}}\right)b^2 + \frac{Y2b^4}{\sqrt{\alpha}}\right] e^{-\alpha b^2} Q(b)\left[-i\,\sigma_x(J_2(qb) + J_o(qb)) + \sigma_y(J_2 - J_0)\right]\left[A + C\,\sigma_y\right] db \qquad \text{(AV-9)}$$

Defin

GE

GE

G

G

F

F

Then

seco

is t

Define

$$GB2S = \int_0^\infty \Gamma(b^2)Q(b)b^2\, e^{-\alpha b^2}\, J_2(qb)db \qquad \text{(AV-10)}$$

$$GB4S = \int_0^\infty \Gamma(b^2)Q(b)b^4\, e^{-\alpha b^2}\, J_2(qb)db \qquad \text{(AV-11)}$$

$$GD2S = \int_0^\infty \Gamma(b^2)Q(b)b^2\, e^{-\alpha b^2}\, J_0(qb)db \qquad \text{(AV-12)}$$

$$GD4S = \int_0^\infty \Gamma(b^2)Q(b)b^4\, e^{-\alpha b^2}\, J_0(qb)db \qquad \text{(AV-13)}$$

$$FBDP = -CON\cdot\sqrt{\tfrac{3}{8}}\cdot \pi \cdot 0.098 \Big[(GB2S + GD2S)\Big(\frac{Y1}{\sqrt{\alpha}} + \frac{Y2}{2\alpha^{3/2}}\Big) + (GB4S + GD4S)\,\frac{Y2}{\sqrt{\alpha}}\Big] \qquad \text{(AV-14)}$$

$$FBDM = -CON\cdot\pi\cdot\sqrt{\tfrac{3}{8}}\cdot 0.098 \Big[(GB2S - GD2S)\Big(\frac{Y1}{\sqrt{\alpha}} + \frac{Y2}{2\alpha^{3/2}}\Big) + (GB4S - GD4S)\,\frac{Y2}{\sqrt{\alpha}}\Big] \qquad \text{(AV-15)}$$

Then

$$SII = \sigma_x\cdot W\cdot FBDP\,[A + c\,\sigma_y] + i\,\sigma_y\cdot FBDM\cdot W\,[A + c\,\sigma_y] \qquad \text{(AV-16)}$$

We can follow the same procedure to evaluate the second term of (AV-1).

$$S(\mu=1, S=0) = iA\cdot SFA1 + iC\cdot W\cdot FBDM + \sigma_x\, A\cdot W\cdot FBDP + \sigma_y(iC\cdot SFA1 + iA\cdot W\cdot FBDM) \qquad \text{(AV-17)}$$

For spin S = 1, we can show that the only non-zero term is the coefficient of σ_z.

$$SPN1z = -2\pi\,\sqrt{2}\,i\; F\; CON\cdot\sqrt{\tfrac{3}{8\pi}}\;\langle 1,1,1,0\,|\,1,1\rangle \int Y^*(\theta,\phi)F^{111}(r)\,\Gamma(b)J_1(-qb)r^2dr\,\sin\theta\, d\theta$$

$$= 2\pi\cdot CON\cdot\sqrt{\tfrac{3}{8}}\cdot F\;\Big(\frac{R1}{\sqrt{\alpha}} + \frac{R2}{2\alpha^{3/2}}\Big)CFB2 + \frac{R2}{\sqrt{\alpha}}\,CFB4 \qquad \text{(AV-18)}$$

Then the addition of (AV-17) and (AV-18) gives the scattering amplitude when the projection quantum number $\mu = 1$. For $\mu = -1$, we get similar results.

We have to repeat the whole process to get the scattering amplitude for $\mu = 0$.

The program shown is for 1^-, T = 1 of O^{16}. The programs for the other states considered have similar structures.

Read in the momentum transfers at Q(N). Then the real and imaginary parts of the two-body scattering amplitudes A, B, C, E and F are stored at AR, AI, BR, BI, CR, CI, ER, EI, FR and FI. The parameters for the distorted waves are read in by the statements 153 and 139. The statement 123 reads in $\Upsilon 1$, $\Upsilon 2$, R1 and R2 for the form factor. WR and WI are the real and imaginary parts of the spin-orbit coupling constants. The results of the integrations performed by (5.18) are stored as the subfunctions FA4, --- FB4, --- T45, --- T09. Only these functions appear for all the states considered, although not all of them are used for a given state. The real parts of the scattering amplitudes are given the following names:

$\mathrm{Re}[S^o(\mu=1)]$ = SAVR1

$\mathrm{Re}[S^x(\mu=1)]$ = SAXR1

$\mathrm{Re}[S^y(\mu=1)]$ = SAYR1

$\mathrm{Re}[S^z(\mu=1)]$ = SAZR1

$\mathrm{Re}[S^o(\mu=0)]$ = SAVR0

$\mathrm{Re}[S^y(\mu=0)]$ = SAYR0

Similar names are given for the imaginary parts. The DO loops

iffe

appro

cross

loops are necessary to evaluate the cross-sections for the different values of the q's and also to consider the Born approximations by making CM=DM=CN=DN=0 and WR=WI=0. The cross-section to be plotted is obtained by 10 x TCROS(mb).

238 LEE H 3

```
 PROGRAM SCATER
 DIMENSION Q(50), ARH(50),AIH(50),CRH(50),CIH(50),
1WRM(5), WIM(5) ,CME(5), CNE(5), DME(5), DNE(5),AE(5), BE(5)  ,
2BRH(50),BIH(50),ERH(50),EIH(50),FRH(50),FIH(50)
 COMMON P
 O 1- T=1
 READ 100, (Q(N), N=1,39)
 FORMAT(8F10.6)
 READ 165,(ARH(N),AIH(N),CRH(N),CIH(N),N=1,39)
 FORMAT(4F10.6)
 READ 167,(BRH(N),BIH(N),ERH(N),EIH(N),FRH(N),FIH(N),N=1,39)
 FORMAT(6F10.6)
 Z=0.0
 P=0.311
 SQP=SQRTF(P)
 CON=1.95
 PEK=-.098
 READ151, (WRM(N), N=1,2)
 READ 151, (WIM(N), N=1,2)
 FORMAT(2F10.5)
 READ 160,CF,CS,DF,DS,R,S
 FORMAT(6F10.5)
 READ 110,(CME(N),CNE(N),DME(N), DNE(N),AE(N),BE(N),N=1,2)
 FORMAT(6F10.5)
 DO 951 JF=1,2
 READ 101, Y1, Y2, R1, R2
 FORMAT(4F10.5)
 YA=-.225*P**2*Y1
 YB=-.225*P**3*Y2
 RA=.159*P**2*R1
 RB=.159*P**3*R2
 PRINT 124, Y1, Y2, R1, R2
 FORMAT(/5X,4F15.3)
 DO 950 L=1,2
 CM=CME(L)
 CN=CNE(L)
 DM=DME(L)
 DN=DNE(L)
 A=AE(L)
 B=BE(L)
 PRINT 135,CM,CN,DM,DN,A,B
 FORMAT(6F10.5)
 DO 910 J=1,2
 WR=WRM(J)
 WI=WIM(J)
 PRINT 170,CF,CS,DF,DS,R,S,WR,WI
 FORMAT(/8F15.5)
 DO 900 I=1,39
 AR=ARH(I)/4.0
 AI=AIH(I)/4.0
 CI=CIH(I)/4.0
 CR=CRH(I)/4.0
 BR=BRH(I)/4.0
 BI=BIH(I)/4.0
 ER=ERH(I)/4.0
 EI=EIH(I)/4.0
```

```
 FR=FRH(I)/4.0
 FI=FIH(I)/4.0
 U=Q(I)
 GB41=CF*T25(R,Z,U)+DF*T25(S,Z,U)-CM*CF*T25(A,R,U)
1-CM*DF*T25(A,S,U)-DM*CF*T25(B,R,U)-DM*DF*T25(B,S,U)
 GB43=CS*T27(R,Z,U)+DS*T27(S,Z,U)-(CN*CF+CM*CS)*T27(A,R,U)
1-(CN*DF+DS*CM)*T27(A,S,U)-(DN*CF+DM*CS)*T27(B,R,U)
2-(DN*DF+DM*DS)*T27(B,S,U)
 GB45=-CN*CS*T29(A,R,U)-CN*DS*T29(A,S,U)-DN*CS*T29(B,R,U)
1-DN*DS*T29(B,S,U)
 GB21=CF*T23(R,Z,U)+DF*T23(S,Z,U)-CF*CM*T23(A,R,U)
1-CF*DM*T23(B,R,U)-CM*DF*T23(A,S,U)-DM*DF*T23(B,S,U)
 GB23=CS*T25(R,Z,U)+DS*T25(S,Z,U)-(CM*CS+CF*CN)*T25(A,R,U)
1-(CS*DM +CF*DN)*T25(B,R,U)-(DS*CM+DF*CN)*T25(A,S,U)
2-(DS*DM+DF*DN)*T25(B,S,U)
 GB25=-CN*CS*T27(A,R,U)-CS*DN*T27(B,R,U)
1-CN*DS*T27(A,S,U)-DN*DS*T27(B,S,U)
 GD21=CF*T03(R,Z,U)+DF*T03(S,Z,U)-CM*CF*T03(A,R,U)-CM*DF*T03(A,S,U)
1  -DM*CF*T03(B,R,U)-DM*DF*T03(B,S,U)
 GD41=CF*T05(R,Z,U)+DF*T05(S,Z,U)-CM*CF*T05(A,R,U)
1-CM*DF*T05(A,S,U)-DM*CF*T05(B,R,U)-DM*DF*T05(B,S,U)
 GD23=CS*T05(R,Z,U)+DS*T05(S,Z,U)-(CM*CS+CF*CN)*T05(A,R,U)
1-(DM*CS+CF*DN)*T05(B,R,U)-(CM*DS+DF*CN)*T05(A,S,U)
2-(DM*DS+DF*DN)*T05(B,S,U)
 GD43=CS*T07(R,Z,U)+DS*T07(S,Z,U)-(CM*CS+CF*CN)*T07(A,R,U)
1-(DM*CS+CF*DN)*T07(B,R,U)-(CM*DS+DF*CN)*T07(A,S,U)
2-(DM*DS+DF*DN)*T07(B,S,U)
 GD25=-CN*CS* T07(A,R,U)-CN*DS*T07(A,S,U)
1- DN*CS*T07(B,R,U)-DN*DS*T07(B,S,U)
 GD45=-CN*CS*T09(A,R,U)-CN*DS*T09(A,S,U)
1-DN*CS*T09(B,R,U)-DN*DS*T09(B,S,U)
 GB4S=GB41+GB43+GB45
 GB2S=GB21+GB23+GB25
 GD2S=GD21+GD23+GD25
 GD4S=GD41+GD43+GD45
 CFB4=FB4(Z,U)-CM*FB4(A,U)-DM*FB4(B,U)-CN*FB6(A,U)-DN*FB6(B,U)
 CFB2=FB2(Z,U)-CM*FB2(A,U)-DM*FB2(B,U)-CN*FB4(A,U)-DN*FB4(B,U)
 AWM=AR*WR-AI*WI
 BWM=BR*WR-BI*WI
 CWM=CR*WR-CI*WI
 EWM=ER*WR-EI*WI
 FWM=FR*WR-FI*WI
 AWP=AR*WI+AI*WR
 BWP=BR*WI+BI*WR
 CWP=CR*WI+CI*WR
 EWP=ER*WI+EI*WR
 FWP=FR*WI+FI*WR
 SFA1=CON*(CFB2*(YA/SQP+YB/(2.0*P*SQP))+YB/SQP*CFB4)*3.84
 FBDP=CON*PEK*((GB2S+GD2S)*(YA/SQP+YB/(2.0*P*SQP))
1+(GB4S+GD4S)*YB/SQP)*1.92
 FBDM=CON*PEK*((GB2S-GD2S)*(YA/SQP+YB/(2.0*P*SQP))
1+(GB4S-GD4S)*YB/SQP)*1.92
 SAVR1=-AI*SFA1-CWP*FBDM
 SAVI1=AR*SFA1+CWM* FBDM
 SAXR1=AWM*FBDP
 SAXI1=AWP*FBDP
 SAYR1=-CI*SFA1-AWP*FBDM
```

```
 SAYI1=CR*SFA1+AWM*FBDM
 QCB=(RA/SQP+RB/(2.0*P*SQP))*CFB2+RB/SQP*CFB4
 AM1Z=CON*QCB*3.84
 SAZR1=-FI*AM1Z
 SAZI1=FR*AM1Z
 GBDP=(RA/SQP+RB/(2.0*P*SQP))*(GB2S+GD2S)
1+RB/SQP*(GB4S+GD4S)
 GBDM=(RA/SQP+RB/(2.0*P*SQP))*(GB2S-GD2S)
1+RB/SQP*(GB4S-GD4S)
 AMA=-5.45*CON*QCB
 AMB=2.72*CON*PEK*GBDP
 AMC=2.72*CON*PEK*GBDM
 SAVR0=CR*AMA+EWM*AMB-BWM*AMC
 SAVI0=CI*AMA+EWP*AMB-BWP*AMC
 SAYR0=BR*AMA-CWM*AMC
 SAYI0=BI*AMA-CWP*AMC
 SCRO=SAVR1**2+SAVI1**2+SAXR1**2+SAXI1**2+SAYR1**2+SAYI1**2
 CROS1=SCRO+SAZR1**2+SAZI1**2
 CROS0=SAVR0**2+SAVI0**2+SAYR0**2+SAYI0**2
 TCROS=2.0*CROS1+CROS0
 SCROS=2.0*SCRO
 PRINT 519, U, SCROS, CROS1, CROS0, TCROS
 FORMAT(5F15.5)
 PRINT 521, QCB,SAZR1,SAZI1,SAVR0,SAVI0,SAYR0,SAYI0
 FORMAT(7E15.4)
 CONTINUE
 CONTINUE
 CONTINUE
 CONTINUE
 GO TO 139
 END
 FUNCTION FA4(X,U)
 COMMON P
 DEN=1.0/(P+X)
 V=  U*U/(4.0*(P+X))
 EVF=EXPF(-V)
 FA4=U**3*EVF*DEN**4/16.0
 RETURN
 END
 FUNCTION FA6(X,U)
 COMMON P
 DEN=1.0/(P+X)
 V=  U*U/(4.0*(P+X))
 EVF=EXPF(-V)
 FA6=U**3*EVF*DEN**5*0.25*(1.0-0.25*V)
 RETURN
 END
 FUNCTION FA8(X,U)
 COMMON P
 DEN=1.0/(P+X)
 V=  U*U/(4.0*(P+X))
 EVF=EXPF(-V)
 FA8=1.25*U**3*DEN**6*EVF*(1.0-0.5*V+0.05*V*V)
 RETURN
 END
 FUNCTION FB2(X,U)
 COMMON P
```

```
DEN=1.0/(P+X)
V=  U*U/(4.0*(P+X))
EVF=EXPF(-V)
FB2=U*EVF*DEN**2*0.25
RETURN
END
FUNCTION FB4(X,U)
COMMON P
DEN=1.0/(P+X)
V=  U*U/(4.0*(P+X))
EVF=EXPF(-V)
FB4=U*DEN**3*EVF*0.5*(1.0-0.5*V)
RETURN
END
FUNCTION FB6(X,U)
COMMON P
DEN=1.0/(P+X)
V=  U*U/(4.0*(P+X))
EVF=EXPF(-V)
FB6=1.5*U*DEN**4*EVF*(1.0-V+V*V/6.0)
RETURN
END
FUNCTION FB8(X,U)
COMMON P
DEN=1.0/(P+X)
V=  U*U/(4.0*(P+X))
EVF=EXPF(-V)
FB8=6.0*U*DEN**5*EVF*(1.0-1.5*V+0.5*V*V-V**3/24.0)
RETURN
END
FUNCTION T45(X,Y,U)
COMMON P
DEN=1.0/(P+X+Y)
V=U*U/(4.0*(P+X+Y))
EVF=EXPF(-V)
T45=U**4*EVF*DEN**5/32.0
RETURN
END
FUNCTION T47(X,Y,U)
COMMON P
DEN=1.0/(P+X+Y)
V=U*U/(4.0*(P+X+Y))
EVF=EXPF(-V)
T47=0.156*U**4*DEN**6*EVF*(1.0-0.2*V)
RETURN
END
FUNCTION T49(X,Y,U)
COMMON P
DEN=1.0/(P+X+Y)
V=U*U/(4.0*(P+X+Y))
EVF=EXPF(-V)
T49=0.94*U**4*DEN**7*EVF*(1.0-0.4*V+0.0333*V*V)
RETURN
END
FUNCTION T411(X,Y,U)
COMMON P
DEN=1.0/(P+X+Y)
```

```
 V=U*U/(4.0*(P+X+Y))
 EVF=EXPF(-V)
 T411=6.55*U** 4*DEN**8*EVF*(1.0-0.6*V+0.1*V*V-0.00476*V**3)
 RETURN
 END
 FUNCTION T25(X,Y,U)
 COMMON P
 DEN=1.0/(P+X+Y)
 V=U*U/(4.0*(P+X+Y))
 EVF=EXPF(-V)
 T25=0.375*U*U*DEN**4*EVF*(1.0-0.333*V   )
 RETURN
 END
 FUNCTION T27(X,Y,U)
 COMMON P
 DEN=1.0/(P+X+Y)
 V=U*U/(4.0*(P+X+Y))
 EVF=EXPF(-V)
 T27=1.5*U*U*DEN**5*EVF*(1.0-0.6667* V+0.0835*V*V)
 RETURN
 END
 FUNCTION T29(X,Y,U)
 COMMON P
 DEN=1.0/(P+X+Y)
 V=U*U/(4.0*(P+X+Y))
 EVF=EXPF(-V)
 T29=7.5*U*U*DEN**6*EVF*(1.0-V+0.25*V*V-0.016667*V**3)
 RETURN
 END
 FUNCTION T211(X,Y,U)
 COMMON P
 DEN=1.0/(P+X+Y)
 V=U*U/(4.0*(P+X+Y))
 EVF=EXPF(-V)
 T211=45.0*U*U*DEN**7*EVF*(1.0-1.333*V+0.5*V*V+0.00278*V**4
1-0.0667*V**3)
 RETURN
 END
 FUNCTION T23(X,Y,U)
 COMMON P
 DEN=1.0/(P+X+Y)
 V=U*U/(4.0*(P+X+Y))
 EVF=EXPF(-V)
 T23=0.125*U*U*DEN**3*EVF
 RETURN
 END
 FUNCTION T03(X,Y,U)
 COMMON P
 DEN=1.0/(P+X+Y)
 V=U*U/(4.0*(P+X+Y))
 EVF=EXPF(-V)
 T03=0.5*DEN**2 *EVF*(1.0-V)
 RETURN
 END
 FUNCTION T05(X,Y,U)
 COMMON P
 DEN=1.0/(P+X+Y)
```

```
V=U*U/(4.0*(P+X+Y))
EVF=EXPF(-V)
T05=EVF*DEN**3*(1.0-2.0*V+0.5*V*V)
RETURN
END
FUNCTION T07(X,Y,U)
COMMON P
DEN=1.0/(P+X+Y)
V=U*U/(4.0*(P+X+Y))
EVF=EXPF(-V)
T07      =3.0*DEN**4*EVF*(1.0-3.0*V+1.5*V*V-0.16667*V** 3)
RETURN
END
FUNCTION T09(X,Y,U)
COMMON P
DEN=1.0/(P+X+Y)
V=U*U/(4.0*(P+X+Y))
EVF=EXPF(-V)
T09=12.0*DEN**5*EVF*(1.0-4.0*V+3.0*V*V-0.6667*V**3+0.0417*V**4)
RETURN
END
FUNCTION T011(X,Y,U)
COMMON P
DEN=1.0/(P+X+Y)
V=U*U/(4.0*(P+X+Y))
EVF=EXPF(-V)
T011=60.0*DEN**6*EVF*(1.0-5.0*V+5.0*V*V-1.667*V**3+0.208*V**4
.-0.00832*V**5)
RETURN
END
END
```

0.192	0.288	0.382	0.479	0.572	0.665	0.760
0.940	1.03	1.12	1.200	1.290	1.38	1.450
1.620	1.690	1.770	1.840	1.910	1.980	2.040
2.160	2.220	2.280	2.330	2.380	2. 30	2.47
2.5550	2.580	2.620	2.640	2.670	2.690	

-.4523	-.0256	-.0029
-.4411	-.0505	-.0050
-.4228	-.0741	-.0055
-.3980	-.0957	-.0037
-.3672	-.1149	.0008
-.3314	-.1131	.0082
-.2915	-.1442	.0187
-.2485	-.1538	.032
-.2035	-.1598	.0479
-.1576	-.1623	.0657
-.1120	-.1613	.0851
-.0675	-.1570	.1054
-.0252	-.1498	.1262
-.0142	-.1399	.1470
.0498	-.1279	.1676
.0812	-.1135	.1877
.1078	-.0978	.2075
.1293	-.0810	.2271
.1454	-.0632	.2466
.1559	-.0448	.2663

.160
.159
.153
.141
.123
.09
.07
.03
-.0
-.0
-.0
-.1
-.2
-.2
-.3
-.3
-.4
-.4
-.53
-.07
-.07
-.06
-.06
-.05
-.05
-.0
-.0
-.0
-.0
-.0
-.
-.
-.
-.
-.2
-.2
-.24
-.26
-.27

58	.1608	-.0260	.2864		
04	.1599	-.0069	.3071		
73	.1533	.0121	.3284		
70	.1410	.0310	.3502		
01	.1230	.0498	.3722		
70	.0994	.0681	.3939		
85	.0704	.0858	.4147		
51	.0362	.1027	.4338		
74	-.0030	.1186	.4503		
56	-.0469	.1331	.4633		
00	-.09500	.1458	.4721		
04	-.1467	.1564	.4757		
63	-.2014	.1644	.4735		
70	-.2580	.1695	.4650		
13	-.3157	.1714	.4500		
76	-.3734	.1696	.4283		
42	-.4298	.1640	.4000		
91	-.4836	.1545	.3653		
00	-.5336	.1412	.3248		
28	-.0721	-1.005	-.0706	-1.519	-.0986
32	-.0704	-.9390	-.0646	-1.492	-.0954
38	-.0676	-.8339	-.0547	-1.447	-.0901
45	-.0640	-.6951	-.0414	-1.388	-.0828
50	-.0597	-.5299	-.0250	-1.317	-.0735
54	-.0548	-.3472	-.0061	-1.238	-.0623
53	-.0498	-.1562	.0146	-1.153	-.0495
47	-.0448	-.0341	.0366	-1.065	-.0351
34	-.0401	.2150	.0590	-.9772	-.0194
14	-.0360	.3794	0.0811	-.8908	-.0027
62	-.0326	.5216	.1023	-.8068	.0149
14	-.0302	.6376	.1217	-.7255	.0329
03	-.0288	.7254	.1389	-.6465	.0511
43	-.0286	.7850	.1531	-.5688	.0690
51	-.0297	.8178	.1639	-.4914	.0862
46	-.0319	.8266	.1709	-.4130	.1025
48	-.0352	.8151	.1737	-.3328	.1173
77	-.0396	.7874	.1721	-.2503	.1304
49	-.0450	.7478	.1661	-.1659	.1412
78	-.0511	.7004	.1554	-.0803	.1494
72	-.0580	.6486	.1402	.0049	.1548
36	-.0656	.5952	.1206	.0874	.1570
68	-.0737	.5421	.0966	.1646	.1557
62	-.0823	.4904	.0686	.2337	.1508
08	-.0915	.4407	.0368	.2921	.1422
94	-.1014	.3929	.0014	.3373	.1298
05	-.1118	.3465	-.0371	.3674	.1137
25	-.1231	.3009	-.0784	.3814	.0939
40	-.1351	.2555	-.1222	.3790	.0706
36	-.1481	.2100	-.1679	.3609	.0441
03	-.1620	.1641	-.2150	.3285	.0148
34	-.1769	.1181	-.2631	.2841	-.0168
26	-.1927	.7235	-.3115	.2304	-.0503
77	-.2092	.0275	-.3596	.1703	-.0849
92	-.2262	-.0157	-.4068	.1069	-.1201
78	-.2435	-0.563	-.4525	.0432	-.1551
42	-.2607	-.0937	-.4958	-.0182	-.1892
95	-.2774	-.1271	-.5361	-.0752	-.2215

-.2931	-.1562	-.5727	-.1262	-.2514
4.31				
-.11				
-11.58	349.2	-5.642	.5	.45
0.0	0.0	0.0	0.0	0.0
-.03459	-2.5859	-.26942	.2	.35
2.175	4.56	-2.85		
-2.57	-4.64	3.32		

APPENDIX VI

To evaluate J_2 and J_3 for the calculations involved in 40 MeV, we have used (26)

$$J_{n-1}(X) + J_{n+1}(X) = \frac{2n}{x} J_n(X) \qquad \text{(AVI.1)}$$

and for $-3 \leqslant X \leqslant 3$

$$J_o(X) = 1 - 2.2499997\left(\frac{x}{3}\right)^2 + 1.2656208\left(\frac{x}{3}\right)^4$$

$$- .3163866\left(\frac{x}{3}\right)^6 + .0444479\left(\frac{x}{3}\right)^8$$

$$- .0039444\left(\frac{x}{3}\right)^{10} + .00021\left(\frac{x}{3}\right)^{12} \qquad \text{(AVI.2)}$$

$$\frac{J_1(X)}{x} = \tfrac{1}{2} - .56549985\left(\frac{x}{3}\right)^2 + .21093573\left(\frac{x}{3}\right)^4$$

$$- .03954289\left(\frac{x}{3}\right)^6 + .00443319\left(\frac{x}{3}\right)^8$$

$$- .00031761\left(\frac{x}{3}\right)^{10} + .00001109\left(\frac{x}{3}\right)^{12} \qquad \text{(AVI.3)}$$

and for $3 \leqslant X < \infty$

$$J_o(X) = \frac{1}{\sqrt{x}} fo \cdot \operatorname{Cos} \theta_o$$

$$fo = .79788456 - .00000077\left(\frac{3}{x}\right) - .00552740\left(\frac{3}{x}\right)^2$$

$$- .00009512\left(\frac{3}{x}\right)^3 + .00137237\left(\frac{3}{x}\right)^4$$

$$- .00072805\left(\frac{3}{x}\right)^5 + .00014476\left(\frac{3}{x}\right)^6$$

$$\theta_o = x - .78539816 - .04166397\left(\frac{3}{x}\right)$$

$$- .00003954\left(\frac{3}{x}\right)^2 + .0026573\left(\frac{3}{x}\right)^3$$

$$-.00054125(\tfrac{3}{x})^4 - .00029333(\tfrac{3}{x})^5 + .00013558(\tfrac{3}{x})^6$$

(AVI.4)

$$J_1 = \frac{f_1}{\sqrt{x}} \cos\theta_1$$

$$f_1 = .79788456 + .00000156(\tfrac{3}{x}) + .01659667(\tfrac{3}{x})^2$$
$$+ .00017105(\tfrac{3}{x})^3 - .00249511(\tfrac{3}{x})^4$$
$$+ .00113653(\tfrac{3}{x})^5 - .0002033(\tfrac{3}{x})^6$$

$$\theta_1 = -2.35619449 + .2499612(\tfrac{3}{x})$$
$$+ .00005650(\tfrac{3}{x})^2 - .00637879(\tfrac{3}{x})^3$$
$$+ .00074348(\tfrac{3}{x})^4 + .00079824(\tfrac{3}{x})^5$$
$$- .00029166(\tfrac{3}{x})^6$$

(AVI.5)

One must be careful in using the above approximation for $X < n$ where n is the order of the Bessel functions as the round-off errors may become large. We have evaluated J_2 and J_3 and compared the results with the values of J_2 and J_3 listed in a standard table. (26) The discrepancies exist for the small values of X where J_2 and J_3 are very near zero. For these points, we have used the values of J_2 and J_3 listed in the tables.

APPENDIX VII

The program listed here calculates the cross-sections of 2^+, $T = 0$ at 4.4 MeV of C^{12} with the incident energy of 40 MeV. The effective form factors are read in by CA, CB, AL, AM. VR, VI, RHR and RHI are the real and imaginary parameters of the two-body potential (V_R, ρ , $V_I, \rho '$). The integral over the impact parameter b is carried out by Simpson's rule in the statements 14 and 27. The functions appearing in the integrands are stored as the sub-functions. GJ2M2 represents the result of the integration over ϕ and z of the effective form factor multiplied by $e^{-iq \cdot r}$ Y_{LM}^* when $M = 2$. GJ2MO has similar meaning for $M = 0$. TRIG x GAMCA represents the distortion while BES is the Bessel functions. The cross-section is given by CROS. This program was written for IBM-1620 at Duquesne University.

```
      DIMENSION SJM2(3,3),SJM0(3,3),   CAD(2),    CBD(2),AMD(2),
     1SAD(2) , SBD(2),BLD(2),BMD(2),ALD(2)
      COMMON  A,B,CA,CB,SA,SB,AL,AM,BL,BM
      READ4 , (CAD(N),N=1,2),(CBD(N),N=1,2),(SAD(N),N=1,2),(SBD(N),N=1,2)
4     FORMAT (8F10.6)
      READ  5 , (ALD(N),N=1,2),(AMD(N),N=1,2),(BLD(N),N=1,2),(BMD(N),N=1,2)
 5    FORMAT (8F10.6)
      READ 6 , VR,VI,RHR,RHI
6     FORMAT (4F10.5)
      EBA=EXPF(-.1)
      CFSQ=COSF(.0)
      SID=SINF(.0)
      SQR=SQRTF(4.0)
      A=-.225*5.52*.084
      B=.0
      Q=.0
      DO 711  L=1,14
      DO 611  K=1,2
      CA=CAD(K)
      CB=CBD(K)
      SA=SAD(K)
      SB=SBD(K)
      AL=ALD(K)
      AM=AMD(K)
      BL=BLD(K)
      BM=BMD(K)
      DO 601  I=1,2
      Z=.0
      DH=.4
      SJM2(I,K)=.0
0     X1=Z+DH
      X2=Z+2.*DH
4     SJM2(I,K)=(YI(Z,I,Q)+4.*YI(X1,I,Q)+YI(X2,I,Q) )*DH/3.+SJM2(I,K)
      Z=X2
      IF(Z-6.)   10,21,21
1     Z=.0
      DH=.4
      SJM0(I,K)=.0
 25   X1=Z+DH
      X2=Z+2.*DH
7     SJM0(I,K)=(YS(Z,I,Q)+4.0*YS(X1,I,Q)+YS(X2,I,Q))*DH/3.+SJM0(I,K)
      Z=X2
      IF(Z-6.)    25,30,30
30    CONTINUE
01    CONTINUE
11    CONTINUE
        SVR2=VR*RHR*SJM2(1,1)-VI*RHI*SJM2(2,2)
      SVR0=VR*RHR*SJM0(1,1)-VI*RHI*SJM0(2,2)
      SVI2=VR*RHR*SJM2(2,1)+VI*RHI*SJM2(1,2)
      SVI0=VR*RHR*SJM0(2,1)+VI*RHI*SJM0(1,2)
      CROS=.58*(.918)**2*(2.0*SVR2**2+SVI2**2*2.+SVR0**2+SVI0**2)
      PUNCH  52,  SJM2(1,1),SJM2(1,2),SJM2(2,1),SJM2(2,2)
52    FORMAT (4F20.6)
      PUNCH  53, SJM0(1,1),SJM0(1,2),SJM0(2,1),SJM0(2,2)
53    FORMAT (4F20.6)
```

```
  PUNCH 51, Q,CROS, SVR2,SVI2,SVR0,SVI0
  FORMAT(6E12.5)
1 Q=Q+.2
  CALL EXIT
  END
:AL,FRE,GAMCA,GJ2M0,GJ2M2,BEFI,BEZE
  FUNCTION YS(X,I,Q)
  R=X*Q
  IF(R-.00001)15,16,16
  BES=1.0
  GO TO 18
  BES=BEZE(R)
  CONTINUE
  FE=FRE(X)
  IF(I-1)21,21,23
  TRIG=COSF(FE)
  GO TO 31
  TRIG=SINF(FE)
  YS=-44.*TRIG*BES*GAMCA(X)*GJ2M0(X)
  RETURN
  END
  FUNCTION YI(X,I,Q)
  R=X*Q
  IF(R-.00001)15,16,16
  BES=.0
  GO TO 18
  BES=BEFI(R)*2./R-BEZE(R)
  CONTINUE
  FE=FRE(X)
  IF(I-1) 21,21,23
  TRIG=COSF(FE)
  GO TO 31
  TRIG=SINF(FE)
  CONTINUE
  YI=54.*TRIG*GAMCA(X)*X**3*BES*GJ2M2(X)
  RETURN
  END
  FUNCTION BEZE(X)
  S=X/3.0
  R=S**2
  V=1.0/S
  T=1.0/R
  IF(3.0-X) 15,15,20
  BEZE=1.0-2.2499997*R+1.2656208*R**2-.3163866*R**3+.0444479*R**4
 1-.0039444*R**5+.00021*R**6
  GO TO 22
  FZE=.79788456            -.0055274*T-.00009512*V*T+.00137237*T**2
 1-.00072805*T*T*V+.00014476*T**3 -.00000077*V
  ANG=X-.78539816-.04166397*V      +      .00262573*T*V
 1-.00054125*T**2 -.00029333*T*T*V+.00013558*T**3-.00003954*T
  BEZE=FZE*COSF(ANG)/SQRTF(X)
  CONTINUE
  RETURN
  END
  FUNCTION BEFI(X)
  S=X/3.0
  R=S*S
```

```
 V=1.0/S
 T=1.0/R
 IF(3.0-X) 15,15,20
 EFI=.5-.56249985*R+.21093573*R**2-.03954289*R**3+.00443319*R**4
1-.00031761*R**5+.00001109*R**6
 BEFI=X*EFI
 GO TO 21
 FI=.79788456          +.01659667*T+.00017105*V*T-.00249511*T**2
1+.00113653*T*T*V-.00020033*T**3+.00000156*V
 ANG=X-2.35619449            +.00005650*T-.00637879*V*T+
1.00074348*T*T+.00079824*V*T*T-.00029166*T**3 +.12499612*V
 BEFI= FI*COSF(ANG)/SQRTF(X)
 CONTINUE
 RETURN
 END
 FUNCTION GJ2M2(X)
 COMMON A,B,CA,CB,SA,SB,AL,AM,BL,BM
 Y=X*X
 GJ2M2=A*(CA*EXPF(-AL*Y)/SQRTF(AL)+CB*EXPF(-AM*Y)/SQRTF(AM) )
1+B*(SA*EXPF(-BL*Y)/SQRTF(BL)+SB*EXPF(-BM*Y)/SQRTF(BM))
 RETURN
 END
 FUNCTION GJ2M0(X)
 COMMON A,B,CA,CB,SA,SB,AL,AM,BL,BM
 Y=X*X
 GJ2M0=A*(CA*EXPF(-AL*Y)*(X-Y*X*AL)/(AL*SQRTF(AL) )
1+CB*EXPF(-AM*Y)*(X-Y*X*AM)/(AM*SQRTF(AM)))
2+B*(SA*EXPF(-BL*Y)*(X-Y*X*BL )/(BL*SQRTF(BL))
3+SB*EXPF(-BM*Y)*(X-Y*X*BM)/(BM*SQRTF(BM)))
 RETURN
 END
 FUNCTION FRE(D)
 CM=.129144
 CN=-.003138
 DM=-.0316928
 DN=-.004752
 A=.12
 B=.51
 F21=(CM+CN*D*D)*EXPF(-A*D*D)+(DM+DN*D*D)*EXPF(-B*D*D)
 FRE=34.5*F21
 RETURN
 END
 FUNCTION GAMCA(X)
 CM=1.00094
 CN=-.0153128
 DM=-.579689
 DN=-.05035
 A=.12
 B=.29
 GAMCA=1.0-(CM+CN*X*X)*EXPF(-A*X*X)-(DM+DN*X*X)*EXPF(-B*X*X)
 RETURN
 END
15518  -.0755   -.057468   -.01687   .34524   .22570   -.73135   -.34119
       .34      .2         .2        .57      .60      .19       .215
97     -.46     1.1        1.6
```

LIST OF REFERENCES

1. A. Kerman, H. McManus, and R.M. Thaler. Ann. Phys. 8, 551, (1959).

2. E. Squires. Nuclear Physics 6, 504, (1958).

3. E. Sanderson. Nuclear Physics 35, 557, (1962).

4. D. Jackson. Nuclear Physics 35, 194, (1962).

5. T. Erickson. Nuclear Physics 55, 497, (1964).

6. X. DeBourd, J. Fos, B. Geofferson, N. Marty, C. Rolland, and B. Tatischeff. Le J. De Physique 24, 1059, (1963).

7. J. Jacmart, J. Garron, R. Riou, and C. Ruhla. "Proceedings at the Conference on Direct Interactions and Nuclear Reaction Mechanism," Padua, 1962. (Gordon and Breach Science Publishers, New York, 1093, (1963).

8. D. Hasselgren, P. Renberg, O. Sunberg, and G. Tibell. Nuclear Physics 69, 81, (1965).

9. P. Roos, Massachusetts Institute of Technology Theses, Unpublished, (1964).

10. G. Satchler, and R. Haybron. Physics Letters 11, 313, (1964).

11. V. Gillet, and N. Vinh-Mau. Nuclear Physics 54, 321, (1964). V. Gillet and E. Sanderson. Nuclear Physics 54, 472, (1964).

12. G.P. McCauley and G.E. Brown. Proceedings Royal Society, 71, 893, (1958).

13. R.J. Glauber. Lectures in Theoretical Physics Vol. 1, Interscience Publishers Co., New York, 315, (1959).

14. D. Jackon. Nuclear Spectroscopy with Direct Reactions II. Unpublished, Argonne National Lab. (1964).

15. M. Goldberger and K. Watson. Collision Theory, John Wiley Co., New York, (1964).

16. G. Brown. The Unified Theory of Nuclear Models. John Wiley Co., New York, 38, (1964).

17. D. Brink and G. Satchler. Nuovo Cimento 4, 549, (1959).

18. D. Brink and G. Satchler. Angular Momentum, Oxford University Press, London, 43, (1962).

19. R. Haybron and H. McManus. Preprint.

20. P. Morse and H. Feshbach. Methods of Theoretical Physics II, 1321, McGraw Hill Co., New York.

21. See any Mathematical Tables, for example, Standard Mathematical Tables, 11th Ed. Chemical Rubber Co., Cleveland. 1957.

22. G. Watson. Theory of the Bessel Functions, Cambridge University Press, 394, 2nd ed.

23. L.R.B. Elton and D. Jackon. Nuclear Physics 35, 209, (1962).

24. M. Fricke and G. Satchler. Phys. Rev. 139, 567, (1965).

25. A. Messiah. Quantum Mechanics I, North Holland Pub. Co., Amsterdam, (1964).

26. F.W.J. Olver. Bessel Functions of Integer Order, Handbook of Mathematical Functions. National Bureau of Standards, 355.

27. P. Hillman, A. Johanson and H. Tyren. Nuclear Physics 4, 648, (1957).

28. M. Perrain, and N. Vinh-Mau. Physics Letters 14, 236, (1965).

29. Preliminary data from Minnesota group, private communications to Hugh McManus, Professor, Michigan State University.

30. L. Elton, R. Shaw, and A. Swift. P.L.A. Progress Report, Rutherford High Energy Lab., Harwell, (1963).

31. Th. A.J. Maris and H. Tyren. Nuclear Physics 4, 662, (1957).

32. R. Alphone, A. Johansson, and G. Tibell. Nuclear Physics 4, 672.

33. M.G. Mayer, and J. Jenson. Elementary Theory of Nuclear Shell Structure. John Wiley, New York, 236, (1955).

34. V. Gillet and M. Melkanoff. Phy. Rev. 133, 1190, (1964).

35. H. McManus and D. Slanina, private communications.

36. Marty, Private communications to Hugh McManus, Professor, Michigan State University.

37. Hooton, D.J. and Ascheroft, N.W. Proceedings Physics Society, 81, 193, (1963).

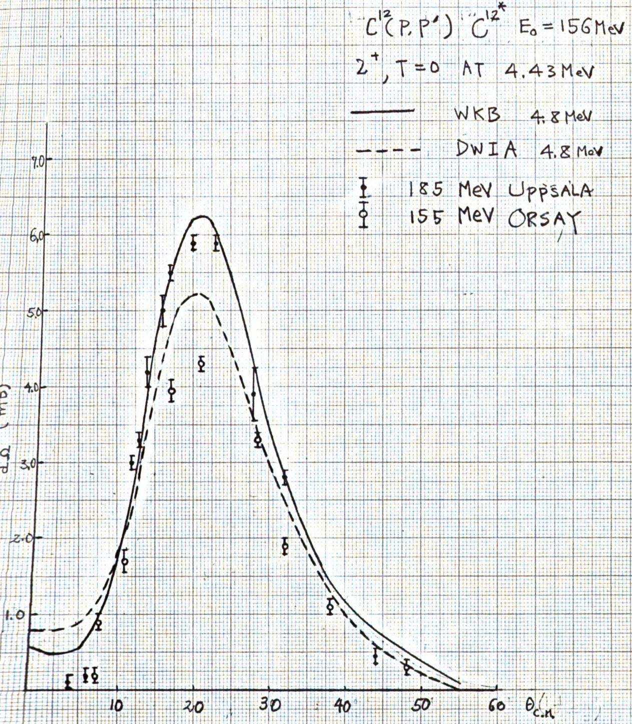

$C^{12}(P,P')C^{12*}$ $E_0 = 156$ MeV
2^+, T=0 AT 4.43 MeV
WKB 4.8 MeV
DWIA 4.8 MeV
185 MeV UPPSALA
155 MeV ORSAY
7.0
6.0
5.0
4.0
3.0
2.0
1.0
10
20
30
40
50
60
$\theta_{c.m.}$

FIG. 1

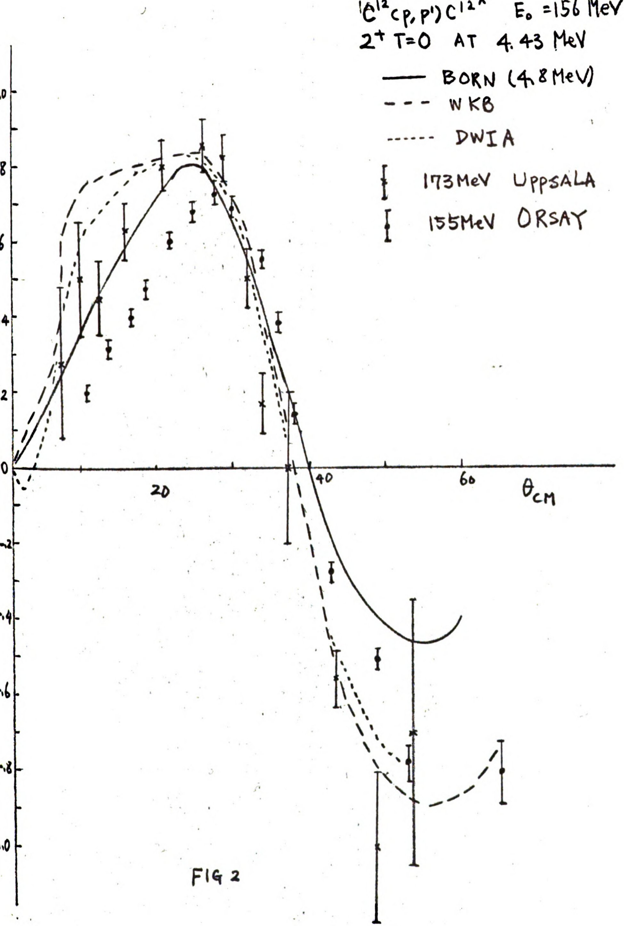
$C^{12}(p,p')C^{12*}$ $E_0 = 156$ MeV
2^+ T=0 AT 4.43 MeV
BORN (4.8 MeV)
WKB
DWIA
173MeV UPPSALA
155MeV ORSAY
20
40
60
θ_{CM}

FIG 2

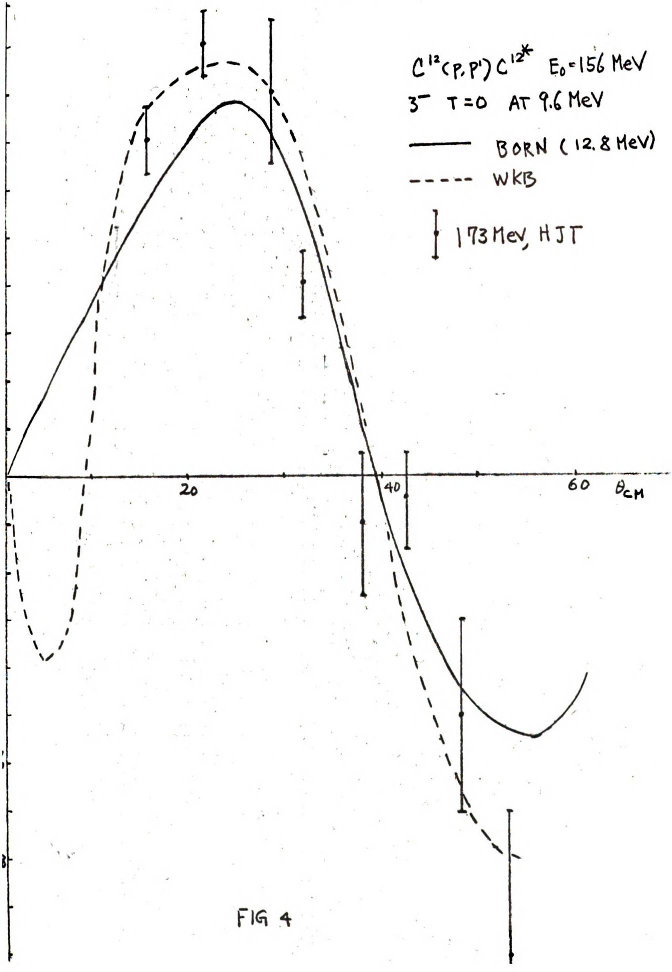

$C^{12}(p,p')C^{12*}$ $E_0 = 156$ MeV
3^- T=0 AT 9.6 MeV
BORN (12.8 MeV)
WKB
173 MeV, HJT
20
40
60
θ_{CM}

FIG 4

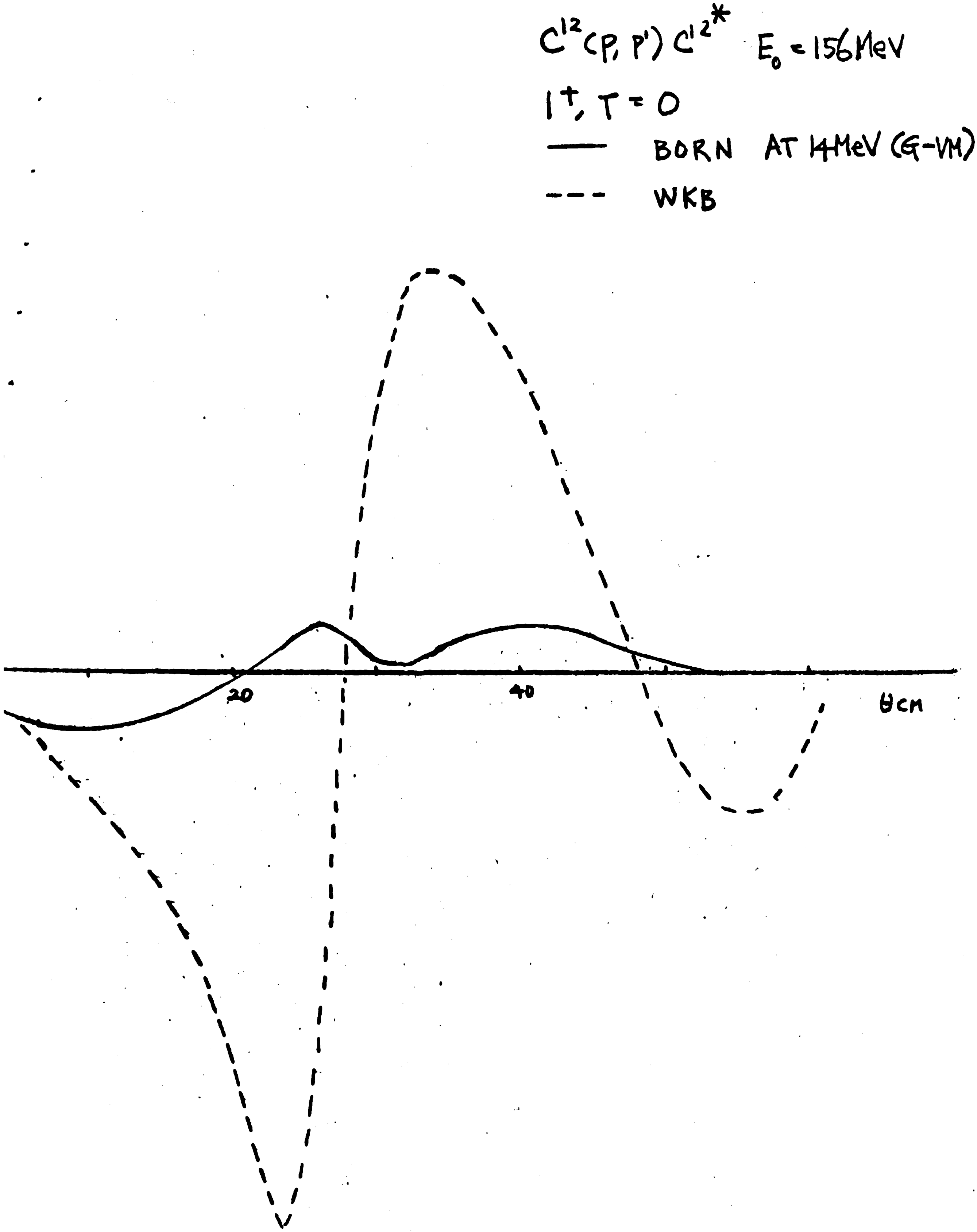

FIG 6

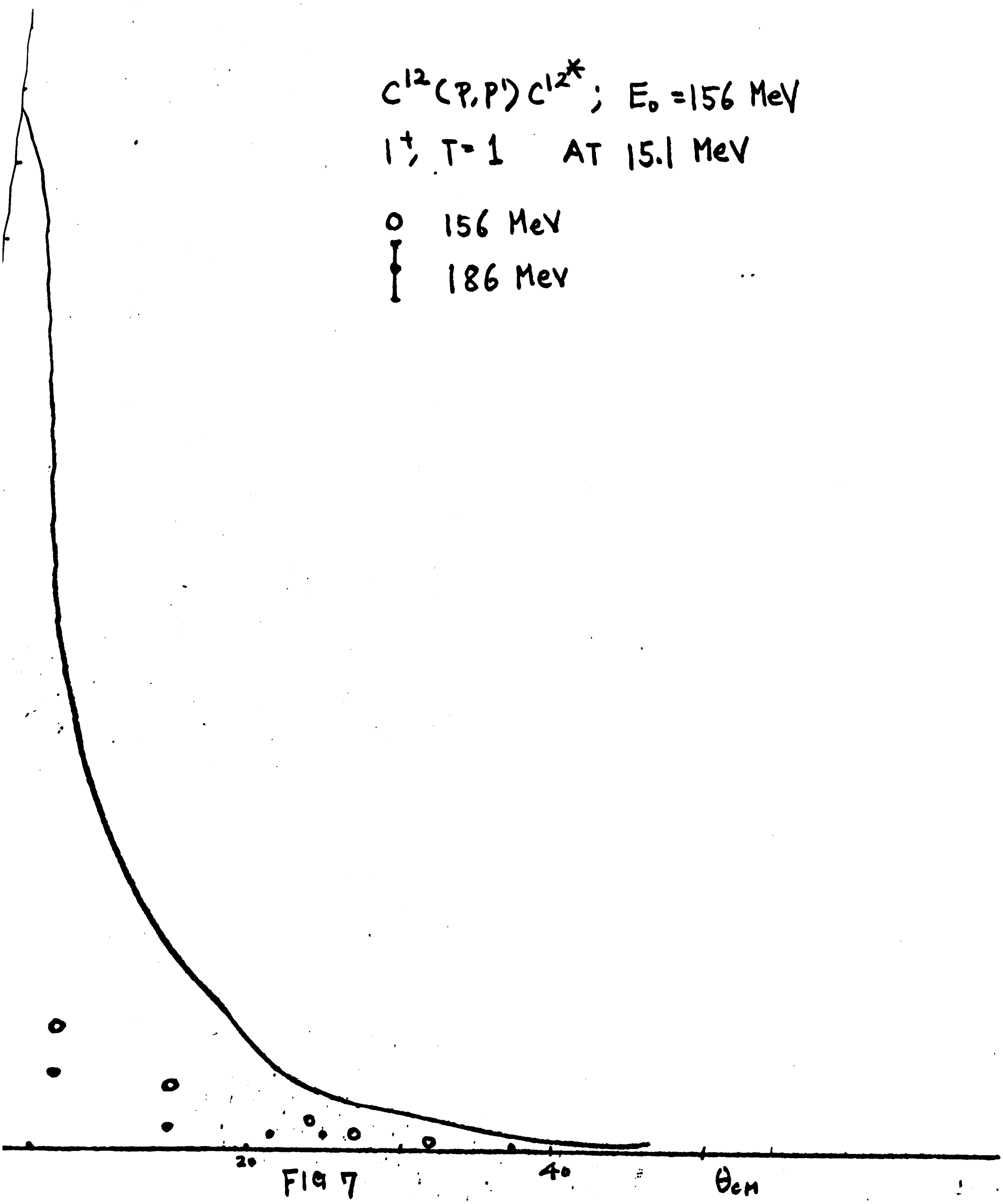
$C^{12}(p,p')C^{12*}$; E_0 = 156 MeV
1^+, T = 1 AT 15.1 MeV
o 156 MeV
186 MeV
20
40
θ_{cm}

FIG 7

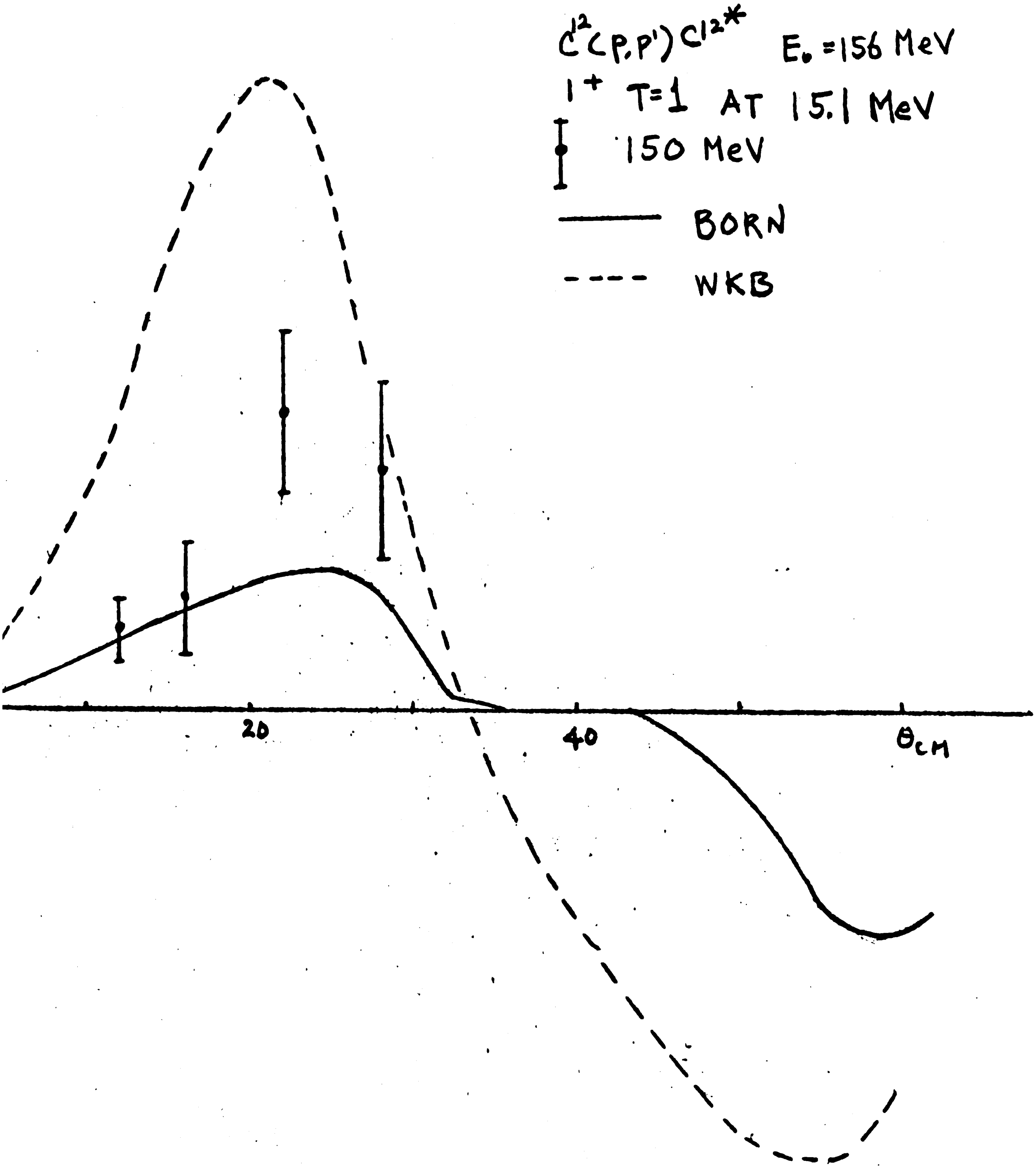
$C^{12}(p,p')C^{12*}$ $E_0 = 156$ MeV
1^+ T=1 AT 15.1 MeV
150 MeV
BORN
WKB
20
40
θ_{CM}

FIG 8

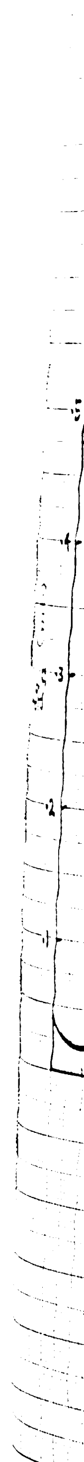

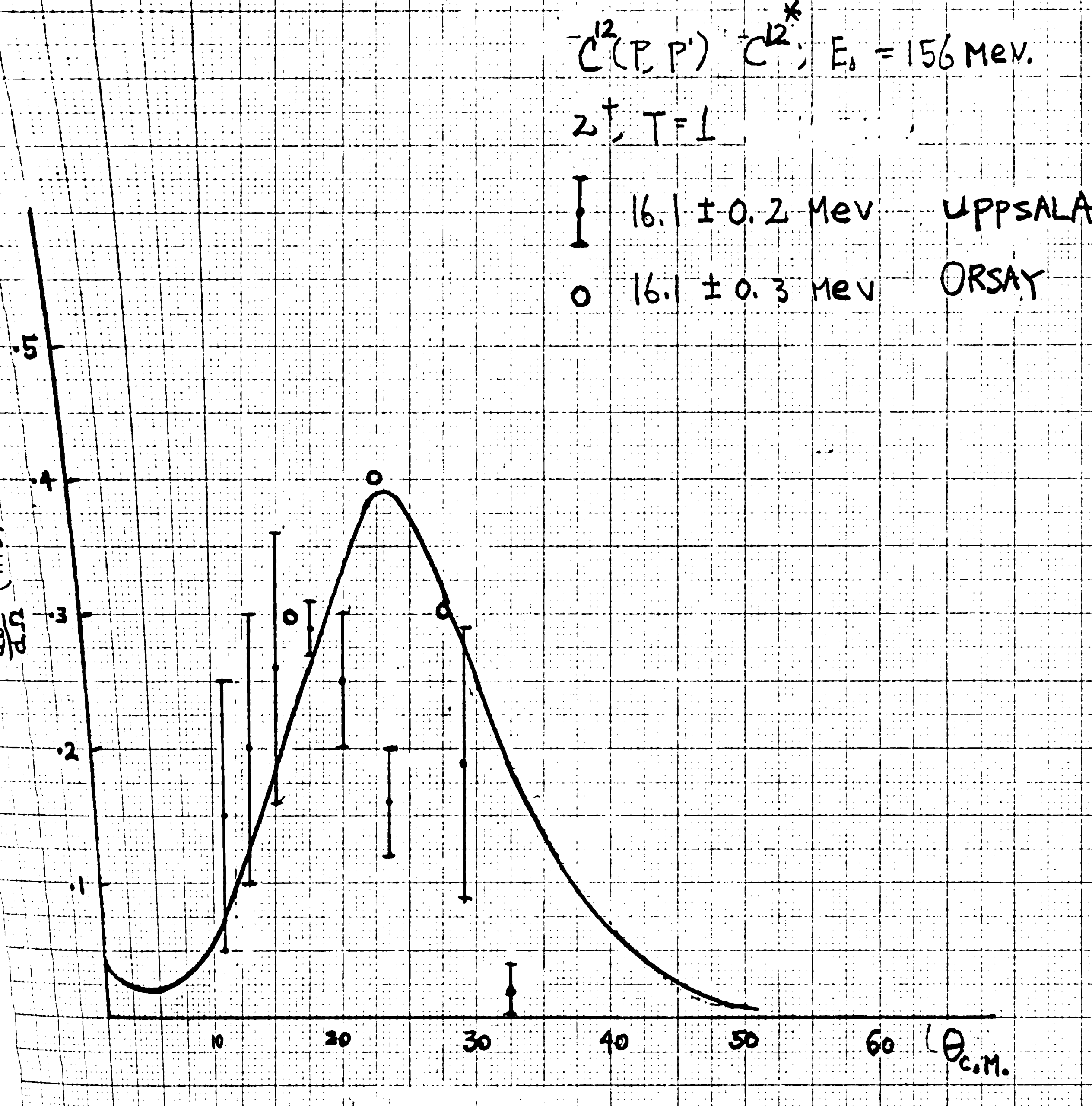
$C^{12}(P, P')\ C^{12*}$; $E_0 = 156$ Mev.
2^+, $T = 1$
16.1 ± 0.2 Mev UPPSALA
16.1 ± 0.3 Mev ORSAY
.5
.4
.3
.2
.1
10
20
30
40
50
60
$\theta_{C.M.}$

FIG 9

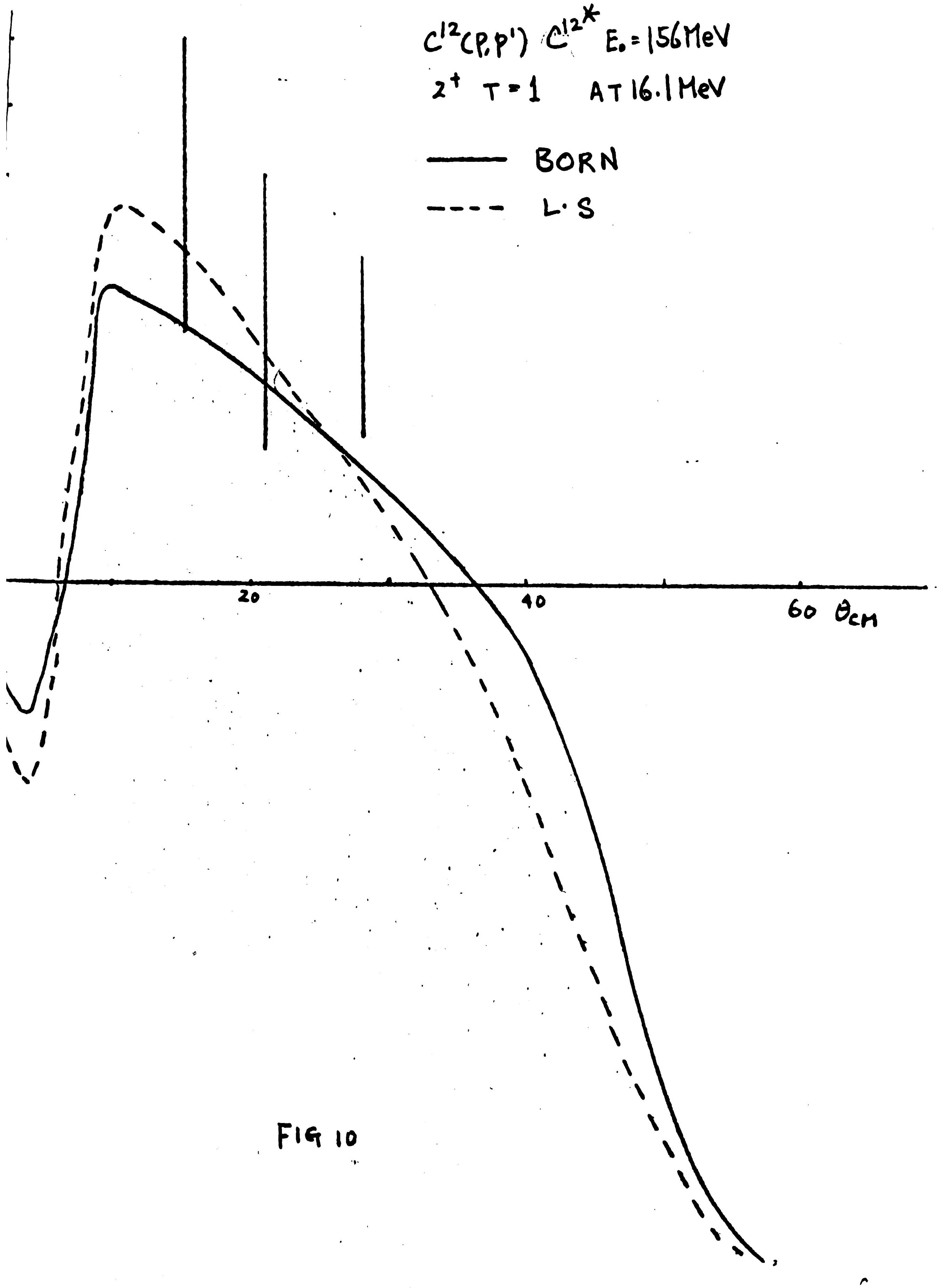

FIG 10

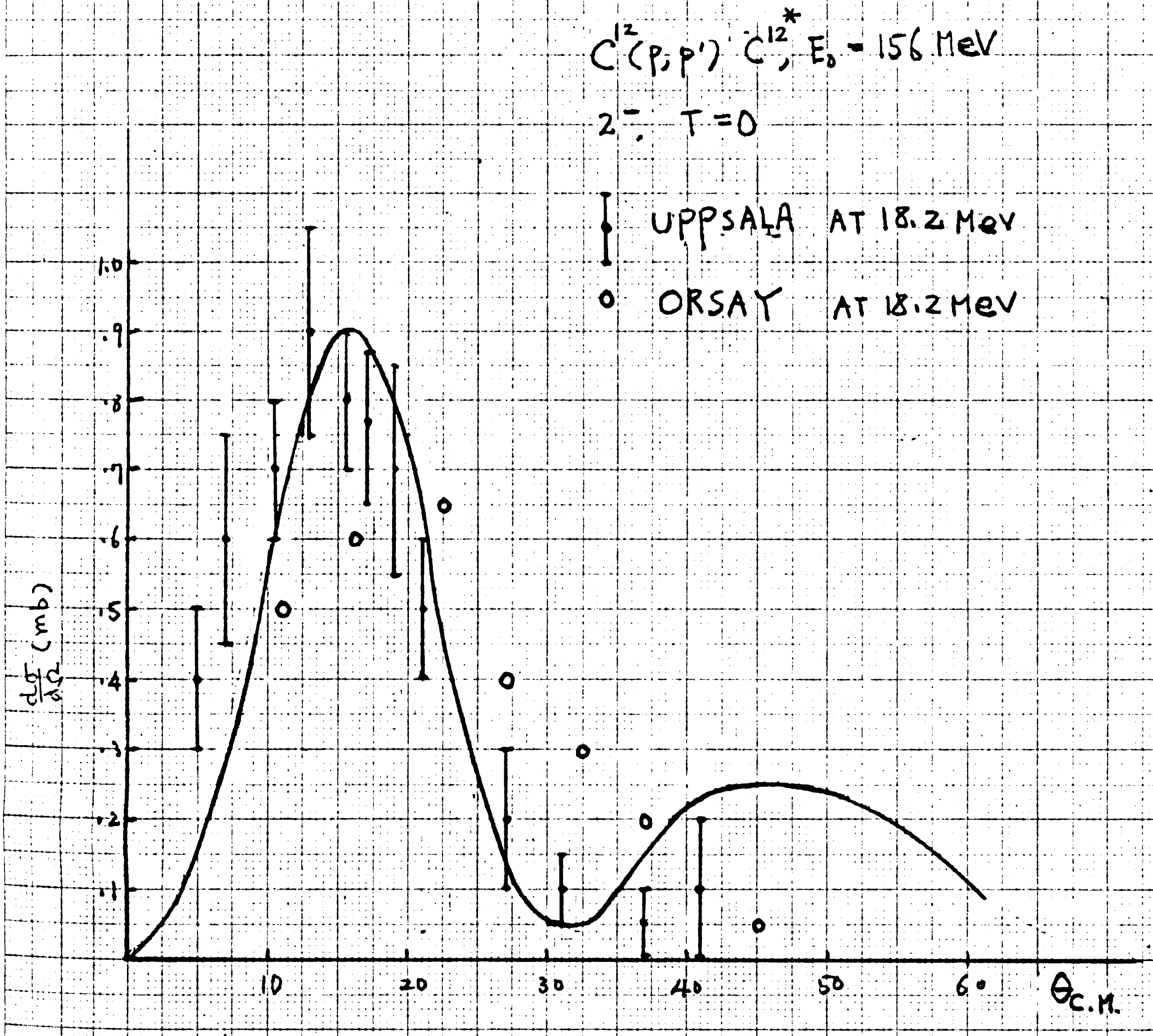
$C^{12}(p,p')C^{12*}$, $E_0 = 156$ MeV
2^-, T=0
UPPSALA AT 18.2 MeV
ORSAY AT 18.2 MeV
$\frac{d\sigma}{d\Omega}$ (mb)
1.0
.9
.8
.7
.6
.5
.4
.3
.2
.1
10
20
30
40
50
60
$\theta_{C.M.}$

FIG 11

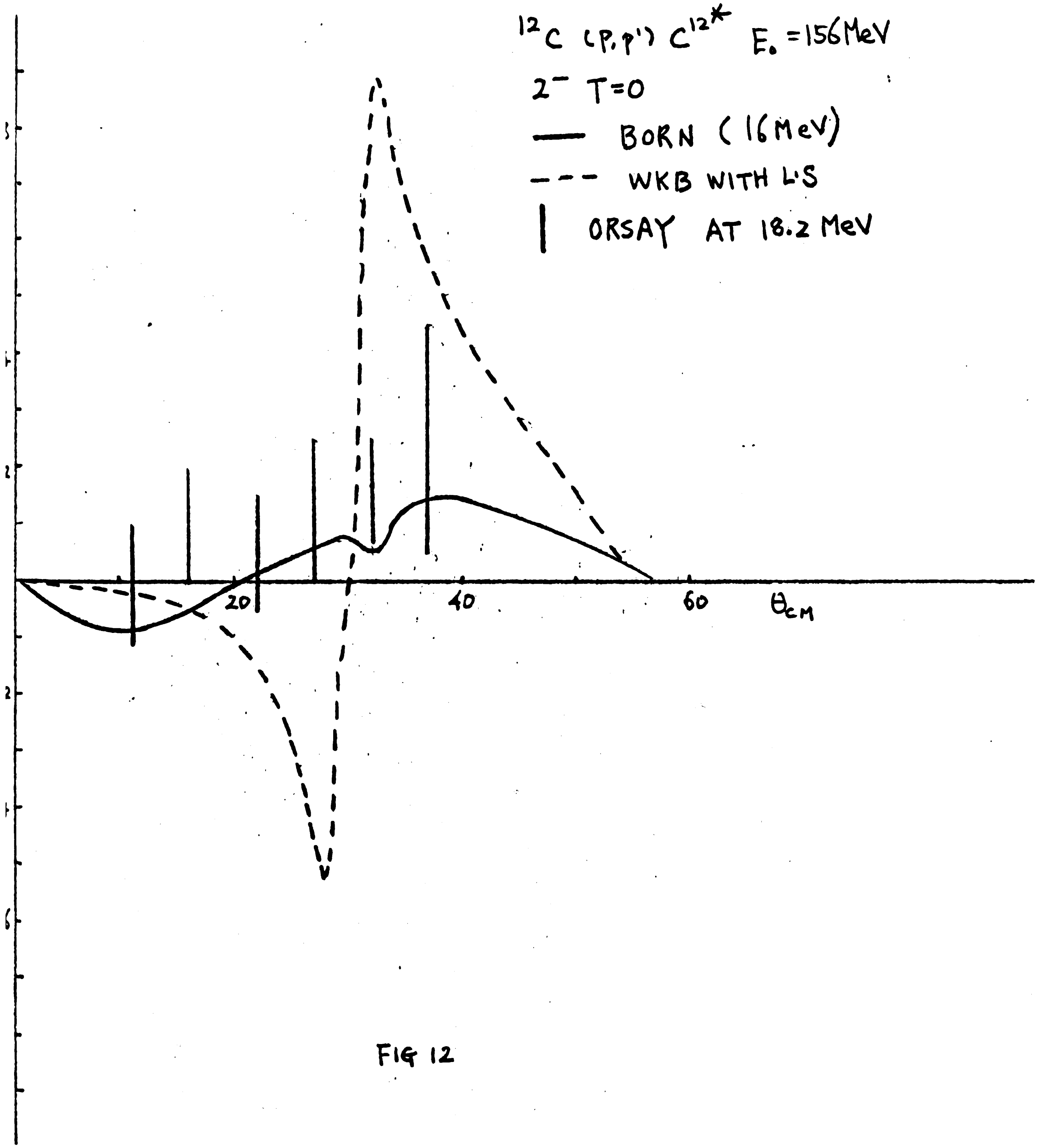

$^{12}C\ (p,p')\ C^{12*}$ $E_0 = 156$ MeV
2^- T=0
BORN (16 MeV)
WKB WITH L·S
ORSAY AT 18.2 MeV
20
40
60
θ_{CM}

FIG 12

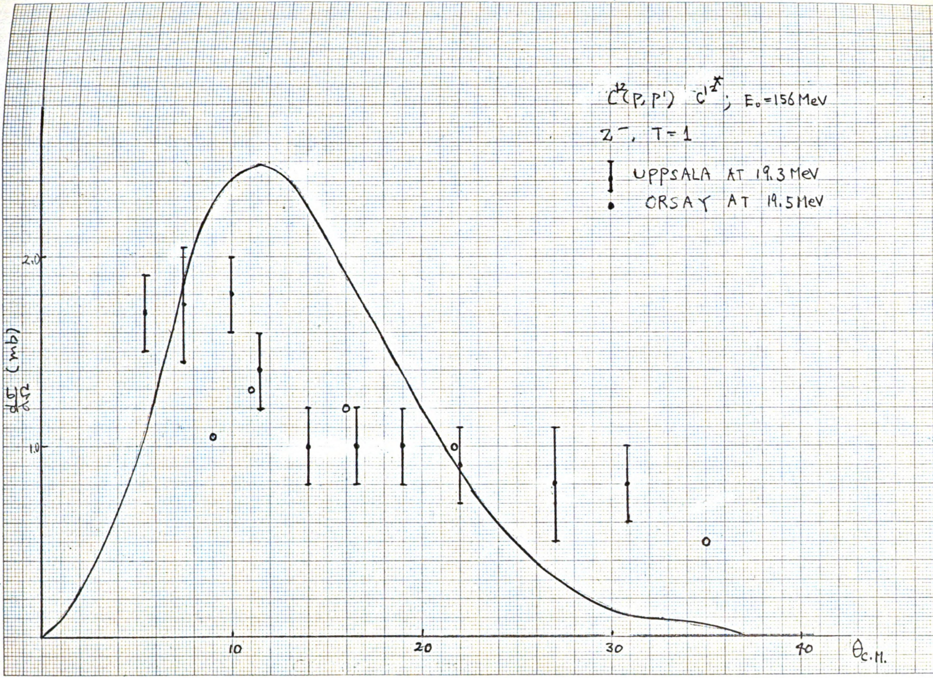
$C^{12}(p,p')\ C^{12*}$; $E_0 = 156$ MeV
2^-, $T=1$
UPPSALA AT 19.3 MeV
ORSAY AT 19.5 MeV
$\frac{d\sigma}{d\Omega}$ (mb)
2.0
1.0
10
20
30
40
$\theta_{C.M.}$

FIG 13

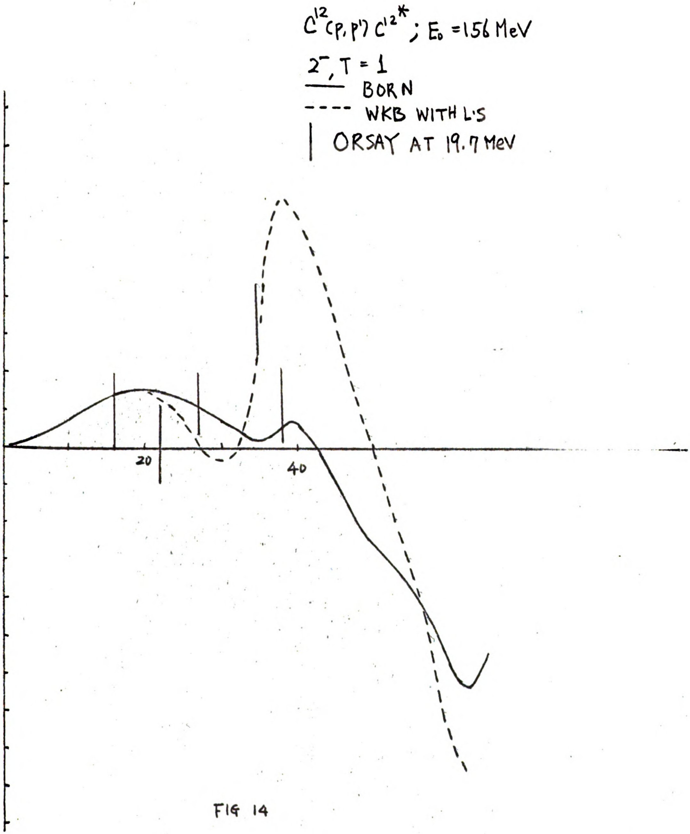

FIG 14

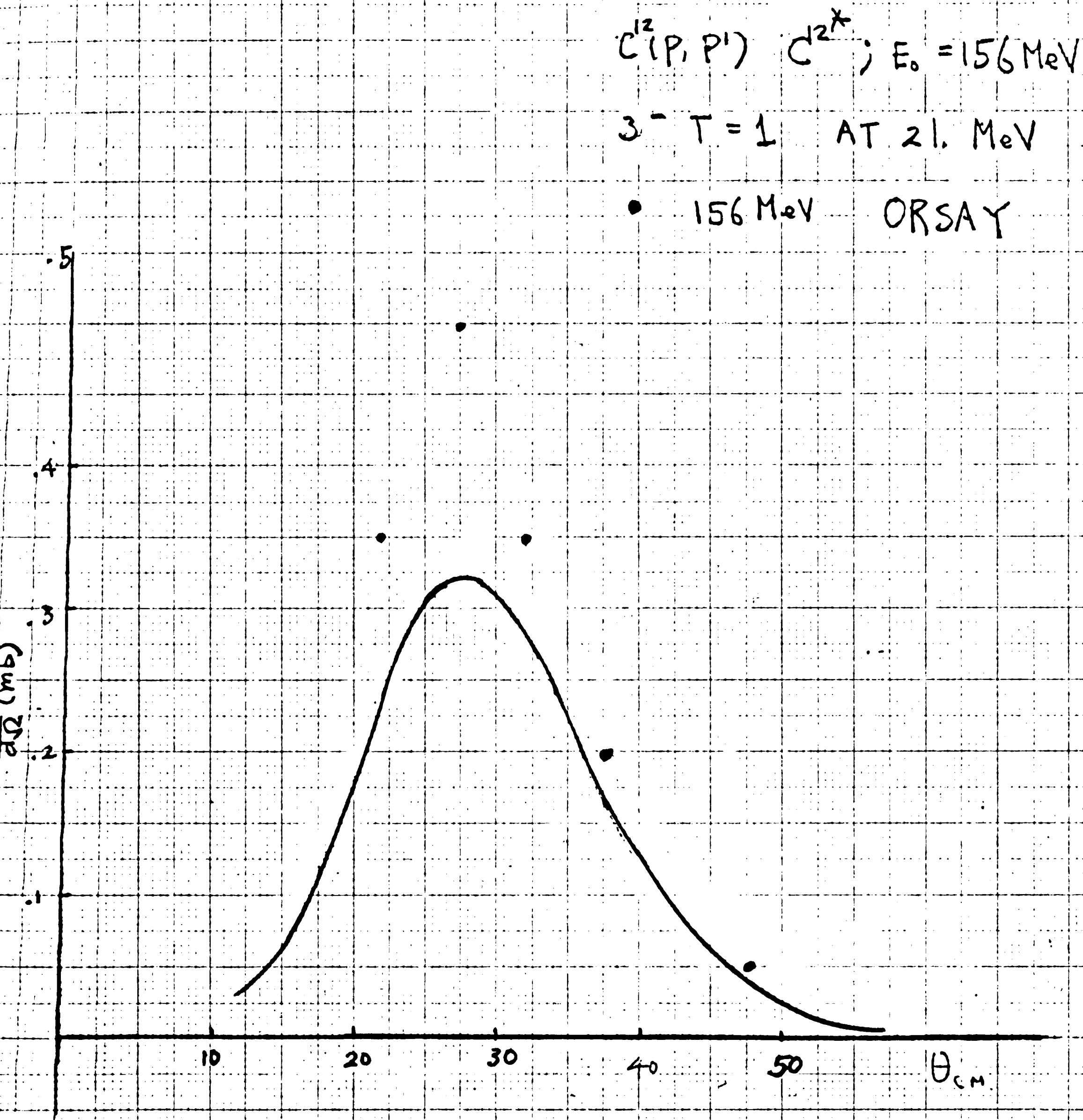

C¹²(P, P') C¹²*; E₀ = 156 MeV
3⁻ T = 1 AT 21. MeV
156 MeV ORSAY
.5
.4
.3
.2
.1
dσ/dΩ (mb)
10
20
30
40
50
θ_CM

FIG 15

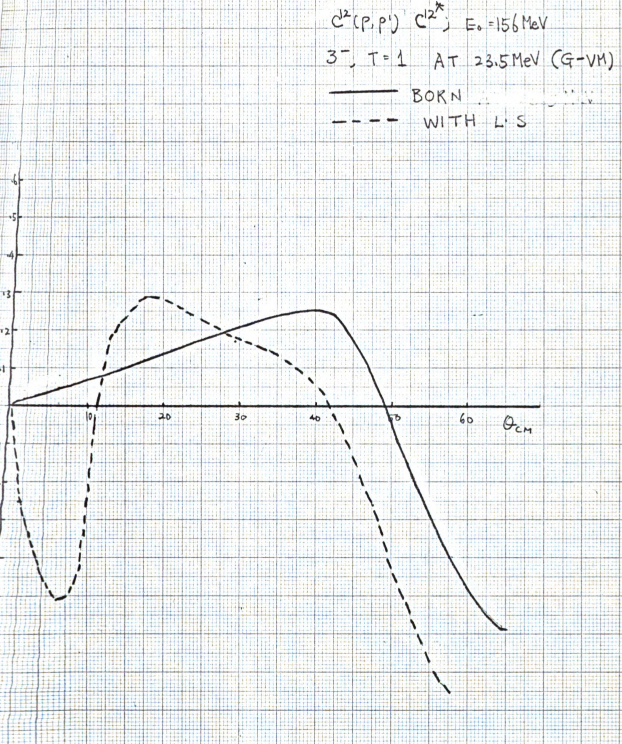

$C^{12}(p,p')\,C^{12*}$; $E_0 = 156$ MeV
3^-, T = 1 AT 23.5 MeV (G-VM)
BORN
WITH L·S
.6
.5
.4
.3
.2
.1
10
20
30
40
50
60
θ_{CM}

FIG 16

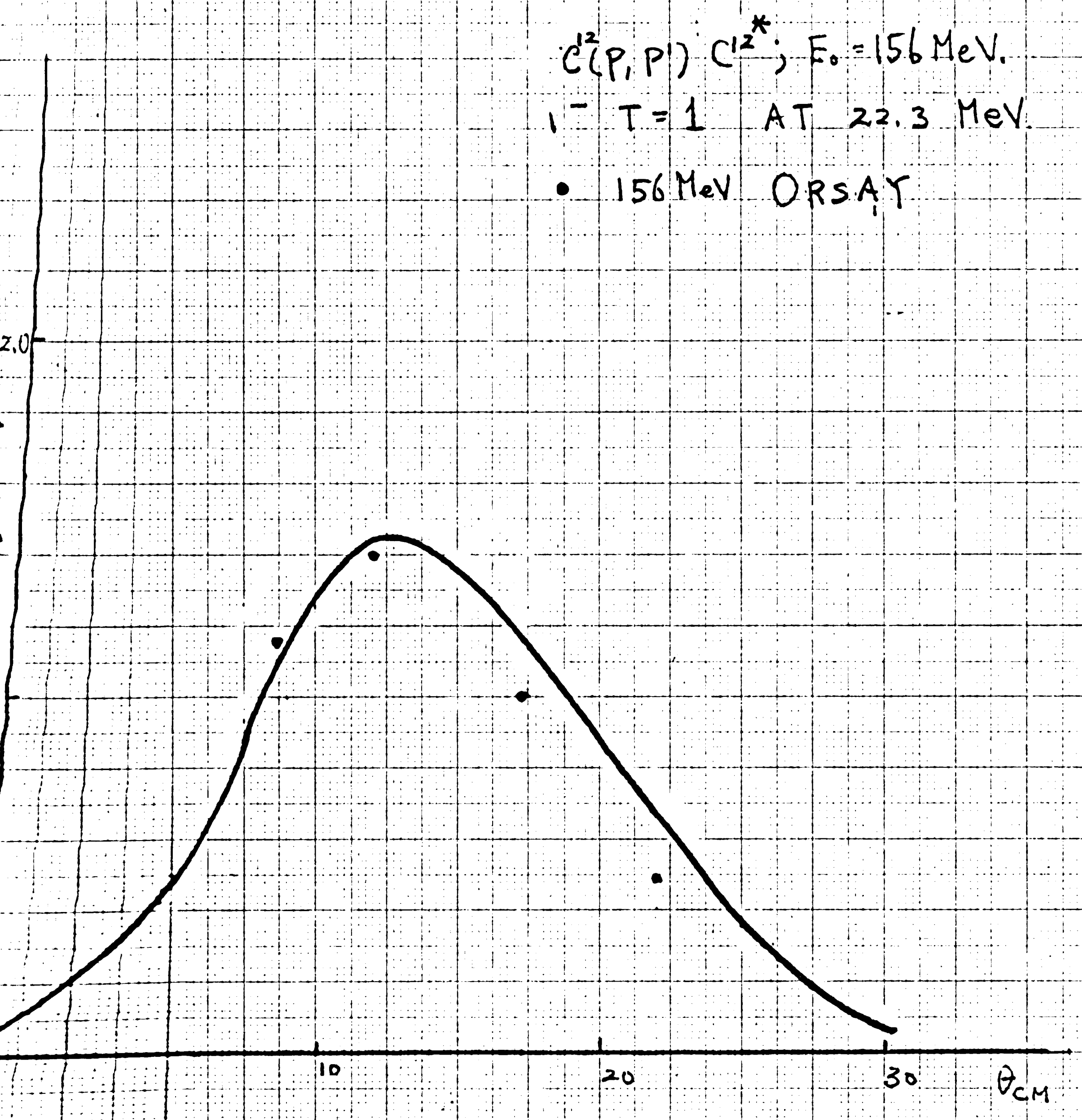

$C^{12}(P,P')C^{12*}$; E_0 = 156 MeV.
1^- T = 1 AT 22.3 MeV
• 156 MeV ORSAY
2.0
10
20
30
θ_{CM}

FIG 17

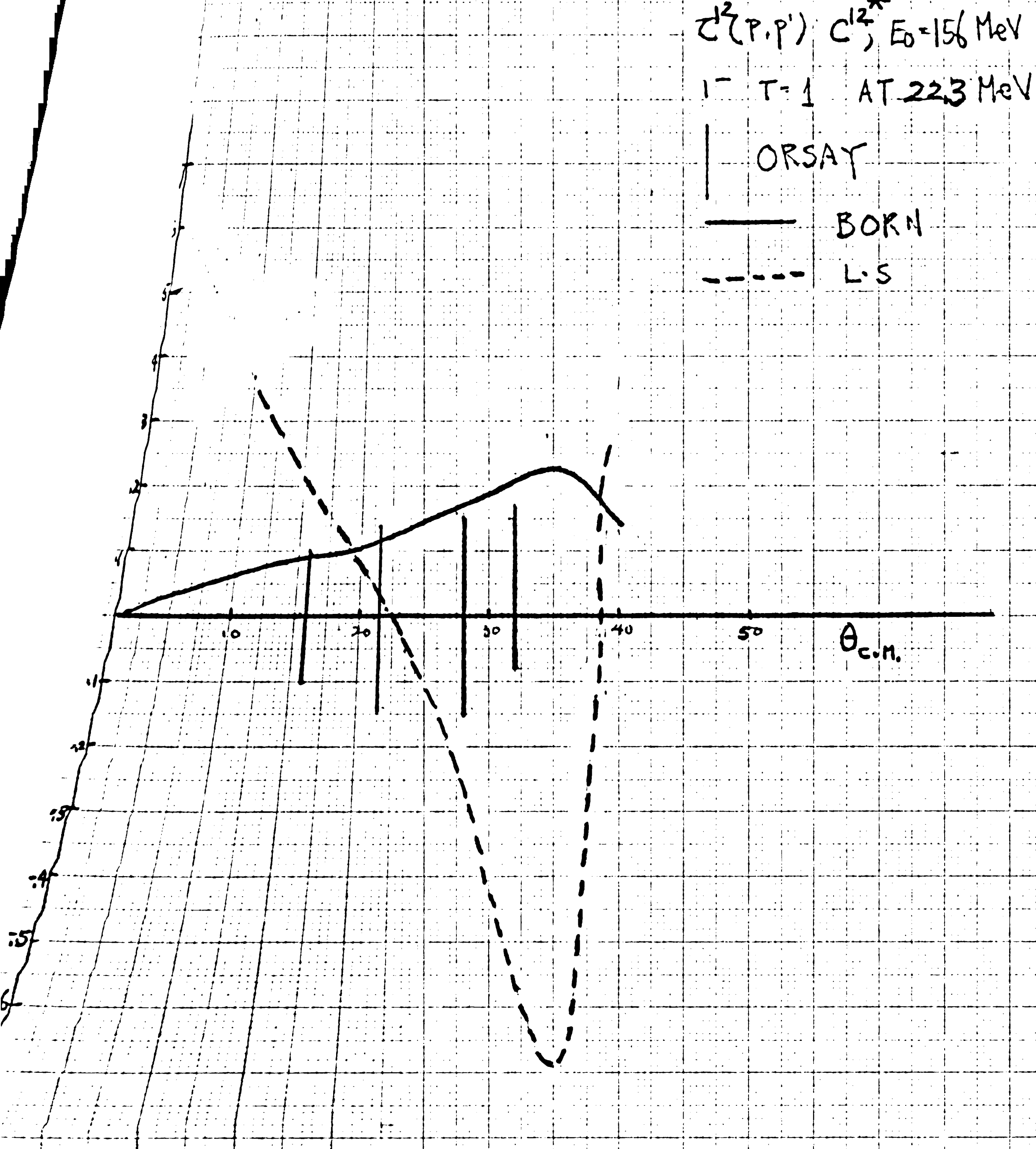
C12(P,P') C12*, E0=156 MeV
1- T=1 AT 22.3 MeV
ORSAY
BORN
L.S
10
20
30
40
50
θc.m.
.1
.2
.3
.4
.5
.6
-.1
-.2
-.3
-.4
-.5
-.6

FIG 18

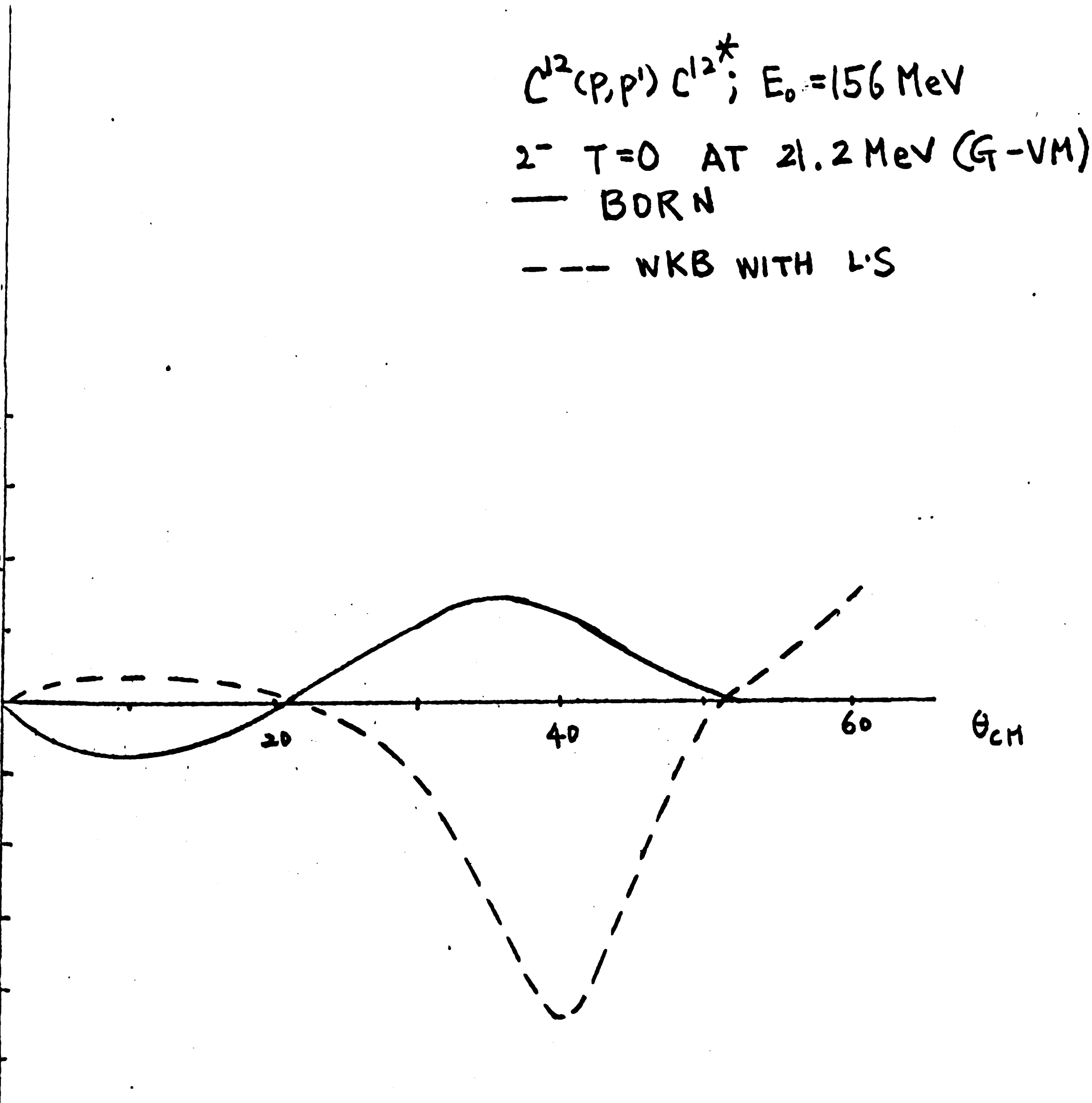
$C^{12}(p,p')C^{12*}$; E_0 =156 MeV
2^- T=0 AT 21.2 MeV (G-VM)
— BORN
--- WKB WITH L·S
20
40
60
θ_{CM}

FIG 20

Fig 20

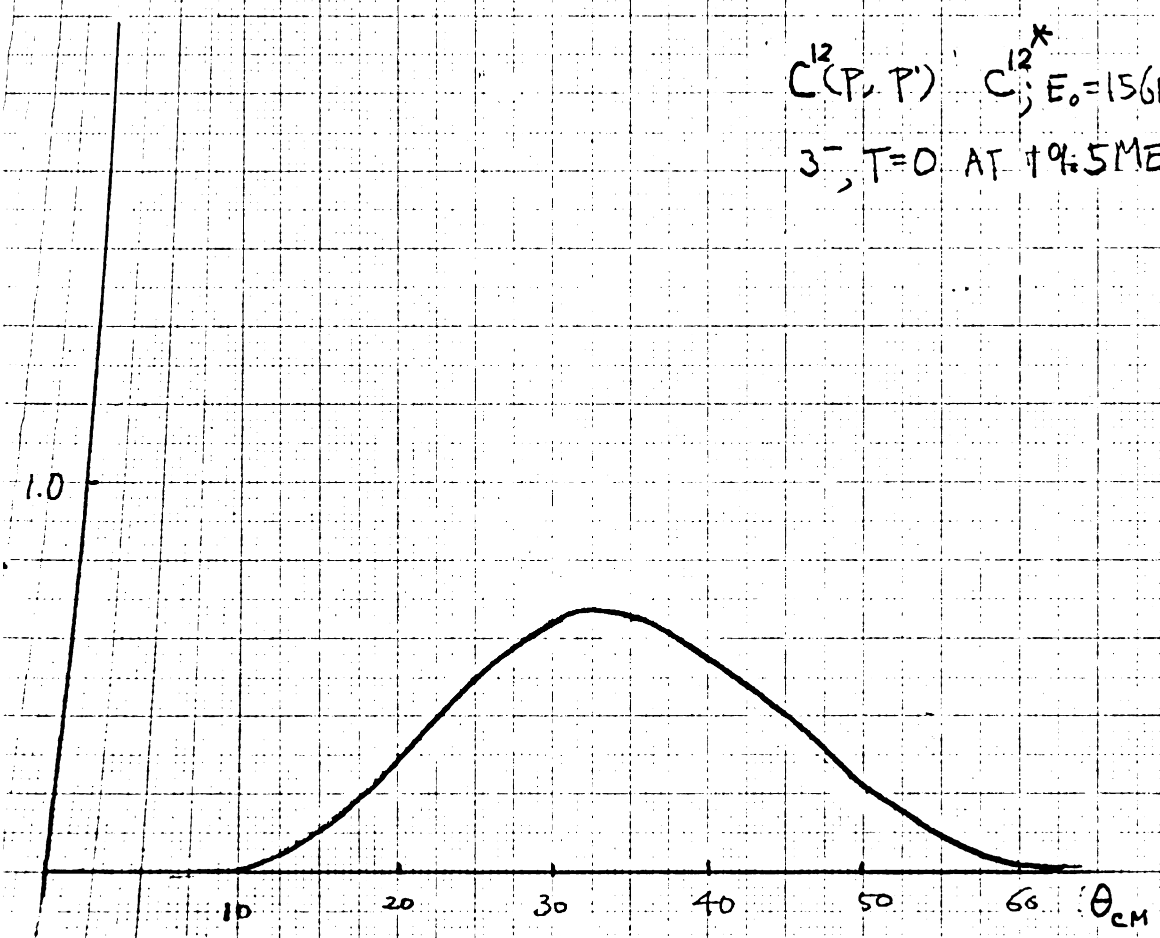

FIG 21

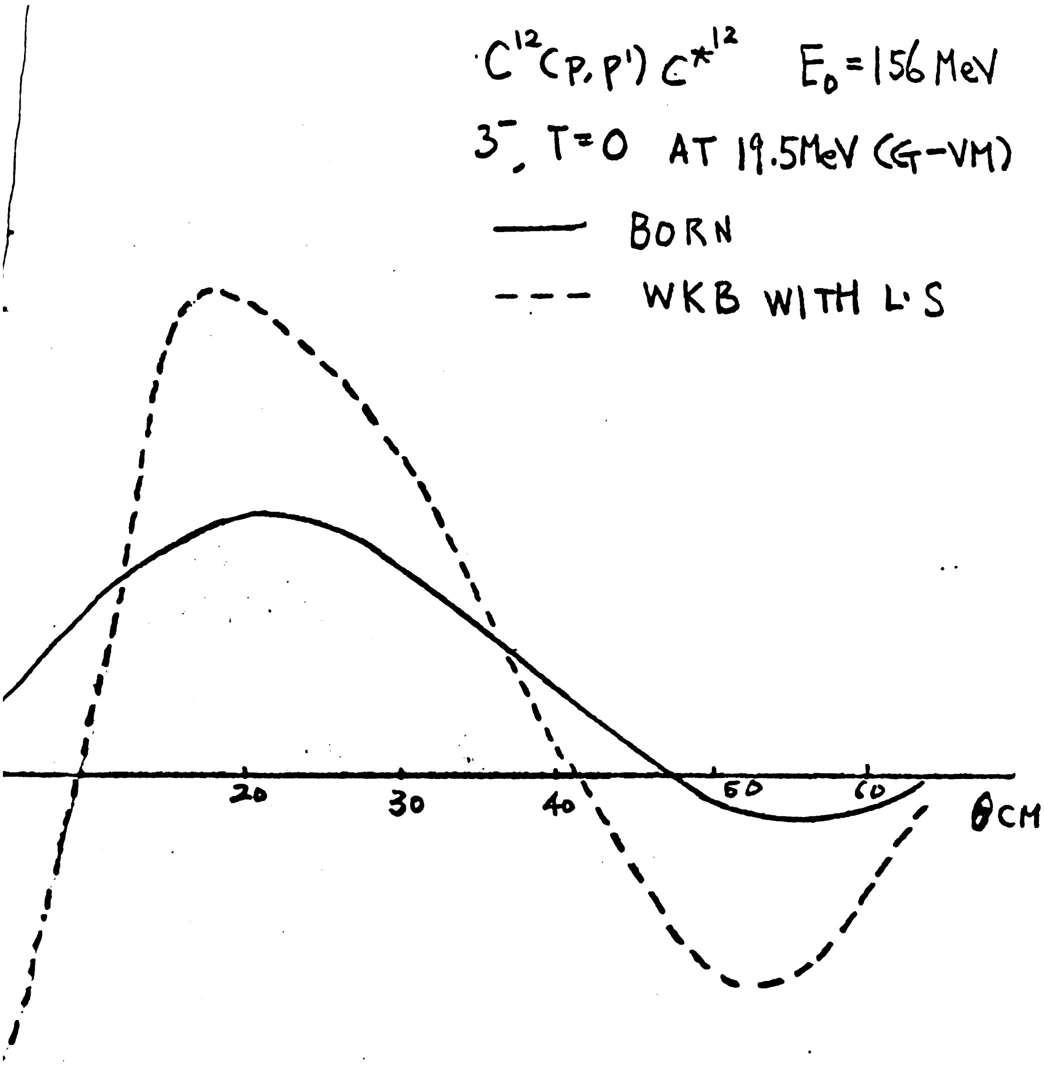

$C^{12}(p,p')C^{*12}$ $E_0=156$ MeV
3^-, T=0 AT 19.5MeV (G-VM)
BORN
WKB WITH L·S
20
30
40
50
60
θCM

FIG 22

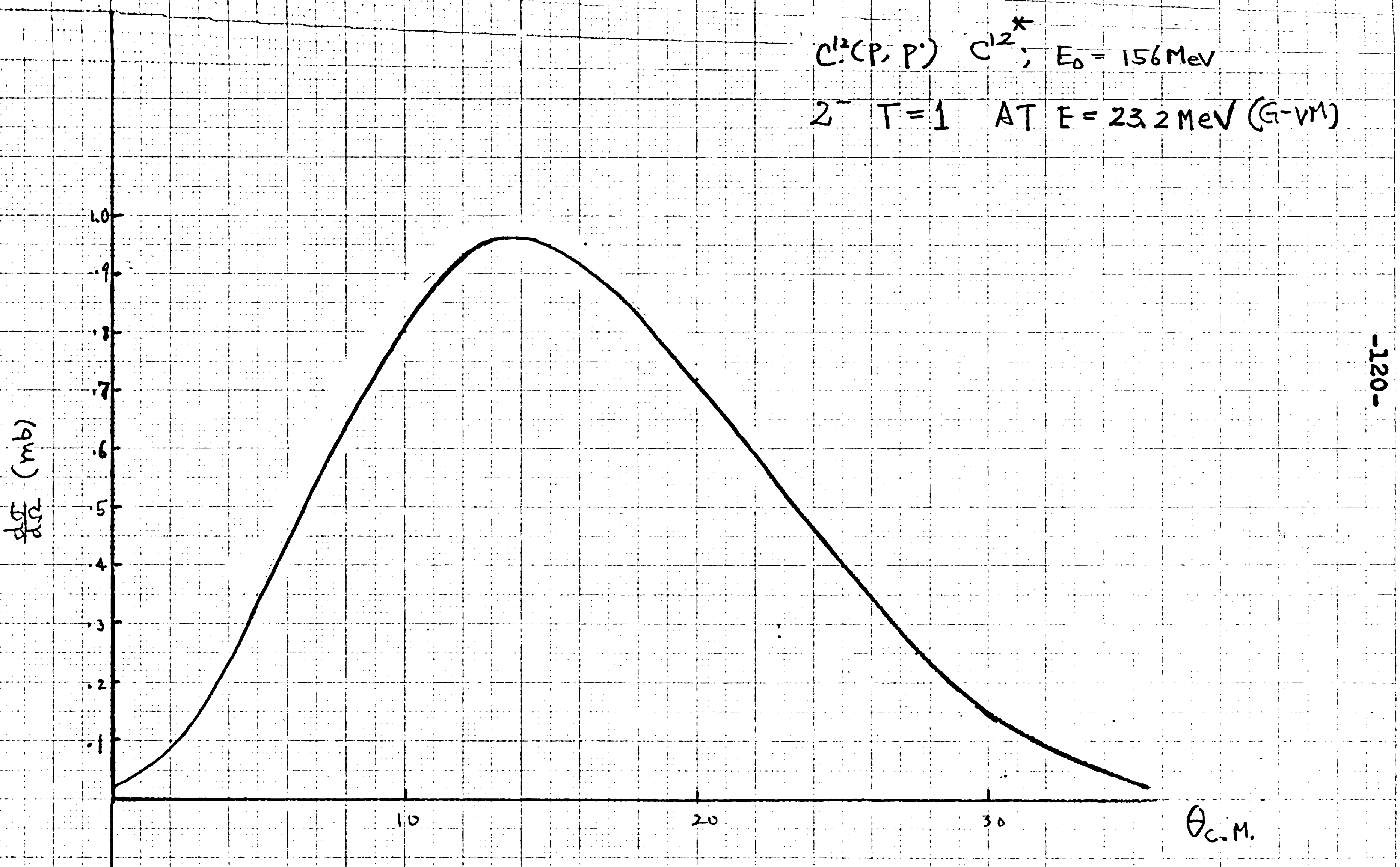
$C^{12}(p, p')\ C^{12*}$; $E_0 = 156$ MeV
2^- T = 1 AT E = 23.2 MeV (G-VM)
$\frac{d\sigma}{d\Omega}$ (mb)
1.0
.9
.8
.7
.6
.5
.4
.3
.2
.1
10
20
30
$\theta_{c.M.}$

FIG 23

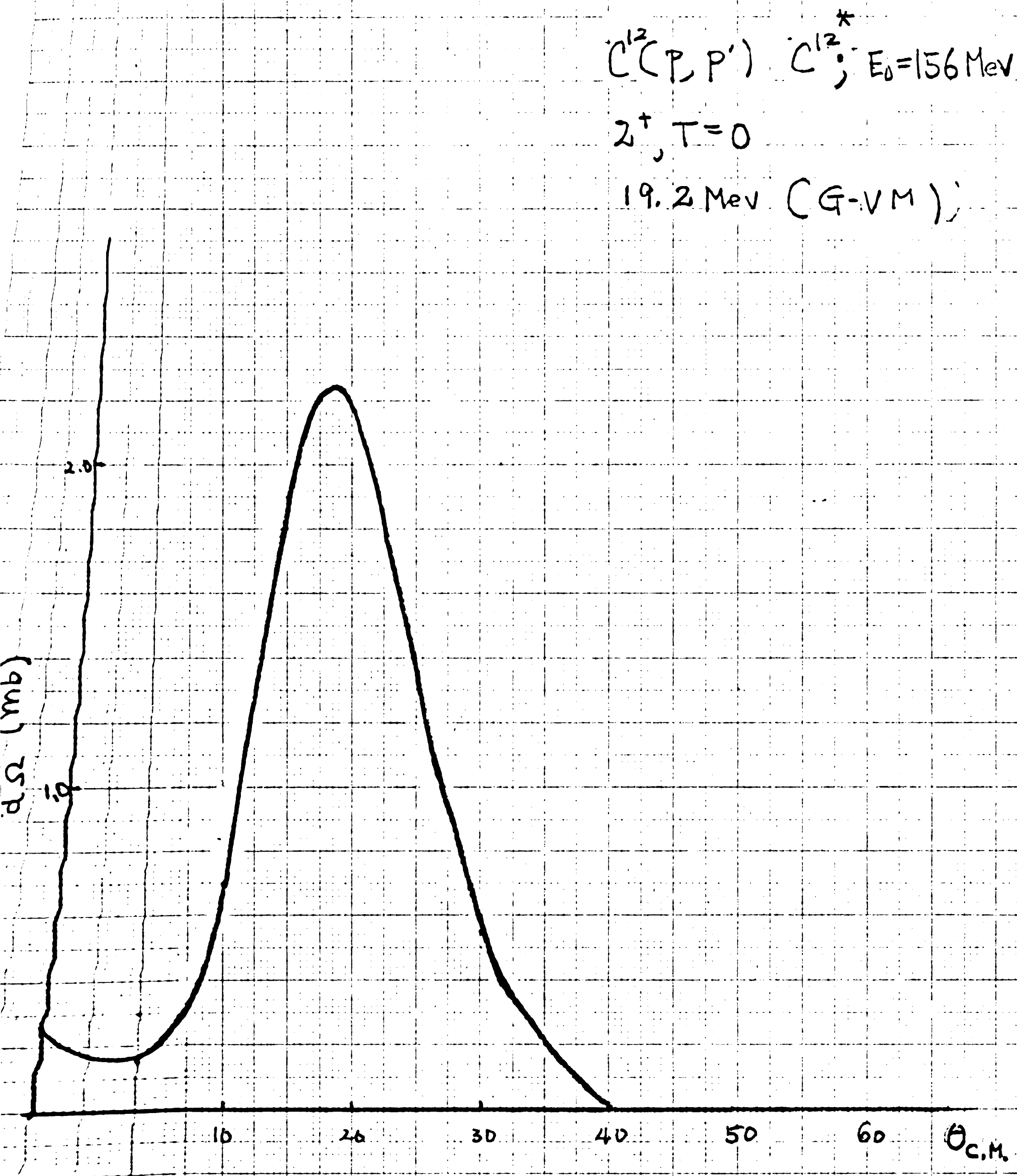
$C^{12}(p, p')\ C^{12*}$; E_0=156 Mev
2^+, T=0
19.2 Mev (G-VM);
2.0
1.0
dσ/dΩ (mb)
10
20
30
40
50
60
$\theta_{C.M.}$

FIG 24

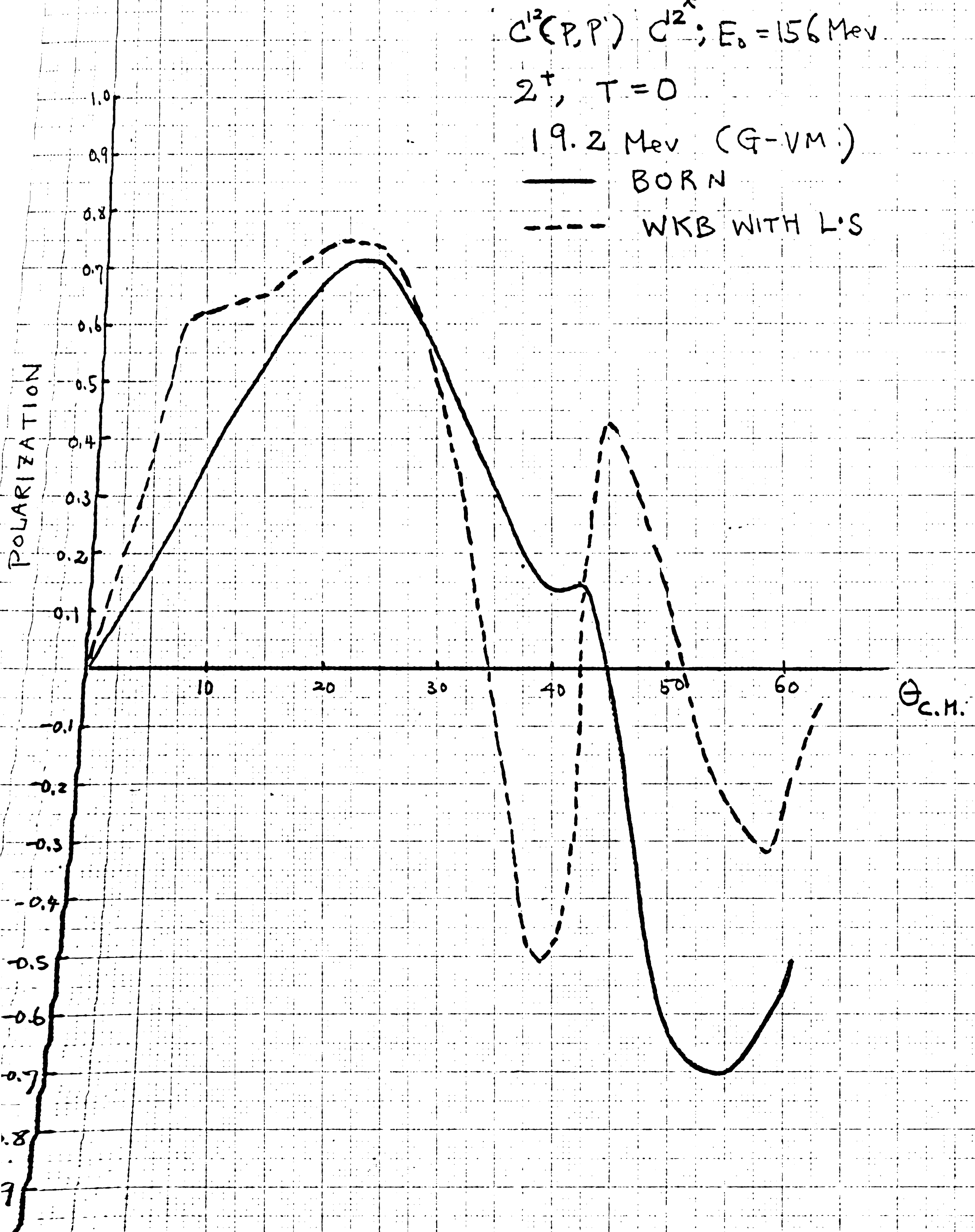
$C^{12}(P,P')\ C^{12*};\ E_0 = 156$ Mev
2^+, T = 0
19.2 Mev (G-VM)
BORN
WKB WITH L·S
POLARIZATION
$\theta_{C.M.}$
1.0
0.9
0.8
0.7
0.6
0.5
0.4
0.3
0.2
0.1
-0.1
-0.2
-0.3
-0.4
-0.5
-0.6
-0.7
10
20
30
40
50
60

FIG. 25

$C^{12}(P,P')\ C^{12*}$ $E_{\circ} = 156$ MeV

1^- $T=1$ AT 24.2 MeV (G-VM)

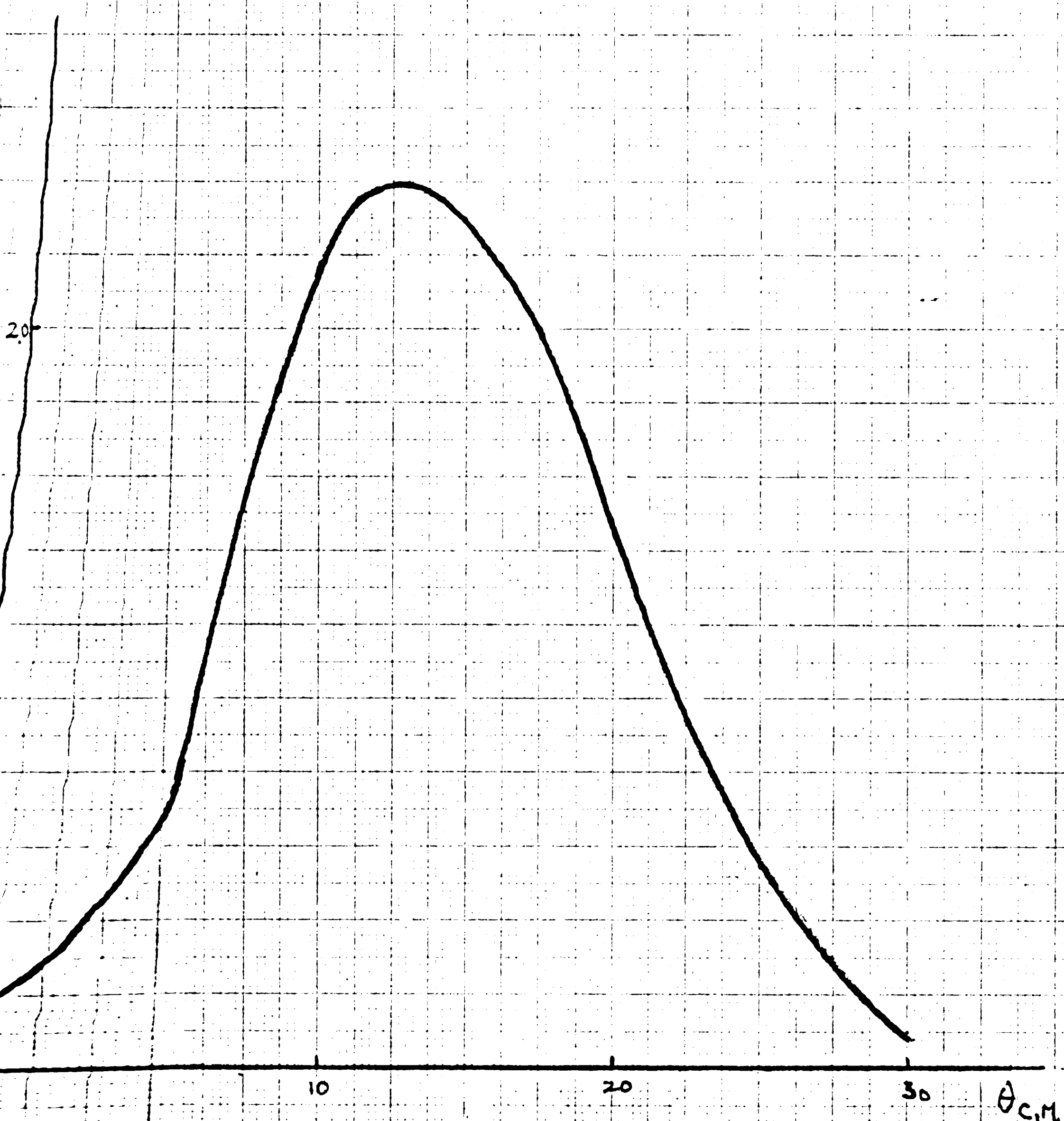

FIG 26

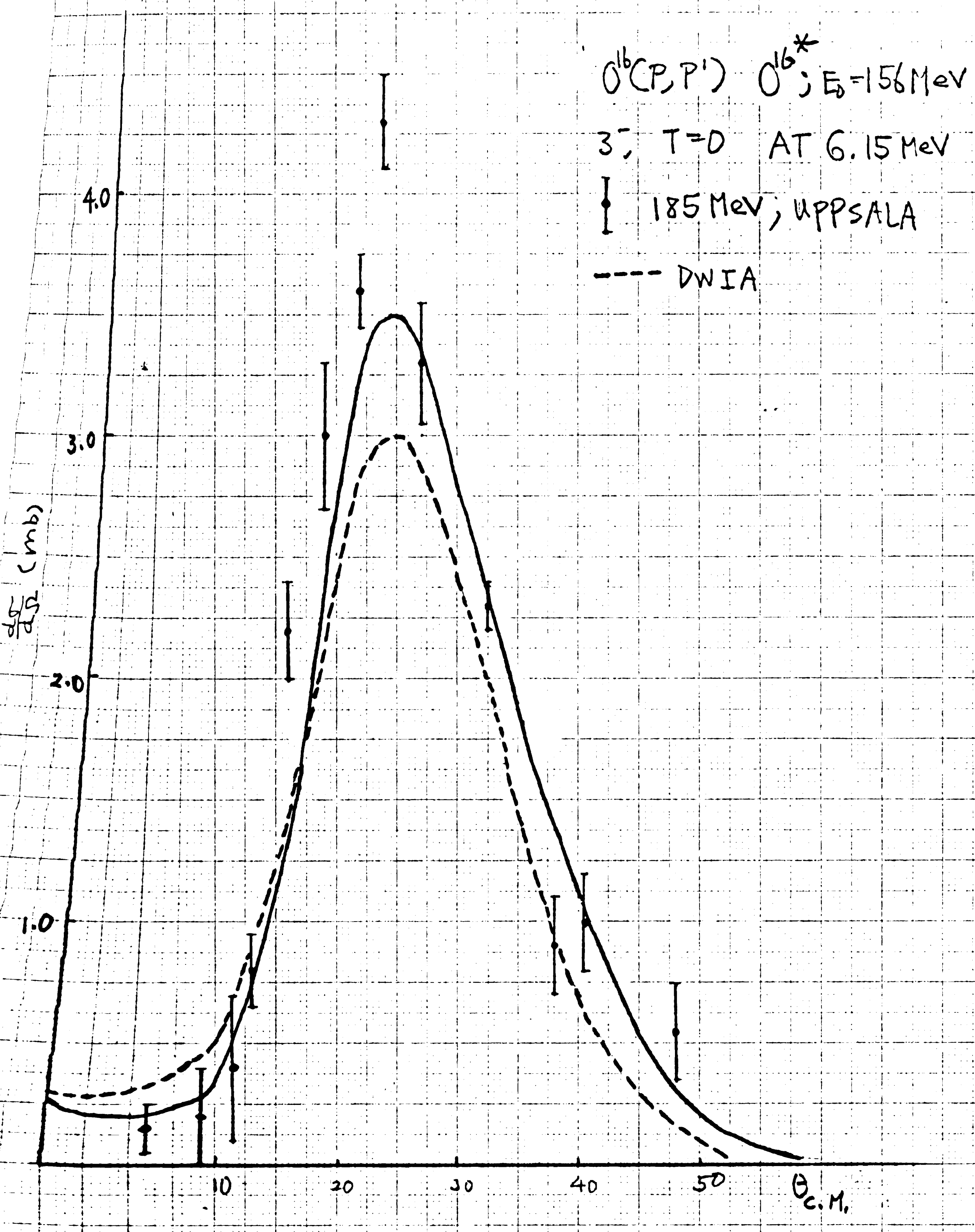
$O^{16}(P,P')\,O^{16*}$; E_0=156 MeV
3⁻; T=0 AT 6.15 MeV
185 MeV; UPPSALA
---- DWIA
4.0
3.0
2.0
1.0
$\frac{d\sigma}{d\Omega}$ (mb)
10
20
30
40
50
$\theta_{c.M.}$

FIG 27

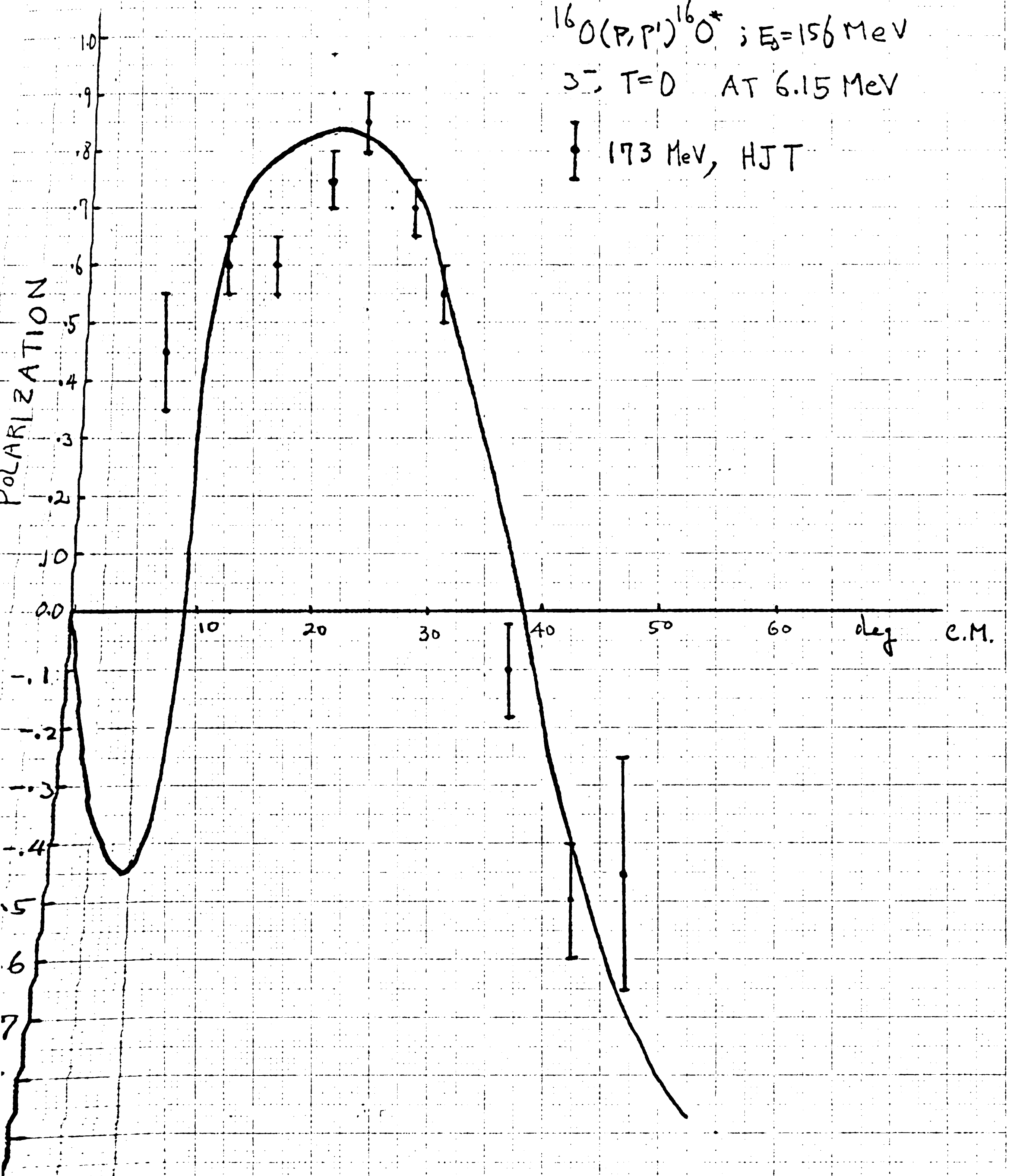

$^{16}O(p,p')^{16}O^{*}$; $E_0=156$ MeV
3^-, T=0 AT 6.15 MeV
173 MeV, HJT
POLARIZATION
1.0
.9
.8
.7
.6
.5
.4
.3
.2
.1 0
0.0
-.1
-.2
-.3
-.4
.5
.6
.7
10
20
30
40
50
60
deg C.M.

FIG 28

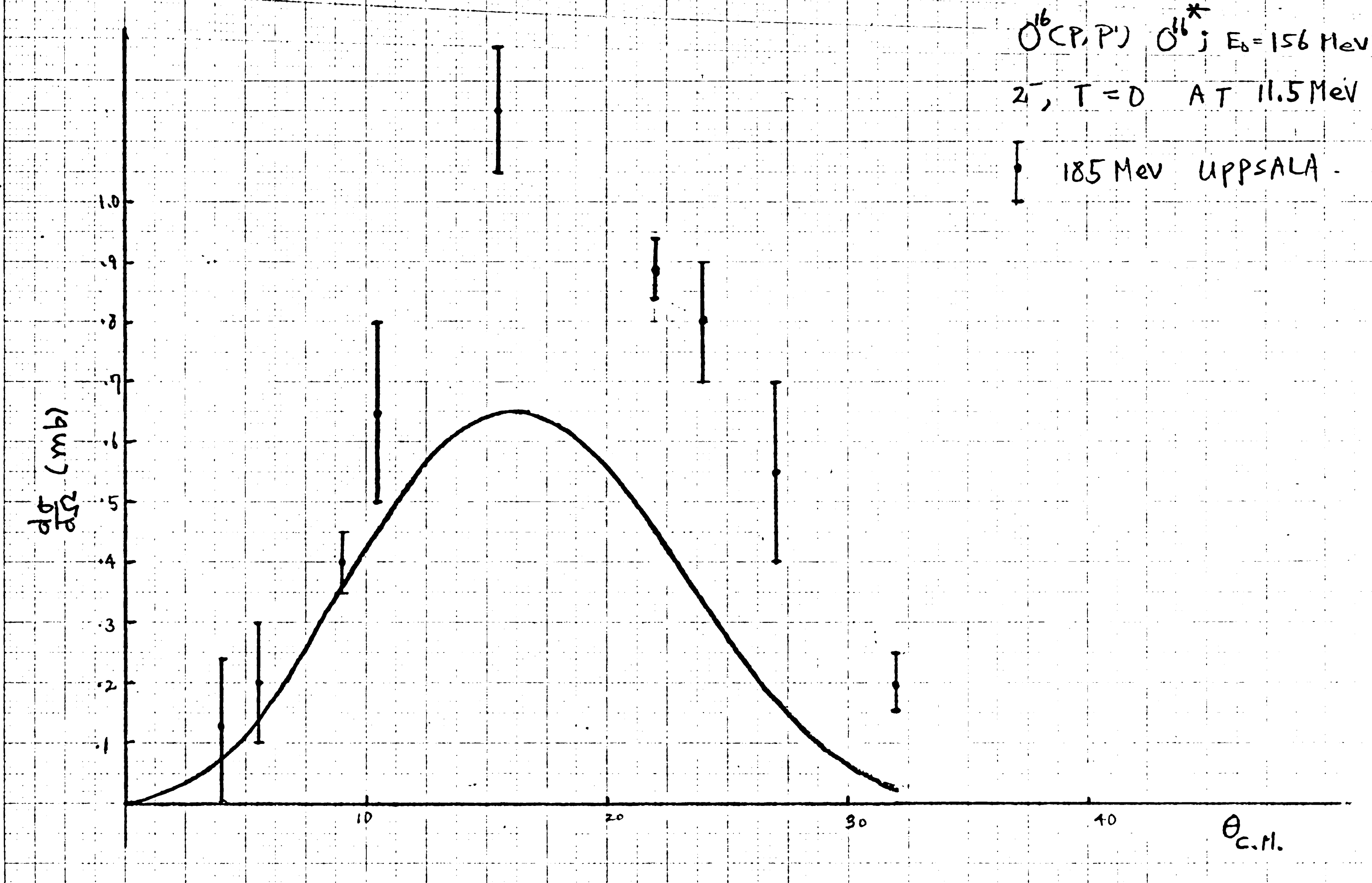
$O^{16}(P,P')\,O^{16*}$; $E_0 = 156$ MeV
2^-, T = 0 AT 11.5 MeV
185 MeV UPPSALA.
$\frac{d\sigma}{d\Omega}$ (mb)
1.0
.9
.8
.7
.6
.5
.4
.3
.2
.1
10
20
30
40
$\theta_{c.m.}$

FIG 29

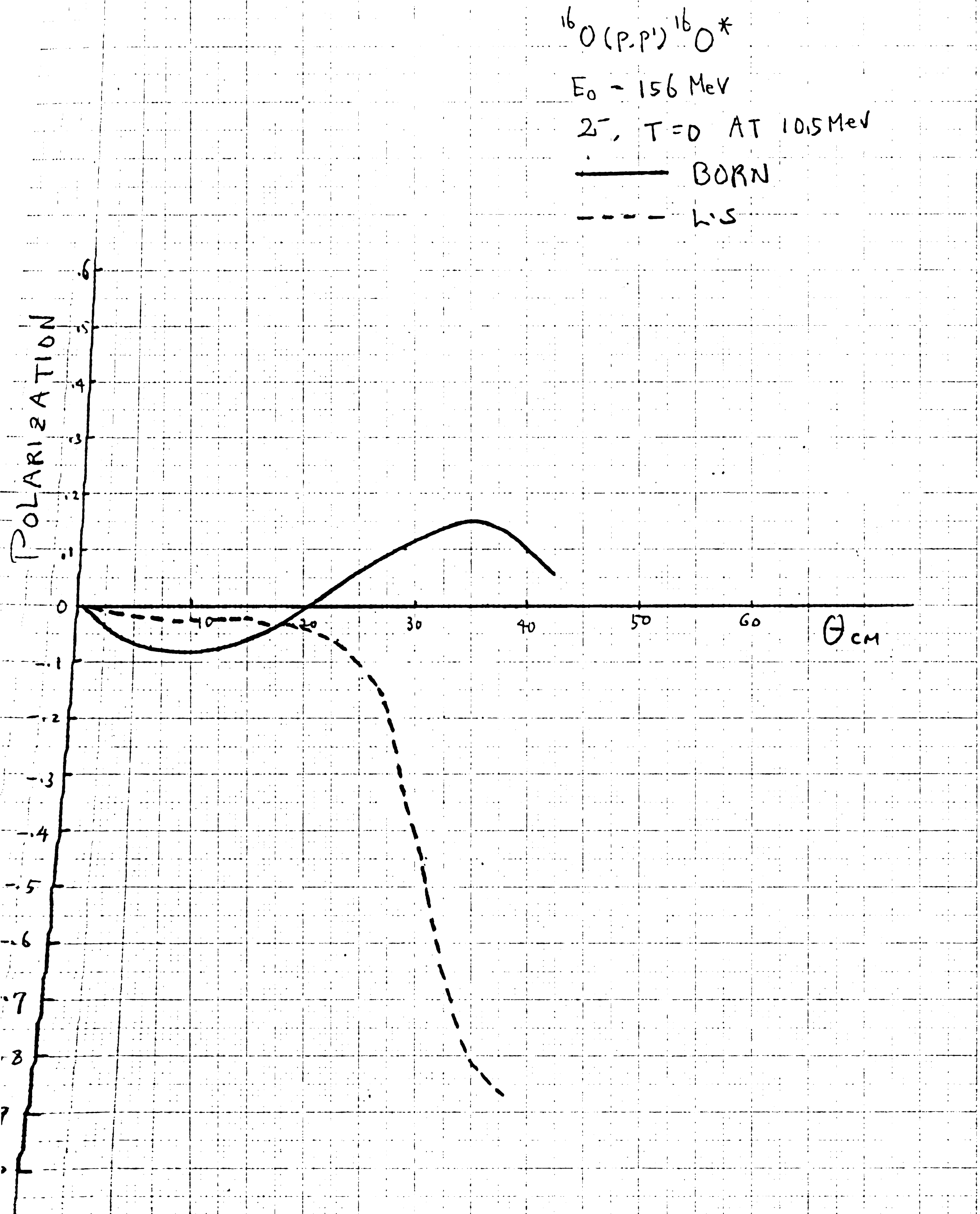
$^{16}O(p,p')^{16}O^*$
E_0 - 156 MeV
2^-, T=0 AT 10.5 MeV
BORN
L·S
POLARIZATION
.6
.5
.4
.3
.2
.1
0
-.1
-.2
-.3
-.4
-.5
-.6
-.7
-.8
10
20
30
40
50
60
θ_{CM}

FIG 30

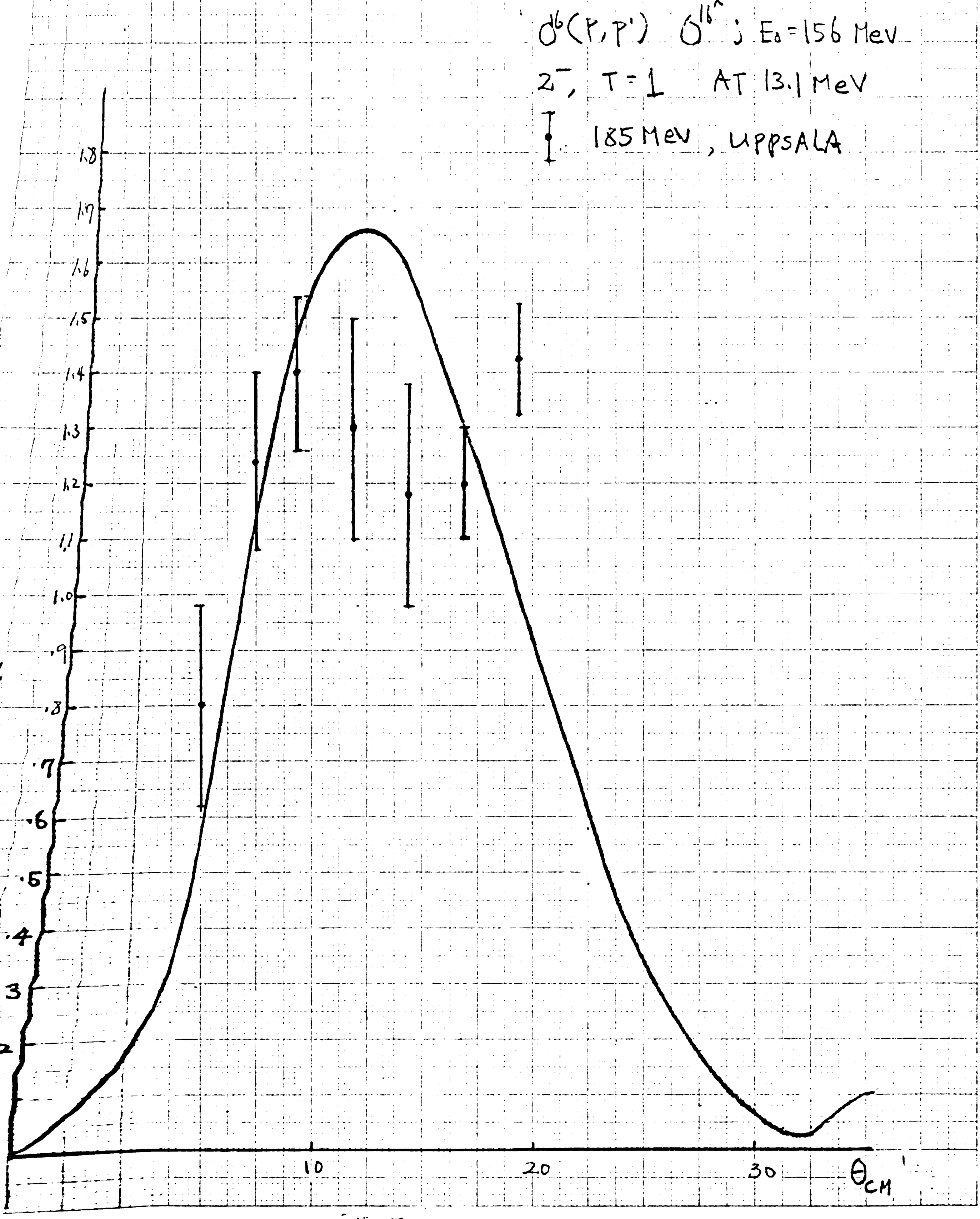
$O^{16}(p,p')\ O^{16*}$; E_0 = 156 MeV
2^-, T = 1 AT 13.1 MeV
185 MeV, UPPSALA
1.8
1.7
1.6
1.5
1.4
1.3
1.2
1.1
1.0
.9
.8
.7
.6
.5
.4
.3
10
20
30
θ_{CM}

FIG 31

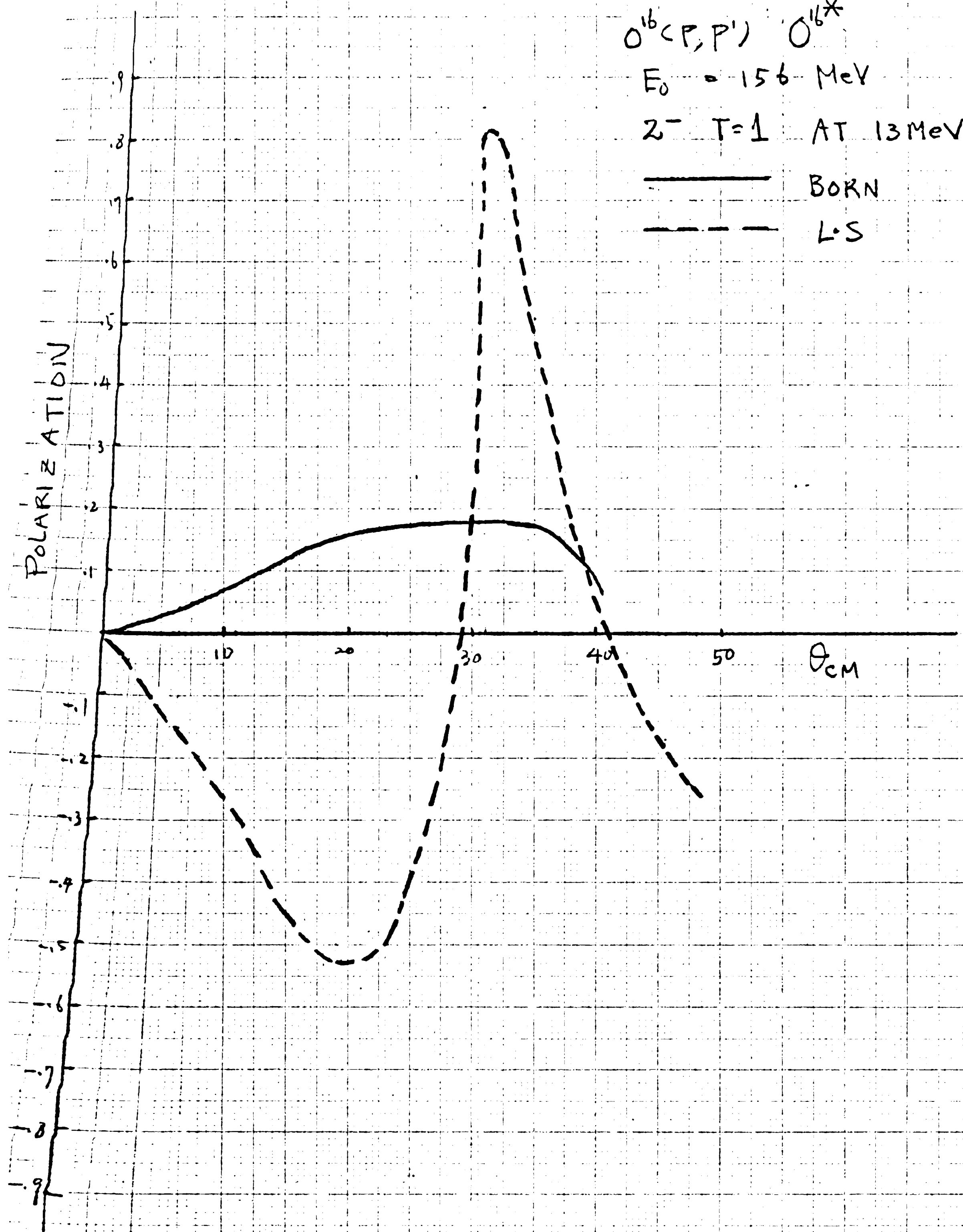
$O^{16}(p,p')\ O^{16*}$
$E_0 = 156$ MeV
2^- T=1 AT 13MeV
BORN
L·S
POLARIZATION
θ_{CM}
.9
.8
.7
.6
.5
.4
.3
.2
.1
-.1
-.2
-.3
-.4
-.5
-.6
-.7
-.8
-.9
10
20
30
40
50

FIG 32

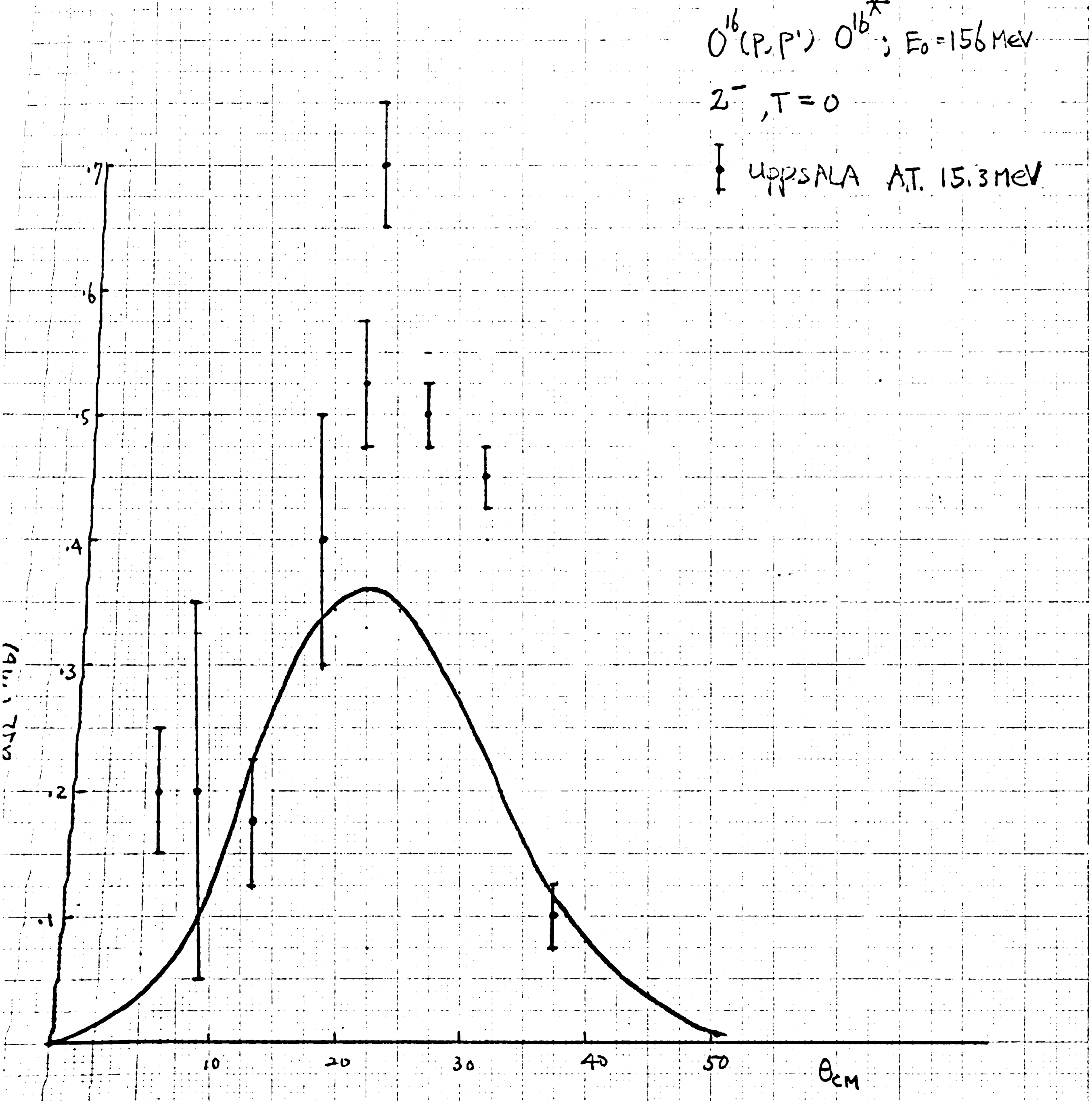
$O^{16}(P,P')\,O^{16*}$; E_0 = 156 MeV
2^-, T = 0
UPPSALA AT 15.3 MeV
.7
.6
.5
.4
.3
.2
.1
10
20
30
40
50
θ_{CM}

FIG 33

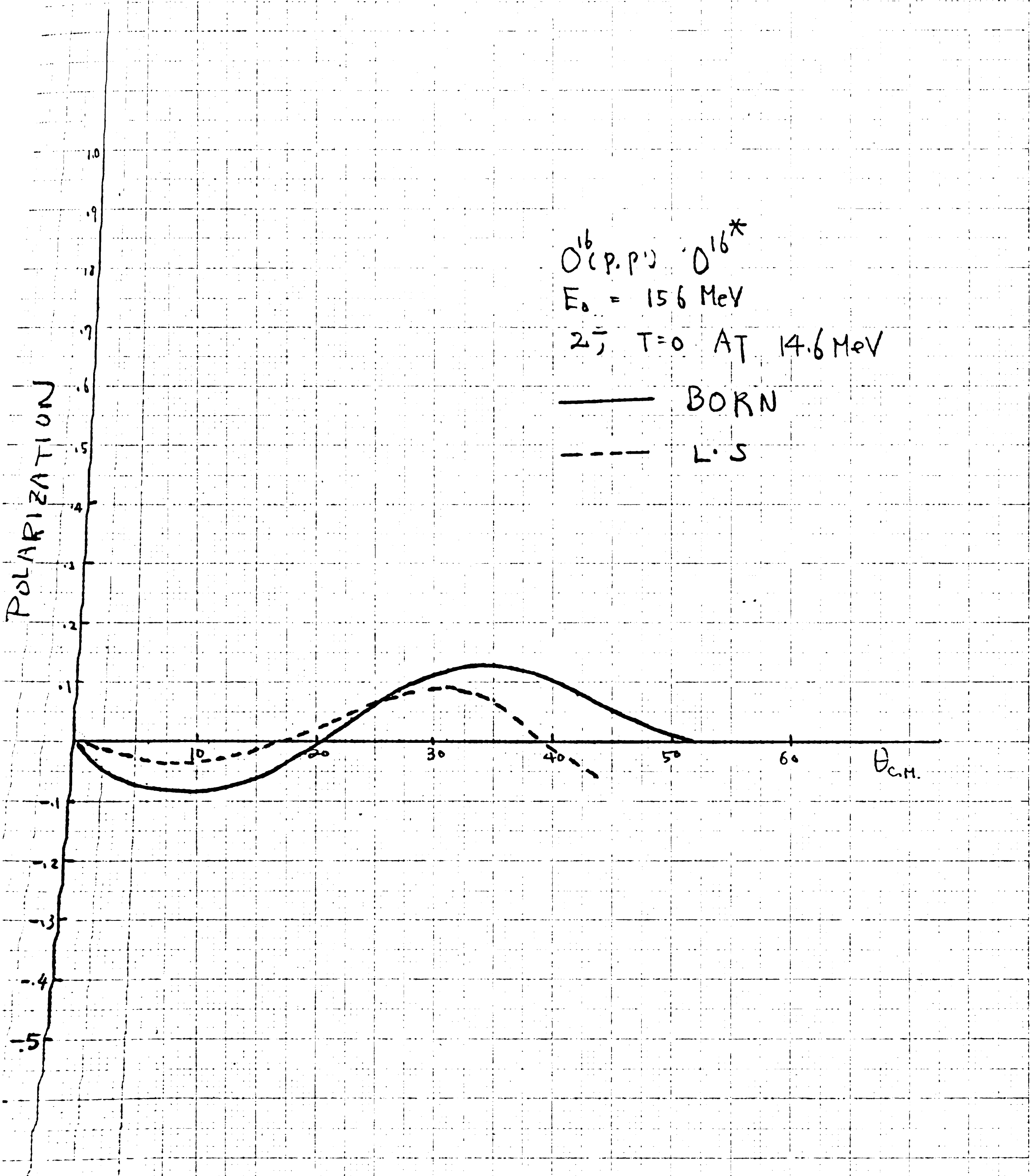
$O^{16}(p,p')O^{16*}$
E_0 = 156 MeV
2^-, T=0 AT 14.6 MeV
BORN
L·S
POLARIZATION
1.0
.9
.8
.7
.6
.5
.4
.3
.2
.1
-.1
-.2
-.3
-.4
-.5
10
20
30
40
50
60
$\theta_{C.M.}$

FIG 34

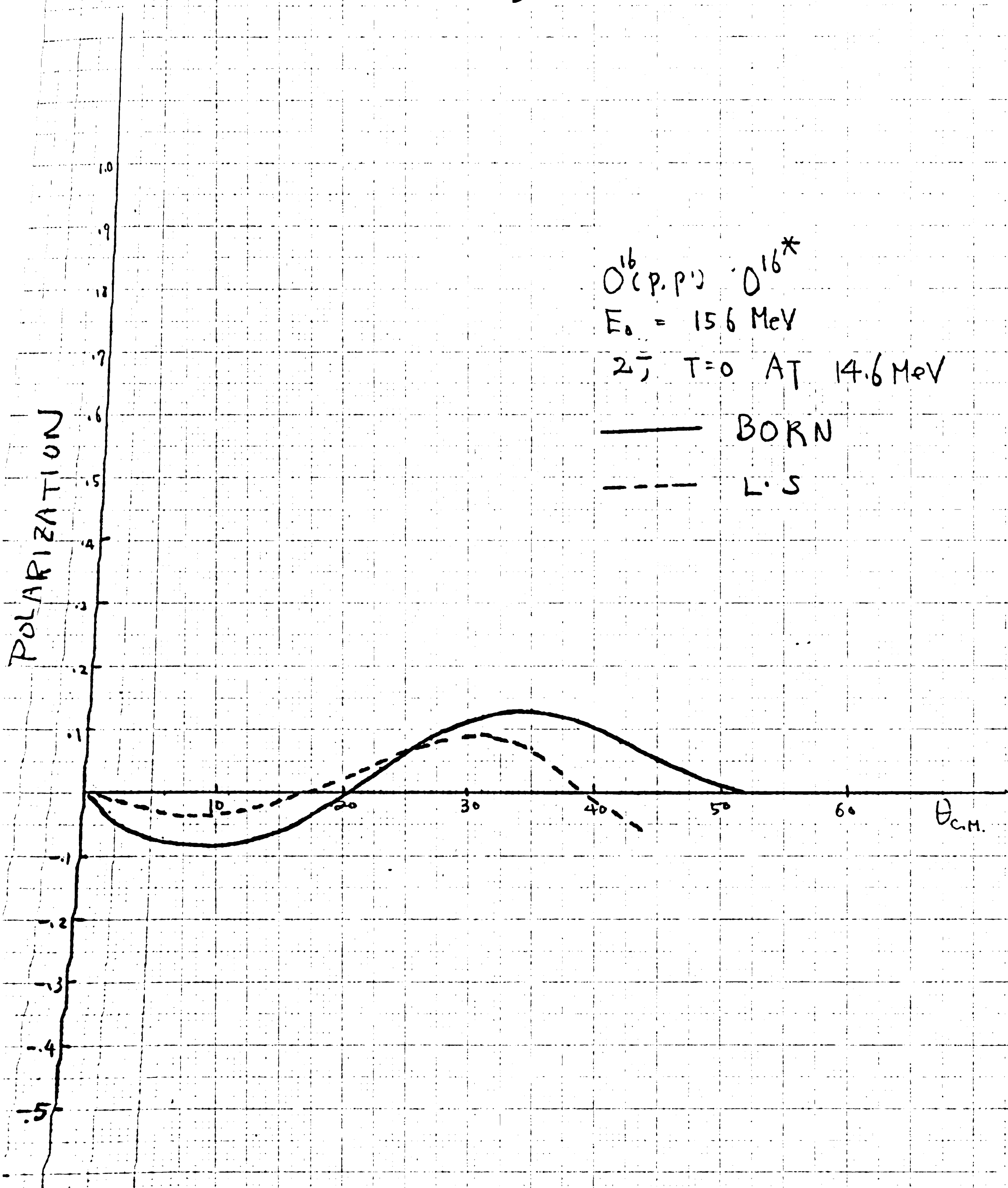

$O^{16}(p,p')O^{16*}$
E_0 = 156 MeV
2^-, T=0 AT 14.6 MeV
BORN
L·S
POLARIZATION
$\theta_{C.M.}$
1.0
.9
.8
.7
.6
.5
.4
.3
.2
.1
-.1
-.2
-.3
-.4
-.5
10
20
30
40
50
60

FIG 34

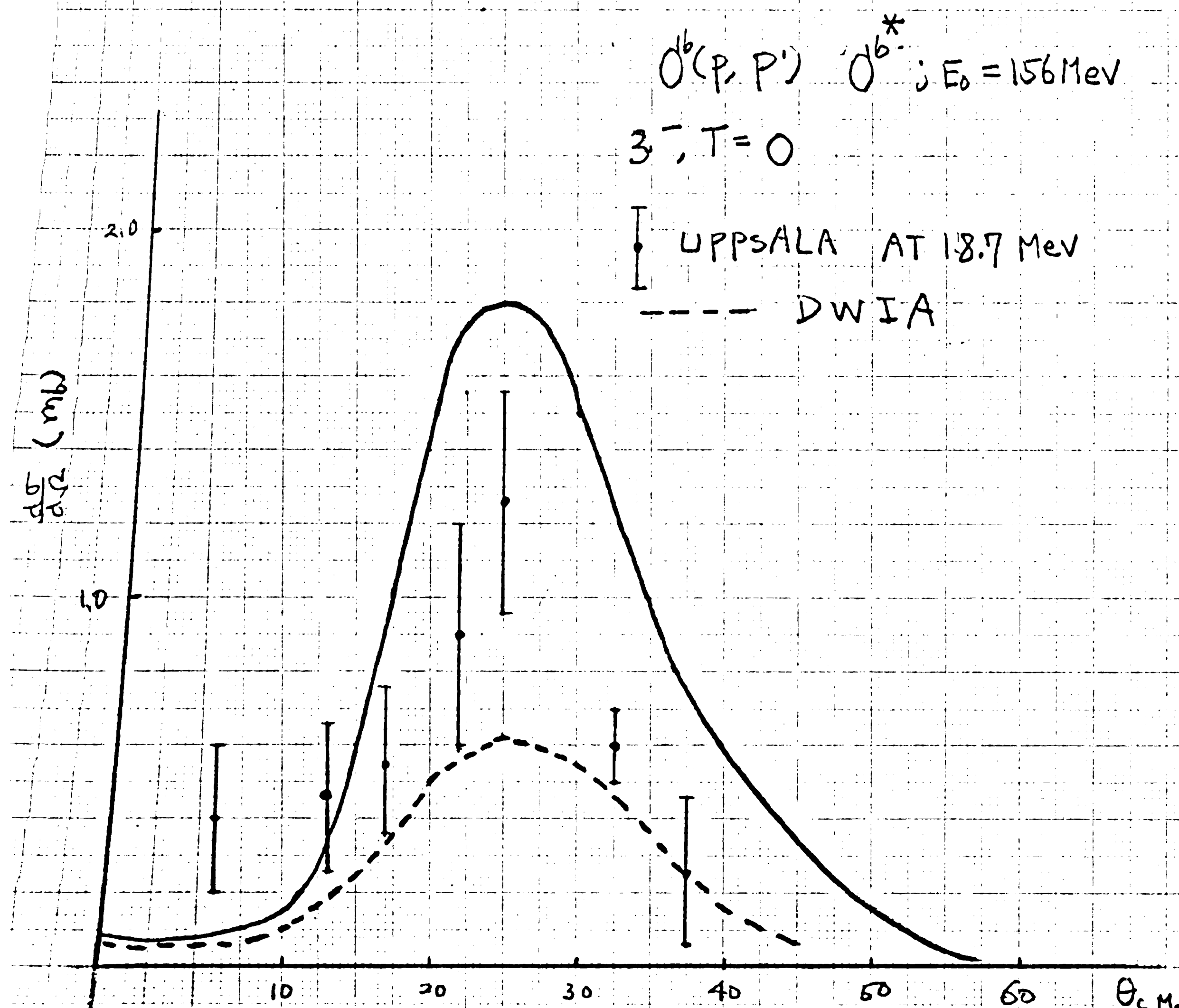

$O^{16}(p, p')\ O^{16*}$; E_0 = 156 Mev
3^-, T = 0
UPPSALA AT 18.7 Mev
DWIA
2.0
1.0
$\frac{d\sigma}{d\Omega}$ (mb)
10
20
30
40
50
60
$\theta_{C.M.}$

FIG 35

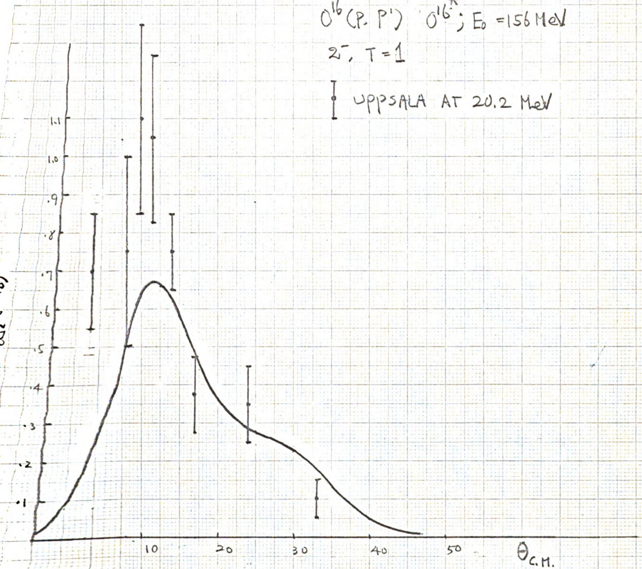
$O^{16}(P.P')\ O^{16*}$; $E_0 = 156$ MeV
2^-, T = 1
UPPSALA AT 20.2 MeV
1.1
1.0
.9
.8
.7
.6
.5
.4
.3
.2
.1
10
20
30
40
50
$\theta_{C.M.}$

FIG 36

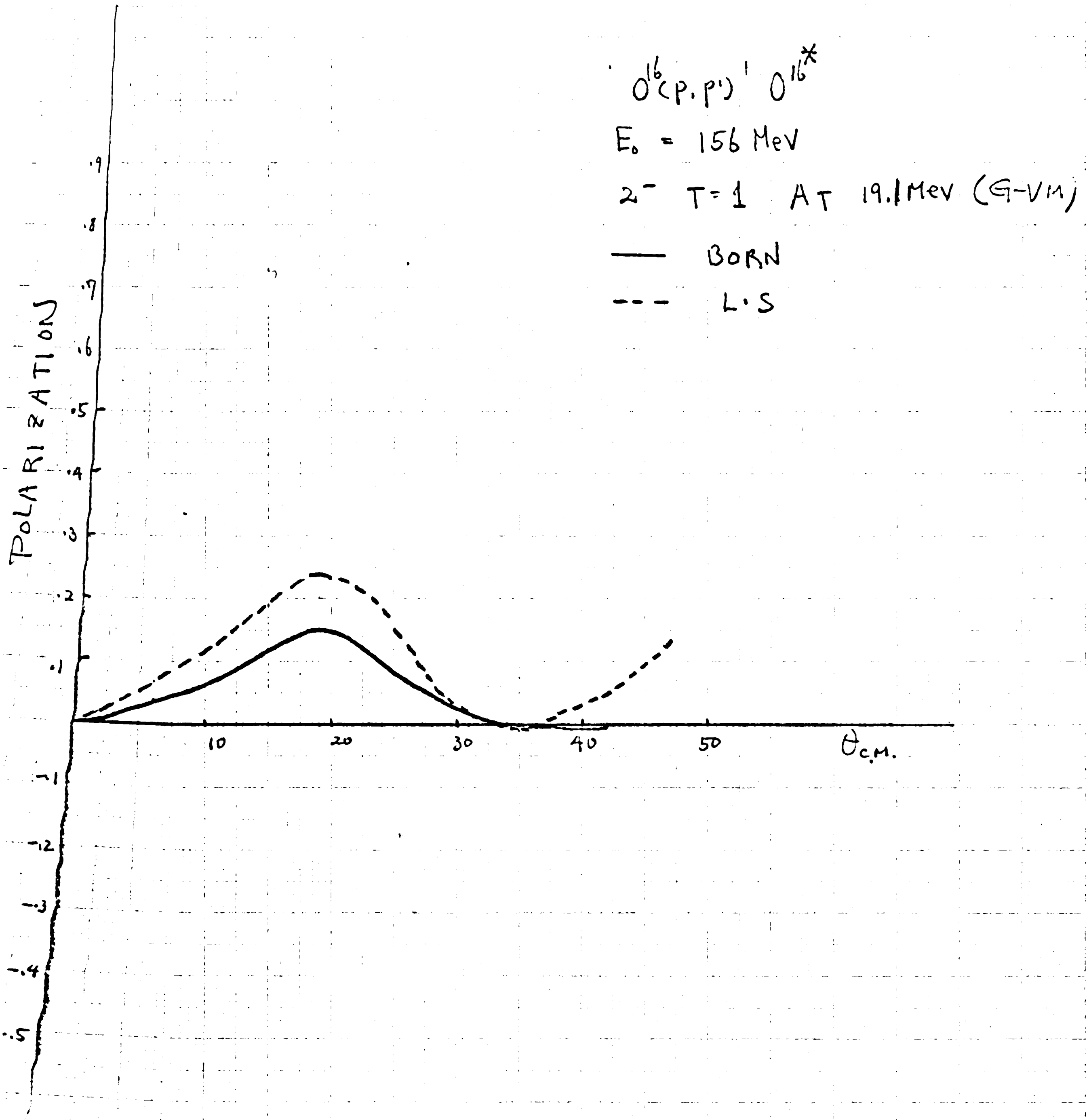

$O^{16}(p,p')O^{16*}$
$E_0 = 156$ MeV
2^- T=1 AT 19.1 MeV (G-VM)
BORN
L·S
POLARIZATION
.9
.8
.7
.6
.5
.4
.3
.2
.1
-.1
-.2
-.3
-.4
-.5
10
20
30
40
50
$\theta_{c.m.}$

FIG 37

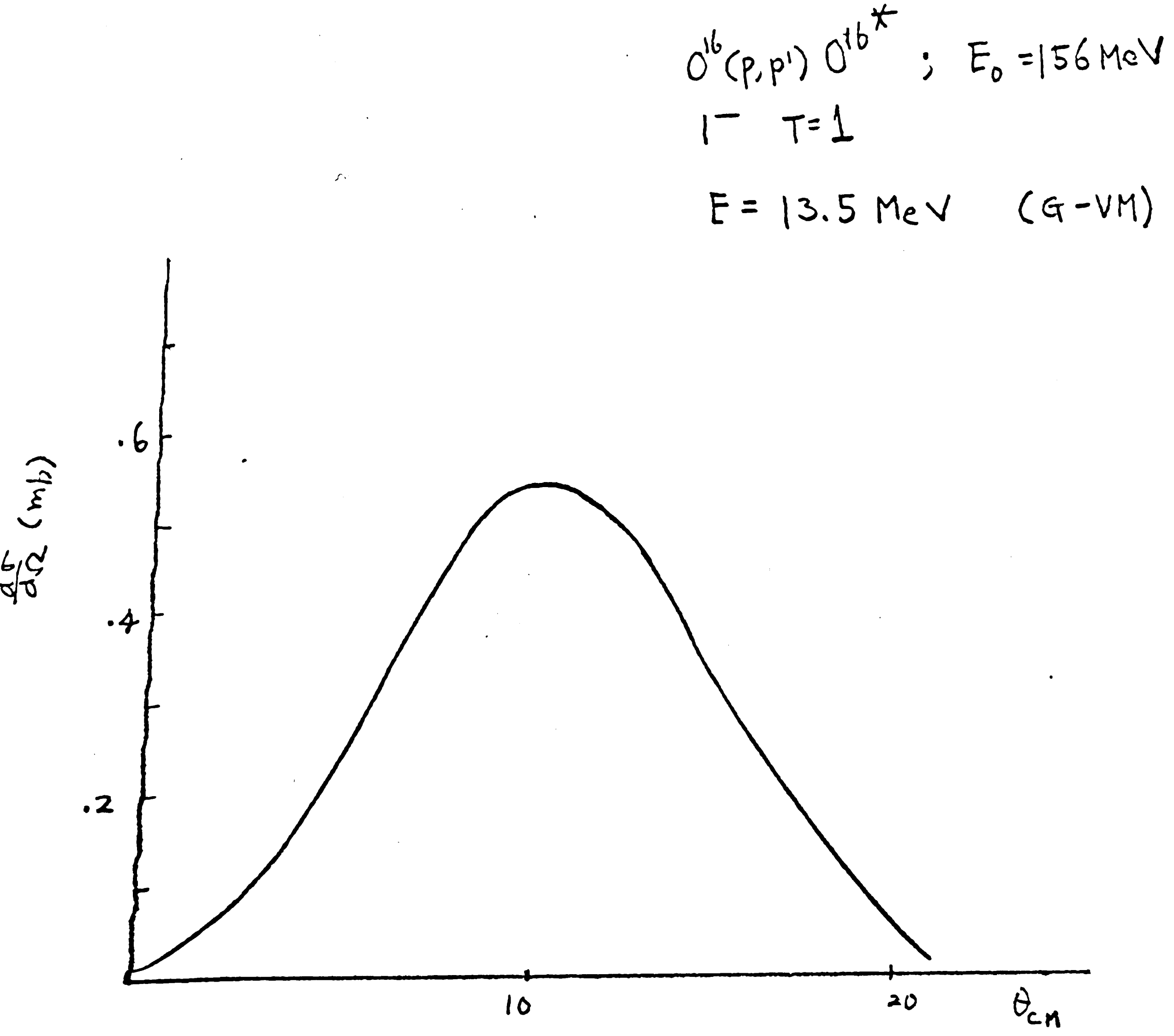
$O^{16}(p,p')\,O^{16*}$; $E_0 = 156$ MeV
1^- T=1
E = 13.5 MeV (G-VM)
$\frac{d\sigma}{d\Omega}$ (mb)
.6
.4
.2
10
20
θ_{cm}

FIG 38

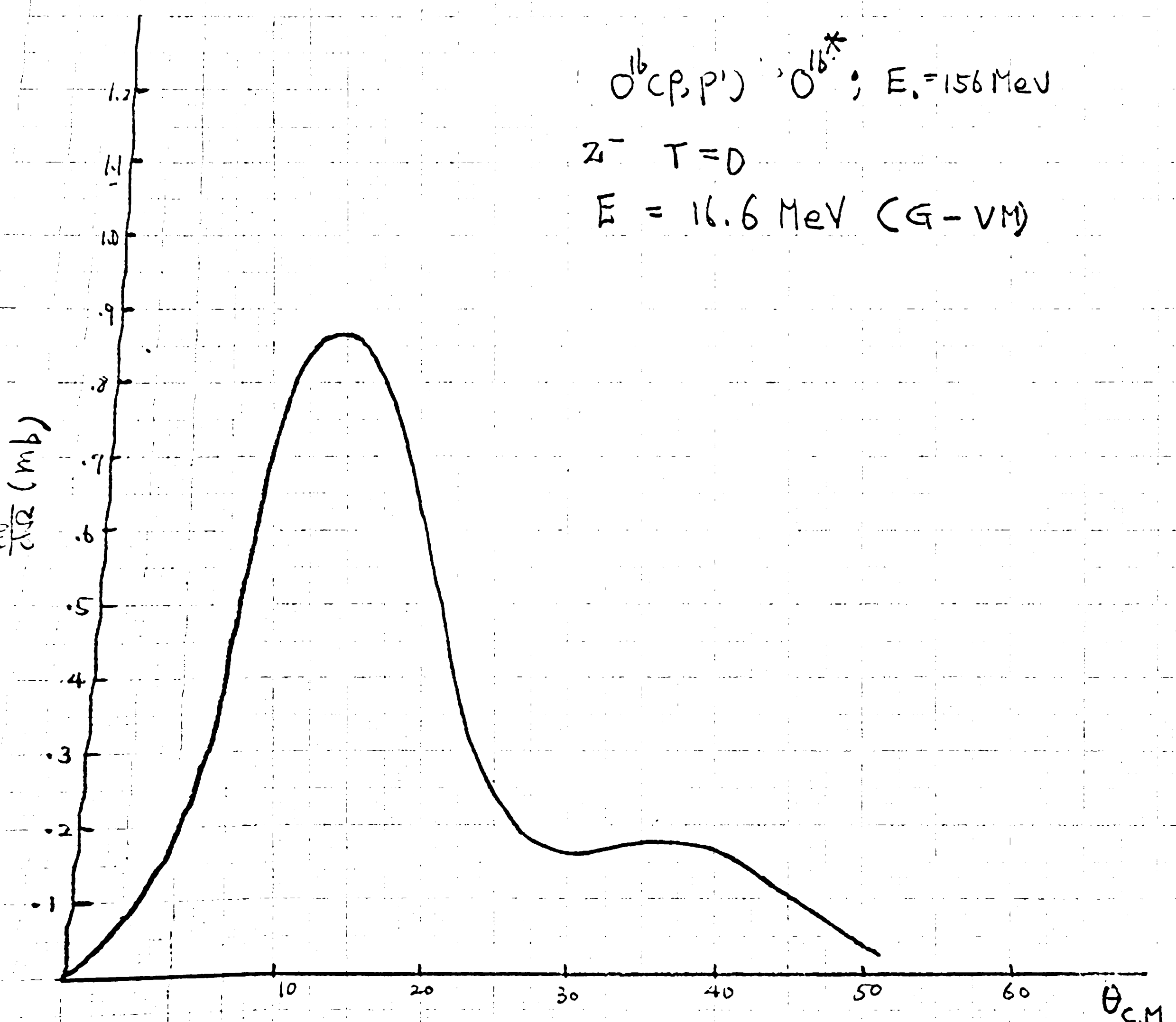
$O^{16}(p,p')O^{16*}$; E_0=156 MeV
2^- T=0
E = 16.6 MeV (G-VM)
$\frac{d\sigma}{d\Omega}$ (mb)
1.2
1.1
1.0
.9
.8
.7
.6
.5
.4
.3
.2
.1
10
20
30
40
50
60
$\theta_{C.M.}$

FIG 39

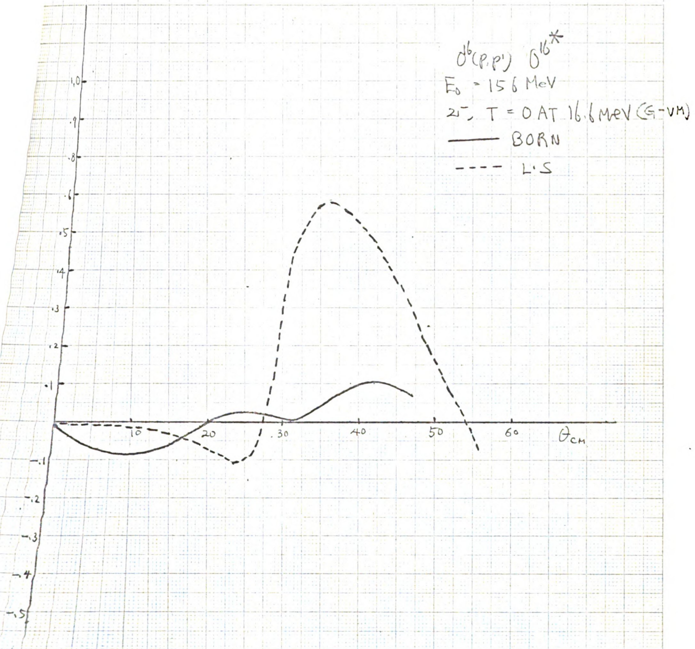
$O^{16}(p,p')\ O^{16*}$
$E_0 = 156$ MeV
2^-, T = 0 AT 16.6 MeV (G-VM)
BORN
L·S
1.0
.9
.8
.6
.5
.4
.3
.2
.1
-.1
-.2
-.3
-.4
-.5
10
20
30
40
50
60
θ_{CM}

FIG 40

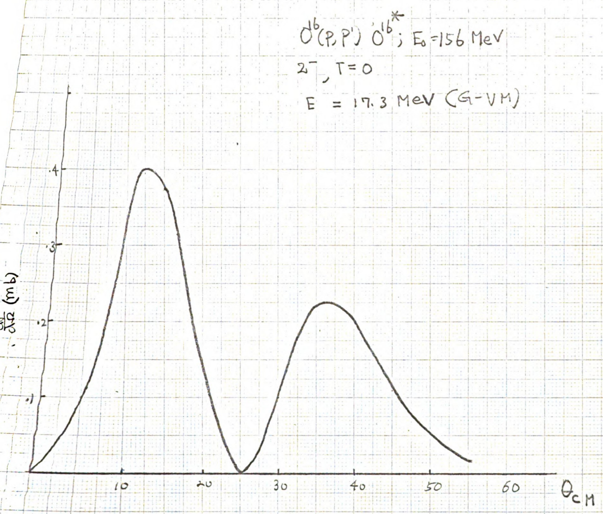

$O^{16}(p,p')O^{16*}$; $E_0 = 156$ MeV
2^-, T=0
E = 17.3 MeV (G-VM)
$\frac{d\sigma}{d\Omega}$ (mb)
.1
.2
.3
.4
10
20
30
40
50
60
θ_{CM}

FIG 41

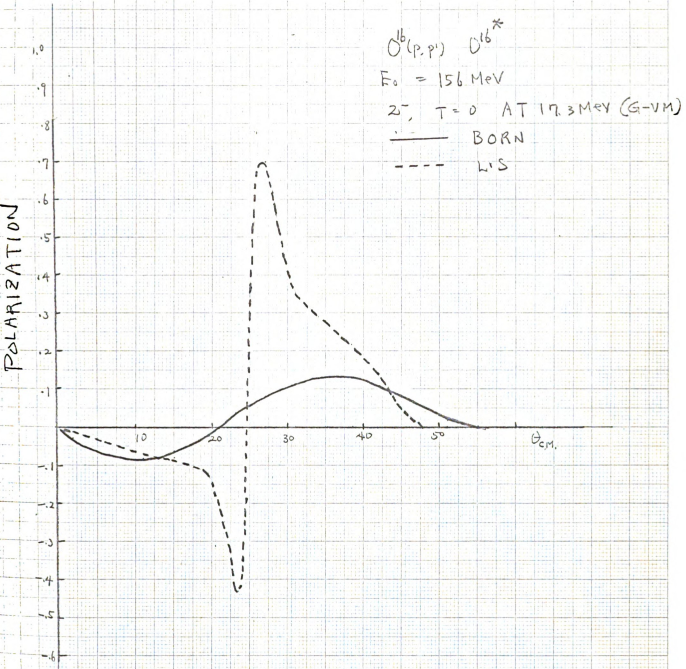

$O^{16}(p,p')\ O^{16*}$
$E_0 = 156$ MeV
2^-, T = 0 AT 17.3 MeV (G-VM)
BORN
L·S
POLARIZATION
$\theta_{C.M.}$

FIG 42

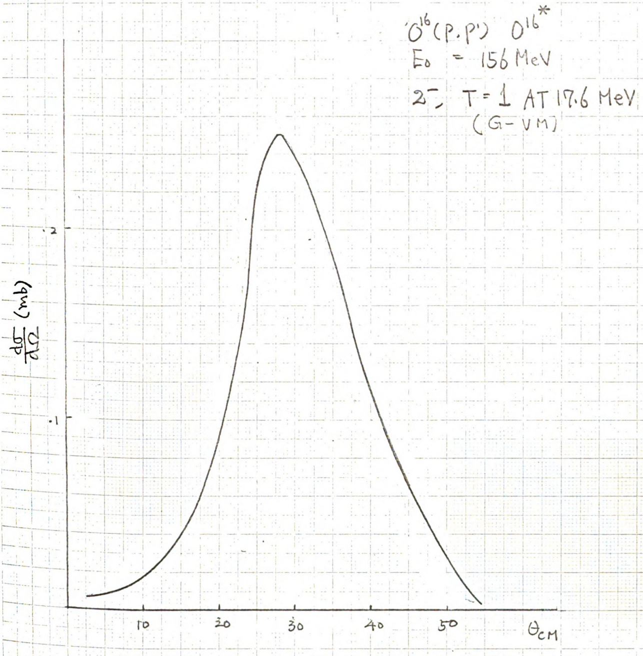

$O^{16}(P,P')\,O^{16*}$
$E_0 = 156$ MeV
2^-, T = 1 AT 17.6 MeV
(G-VM)
.2
.1
$\frac{d\sigma}{d\Omega}$ (mb)
10
20
30
40
50
θ_{CM}

FIG 43

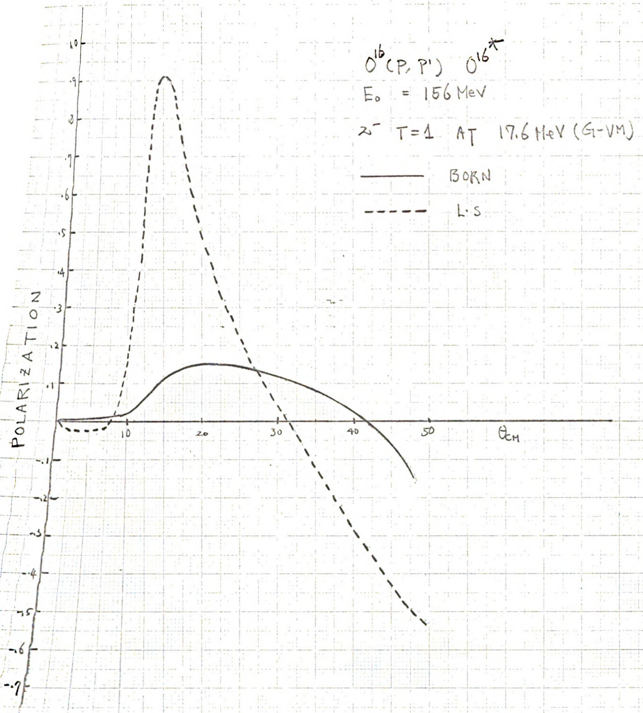

$O^{16}(P, P')\ O^{16*}$
$E_0 = 156$ MeV
2^- T=1 AT 17.6 MeV (G-VM)
BORN
L·S
POLARIZATION
1.0
.9
.8
.7
.6
.5
.4
.3
.2
.1
-.1
-.2
-.3
-.4
-.5
-.6
-.7
10
20
30
40
50
θ_{CM}

FIG 44

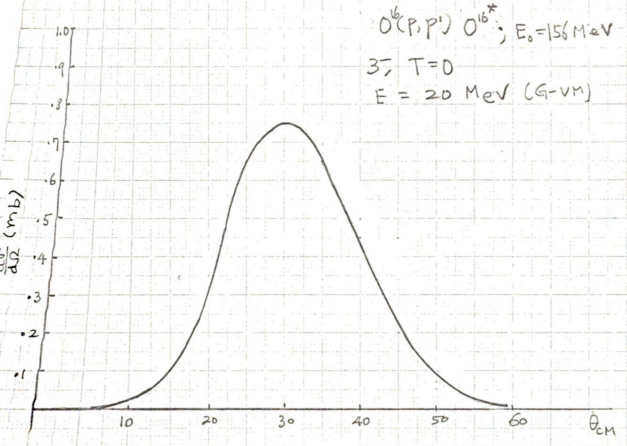
$O^{16}(p,p')\,O^{16*}$; $E_0 = 156$ MeV
3^-, $T=0$
E = 20 MeV (G-VM)
1.0
.9
.8
.7
.6
.5
.4
.3
.2
.1
$\frac{d\sigma}{d\Omega}$ (mb)
10
20
30
40
50
60
θ_{CM}

FIG 45

$O^{16}(p,p')O^{16*}$; $E_0 = 156$ MeV

3^- T=0

E = 20 MeV (G-VM)

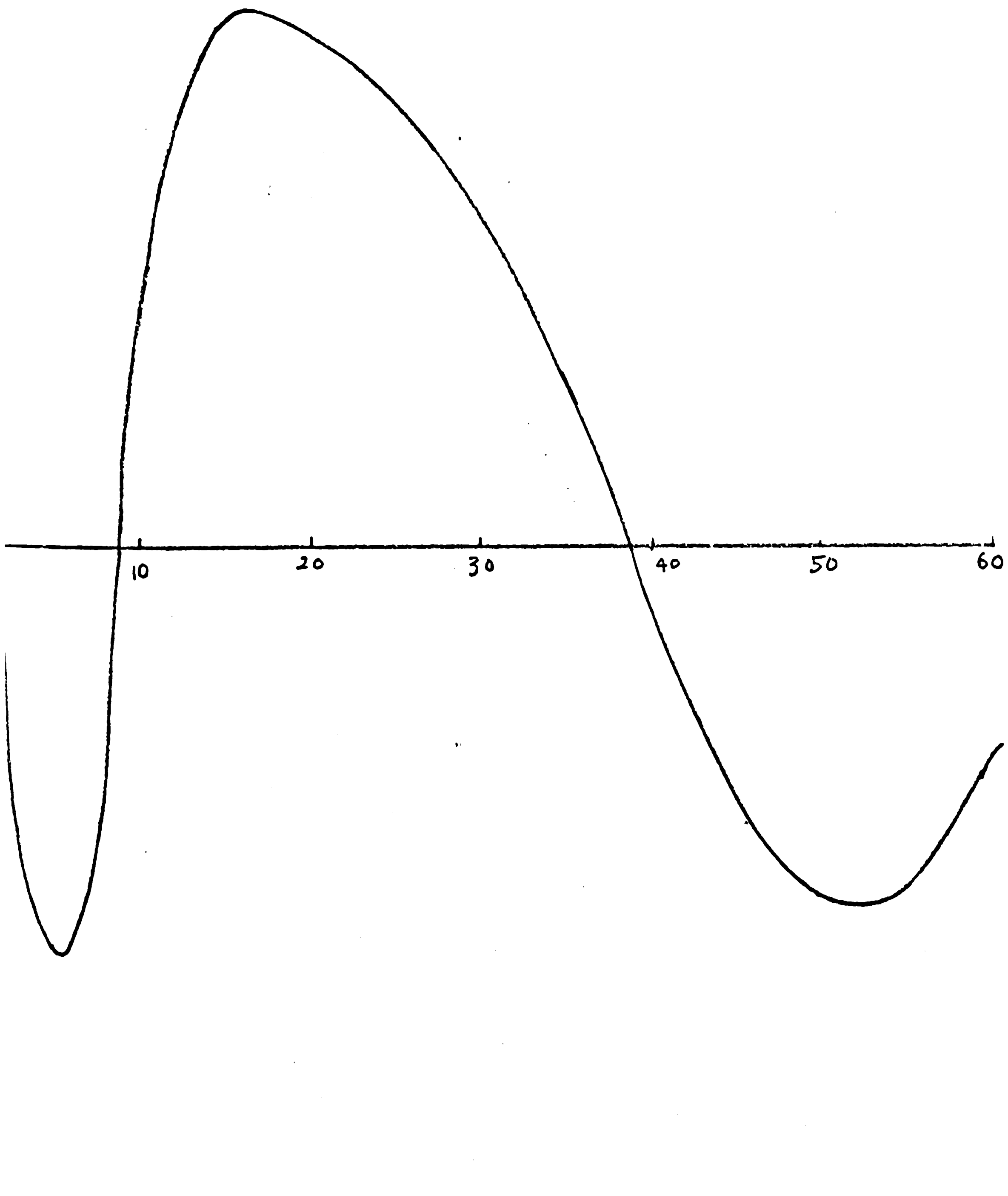

FIG. 46

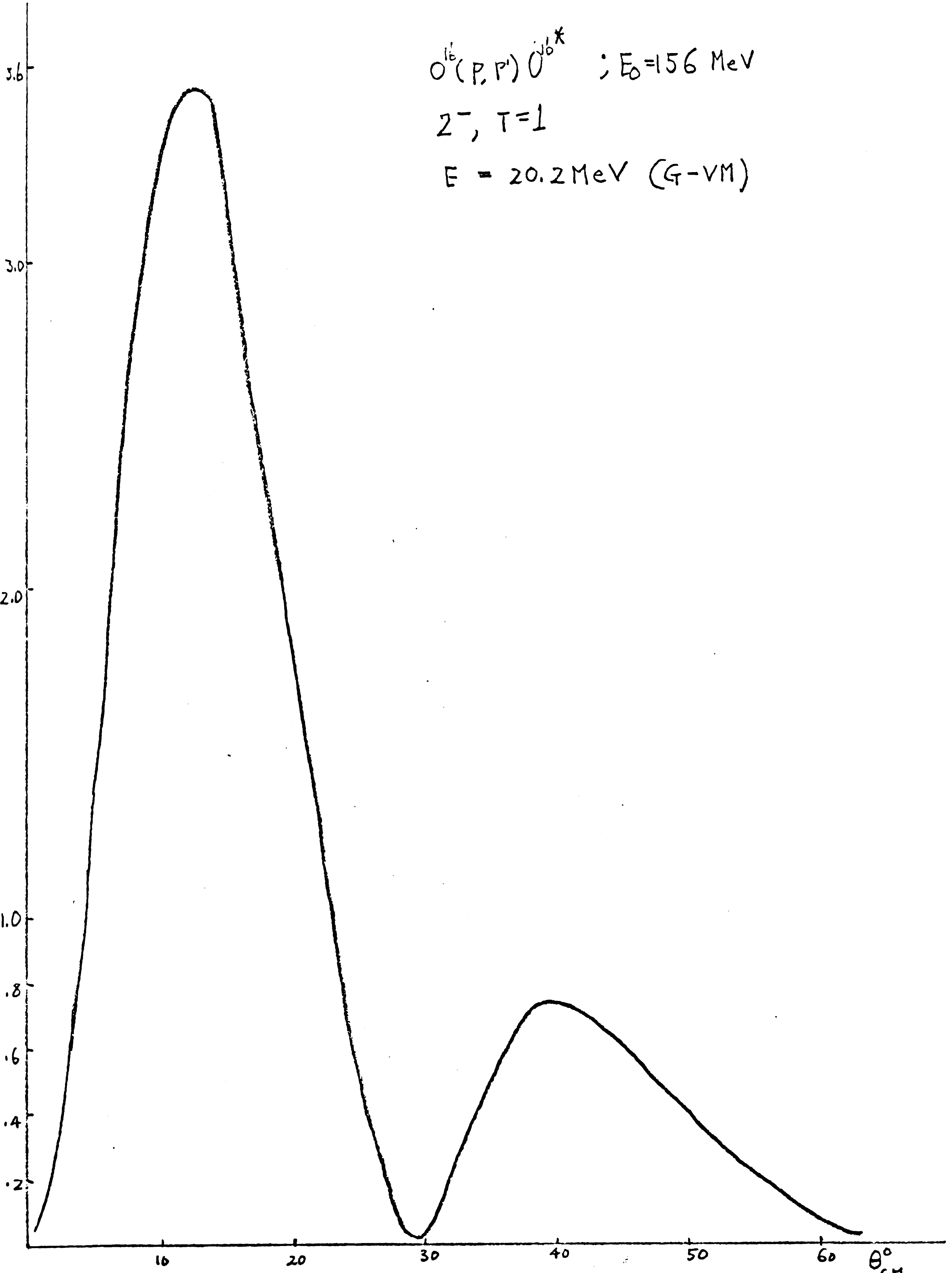

$O^{16}(p,p')O^{16*}$; E_0=156 MeV
2^-, T=1
E = 20.2MeV (G-VM)
3.6
3.0
2.0
1.0
.8
.6
.4
.2
10
20
30
40
50
60
$\theta^o_{C.M.}$

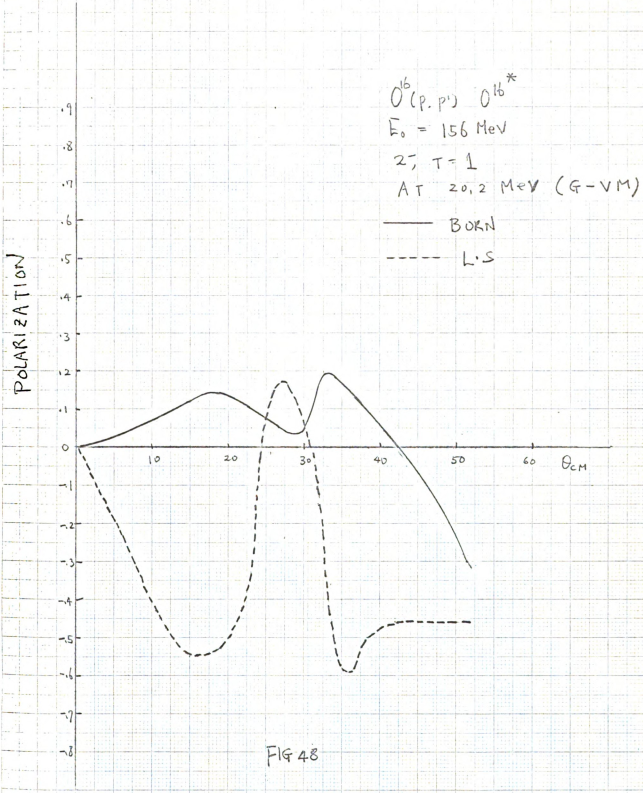
$O^{16}(p, p')\ O^{16*}$
E_0 = 156 MeV
2^-, T = 1
AT 20,2 MeV (G-VM)
BORN
L·S
POLARIZATION
θ_{CM}
.9
.8
.7
.6
.5
.4
.3
.2
.1
0
-.1
-.2
-.3
-.4
-.5
-.6
-.7
-.8
10
20
30
40
50
60

FIG 48

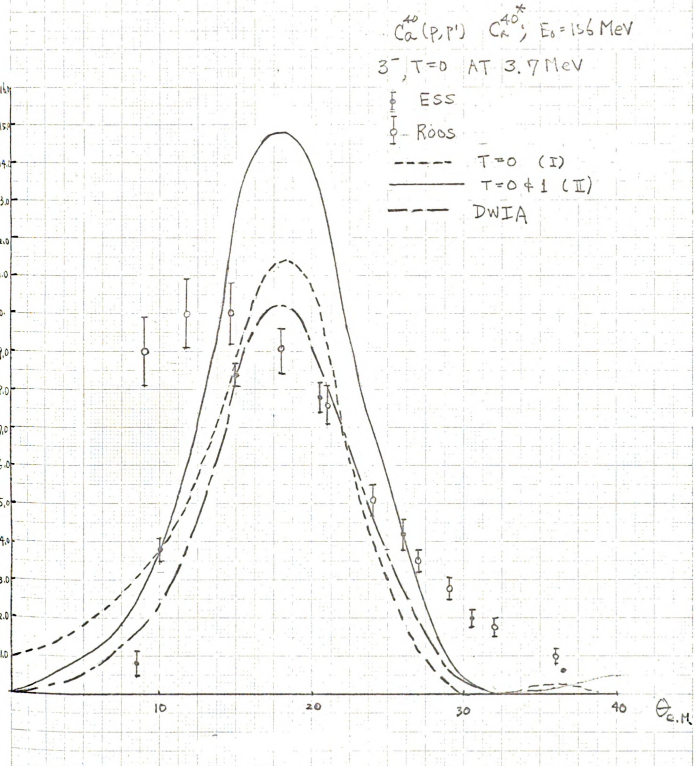

$Ca^{40}(p,p')\ Ca^{40*}$; $E_0 = 156$ MeV
3^-, T=0 AT 3.7 MeV
ESS
Roos
T=0 (I)
T=0 + 1 (II)
DWIA
1.0
2.0
3.0
4.0
5.0
7.0
8.0
9.0
10
20
30
40
$\theta_{c.M.}$

FIG 49

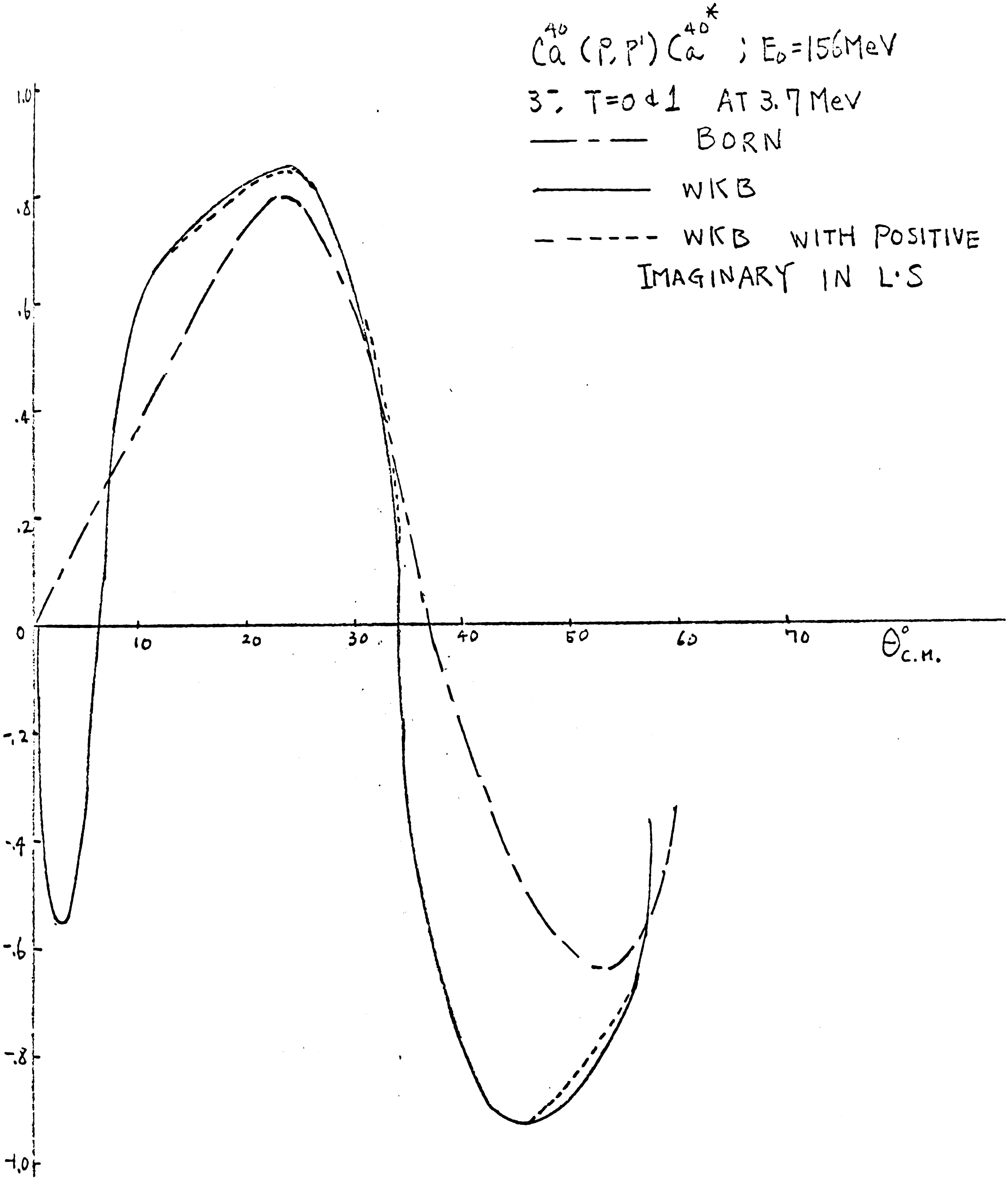

$Ca^{40}(p,p')Ca^{40*}$; E_0=156MeV
3^-, T=0 & 1 AT 3.7 MeV
BORN
WKB
WKB WITH POSITIVE IMAGINARY IN L·S
1.0
.8
.6
.4
.2
0
-.2
-.4
-.6
-.8
-1.0
10
20
30
40
50
60
70
$\theta^{\circ}_{C.M.}$

FIG. 50

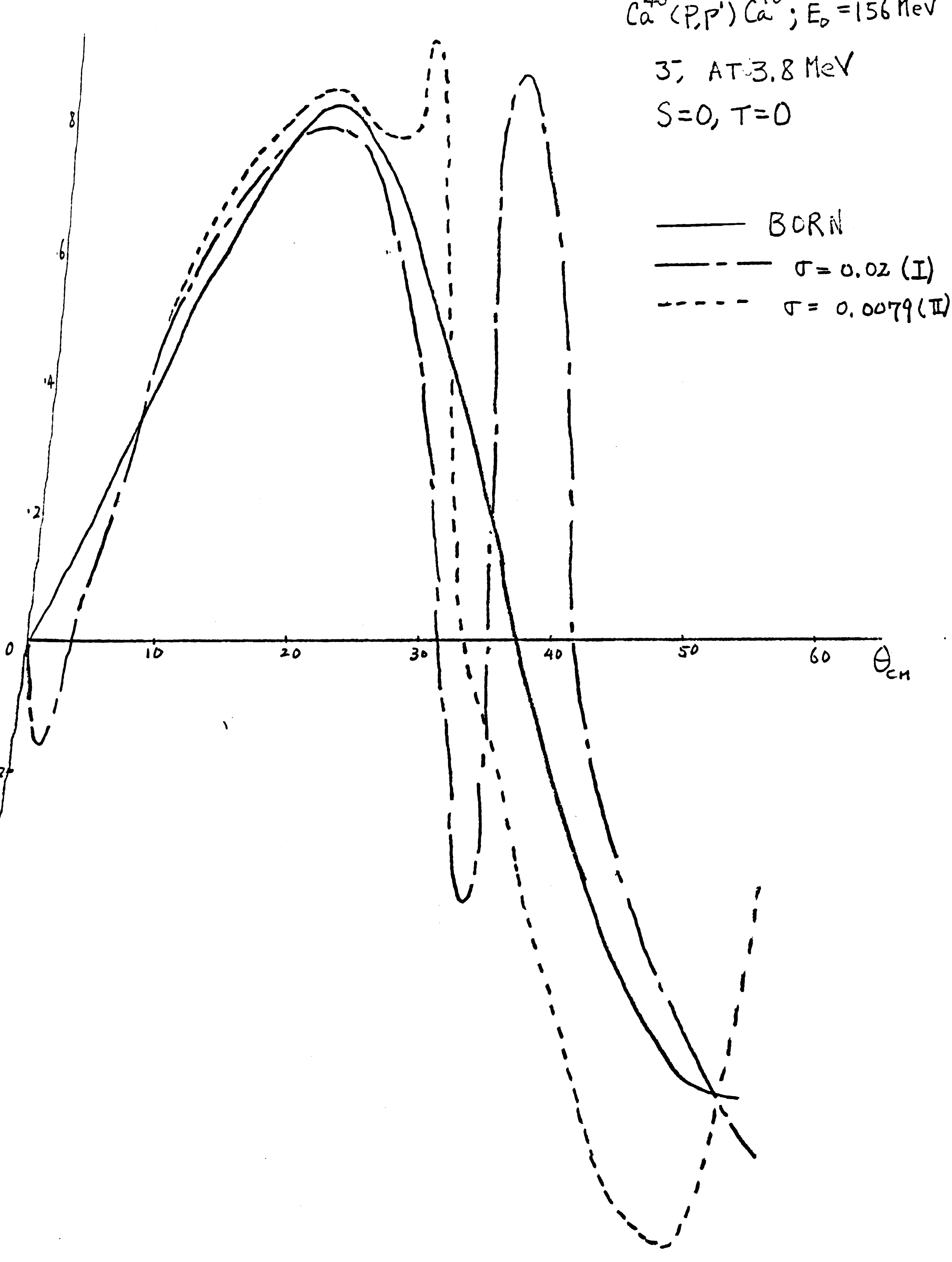

$Ca^{40}(P,P')Ca^{40*}$; E_0 = 156 MeV
3^-, AT 3.8 MeV
S=0, T=0
BORN
σ = 0.02 (I)
σ = 0.0079 (II)
.8
.6
.4
.2
0
10
20
30
40
50
60
θ_{CM}

FIG 51

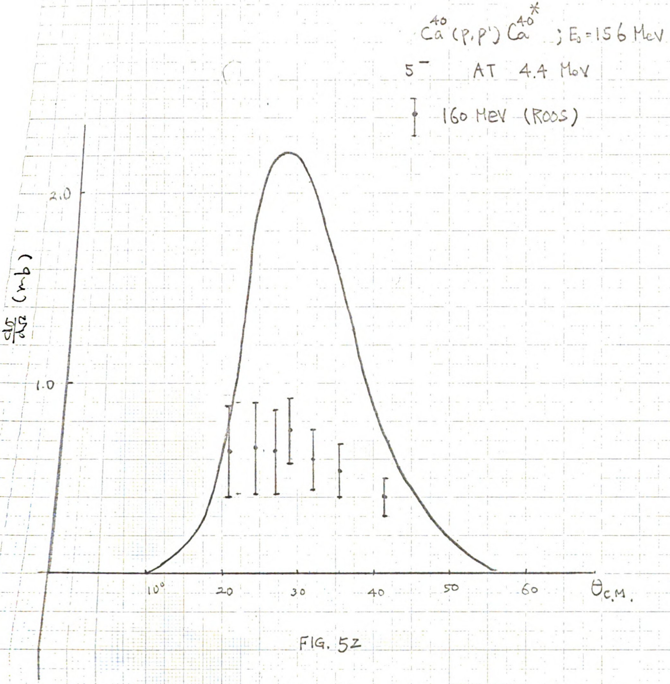

$Ca^{40}(p,p')Ca^{40*}$; E_0 = 156 MeV
5^- AT 4.4 MeV
160 MeV (ROOS)
$\frac{d\sigma}{d\Omega}$ (mb)
2.0
1.0
10°
20
30
40
50
60
$\theta_{C.M.}$

FIG. 52

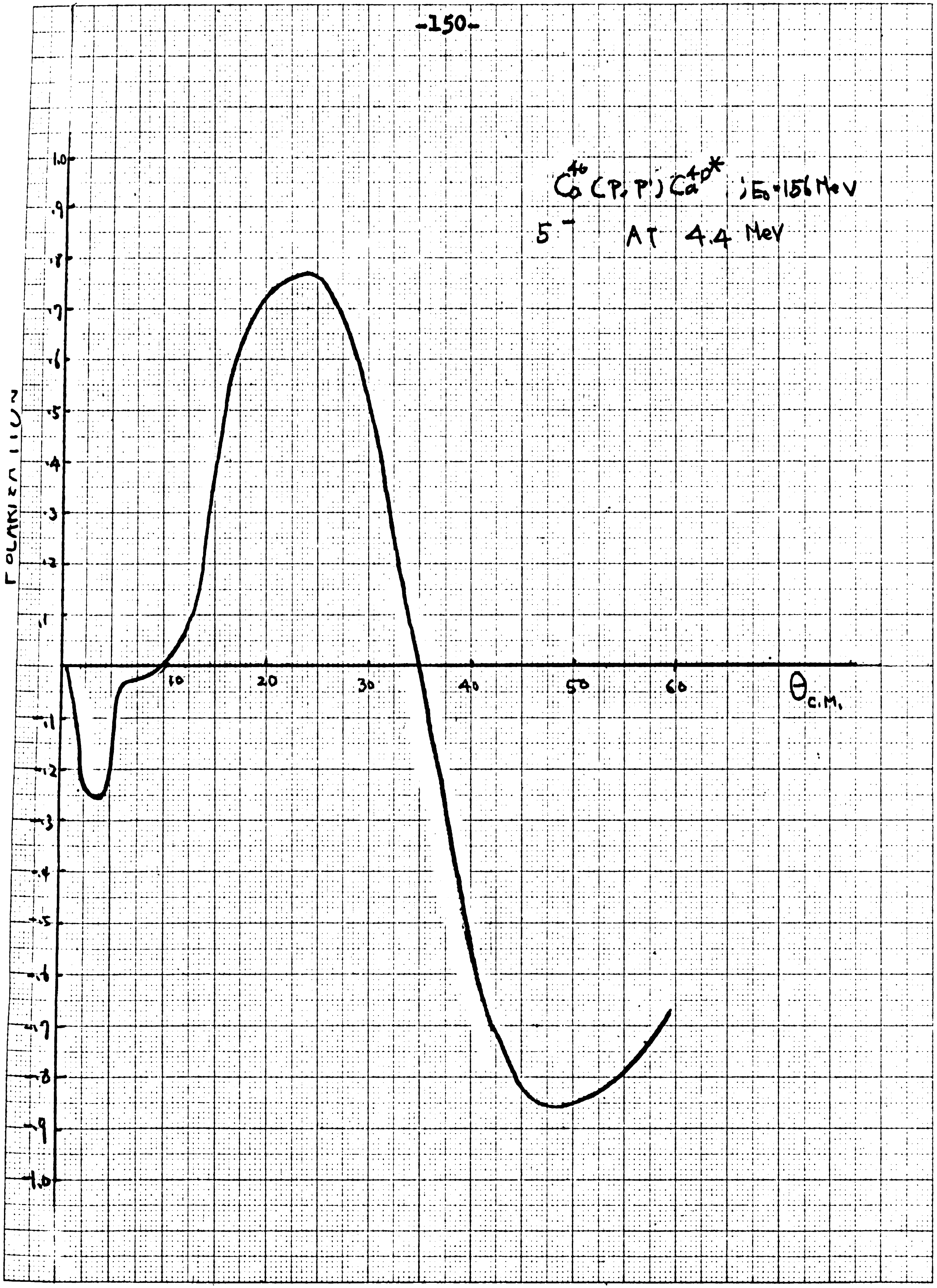

$Ca^{40}(p,p')Ca^{40*}$; E_0=156 MeV
5^- AT 4.4 MeV
POLARIZATION
1.0
.9
.8
.7
.6
.5
.4
.3
.2
.1
-.1
-.2
-.3
-.4
-.5
-.6
-.7
-.8
-.9
-1.0
10
20
30
40
50
60
$\theta_{C.M.}$

FIG 53

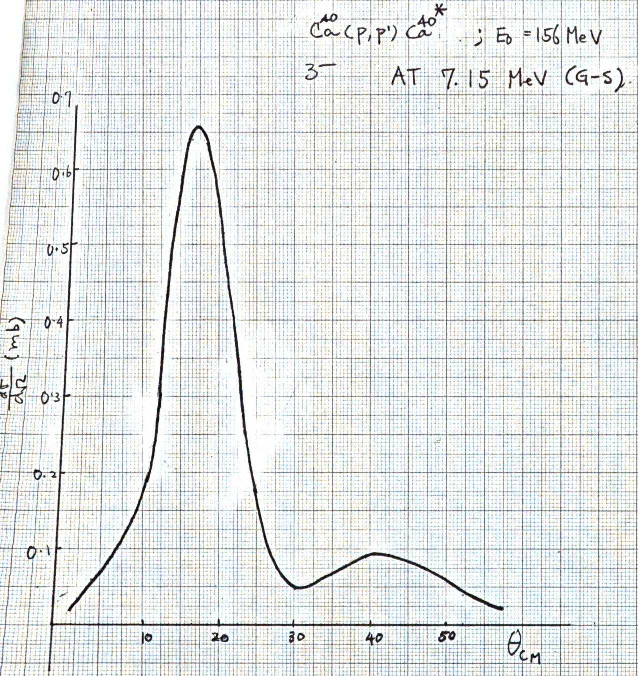

$Ca^{40}(p,p')Ca^{40*}$; $E_0 = 156$ MeV
3^- AT 7.15 MeV (G-S)
0.7
0.6
0.5
0.4
0.3
0.2
0.1
$\frac{d\sigma}{d\Omega}$ (mb)
10
20
30
40
50
θ_{CM}

FIG 54

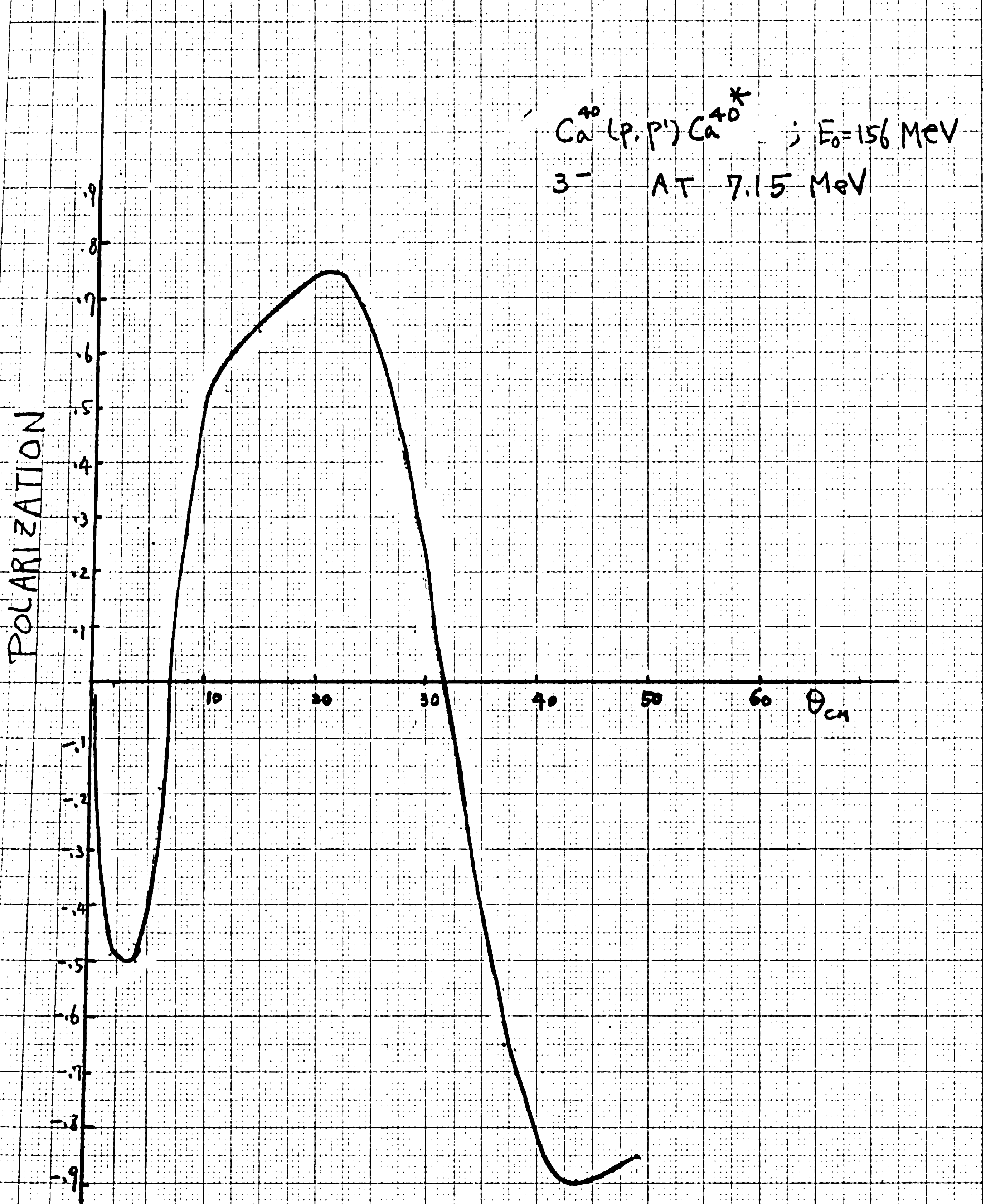
$Ca^{40}(p,p')Ca^{40*}$; E_0=156 MeV
3^- AT 7.15 MeV
POLARIZATION
θ_{CM}
.9
.8
.7
.6
.5
.4
.3
.2
.1
-.1
-.2
-.3
-.4
-.5
-.6
-.7
-.8
-.9
10
20
30
40
50
60

FIG 55

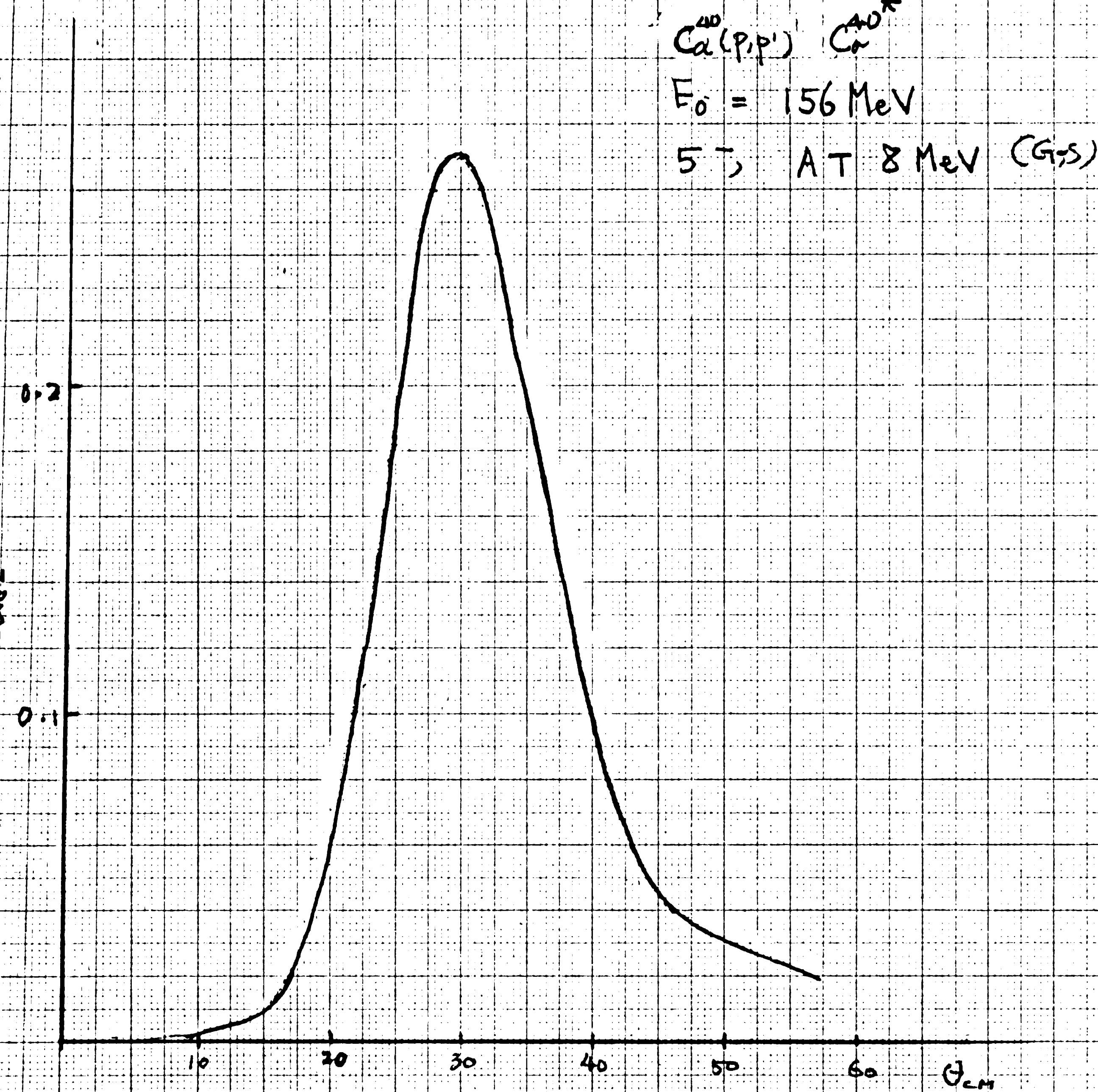
$Ca^{40}(p,p')\,Ca^{40*}$
$E_0 = 156$ MeV
5^-, AT 8 MeV (G.S)
0.2
0.1
$\frac{d\sigma}{d\Omega}$ (mb)
10
20
30
40
50
60
θ_{CM}

FIG. 58

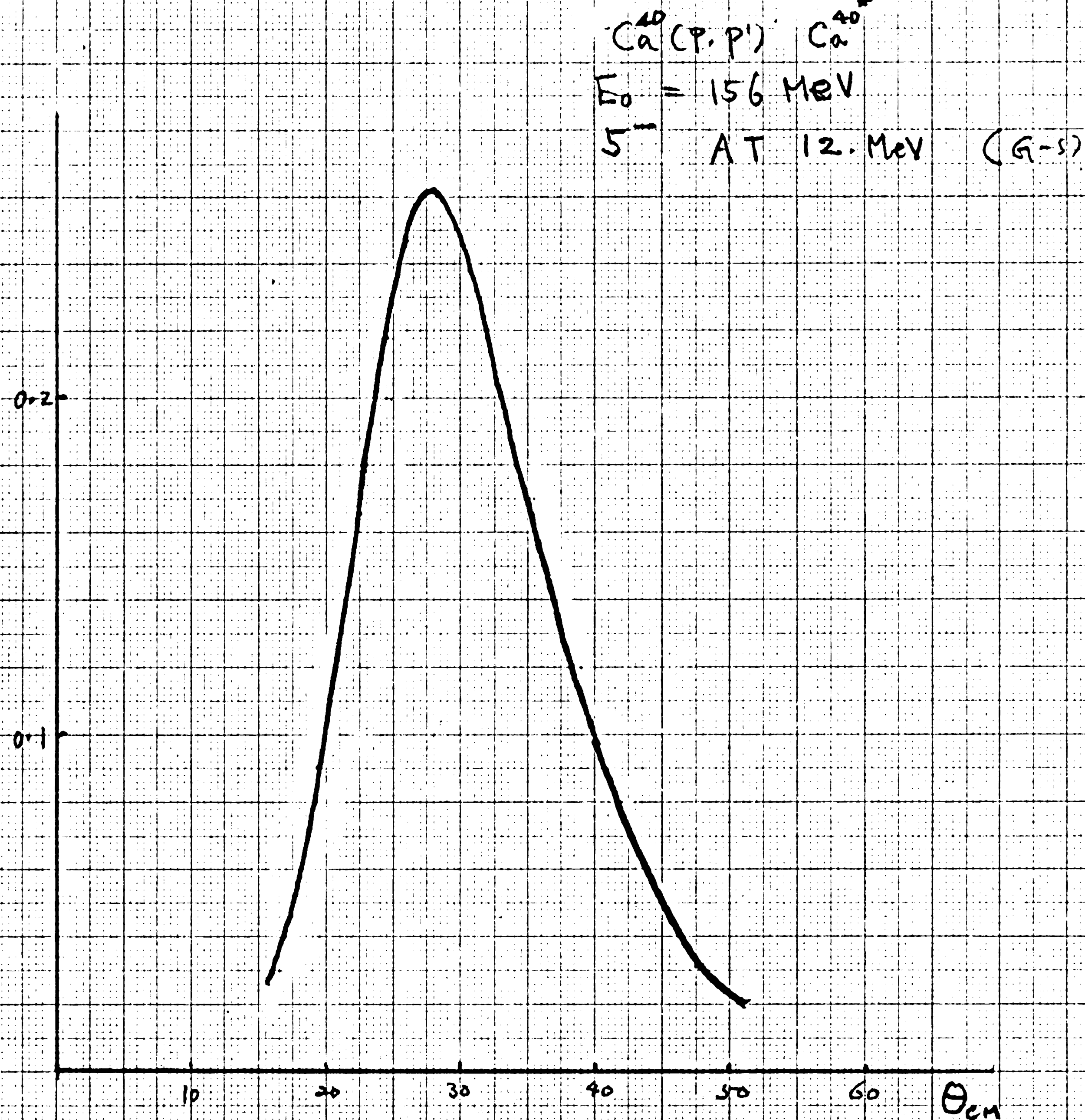

$Ca^{40}(p, p')\ Ca^{40*}$
$E_0 = 156$ MeV
5^- AT 12. MeV (G-S)
0.2
0.1
$\frac{d\sigma}{d\Omega}$ (mb)
10
20
30
40
50
60
θ_{CM}

FIG. 59

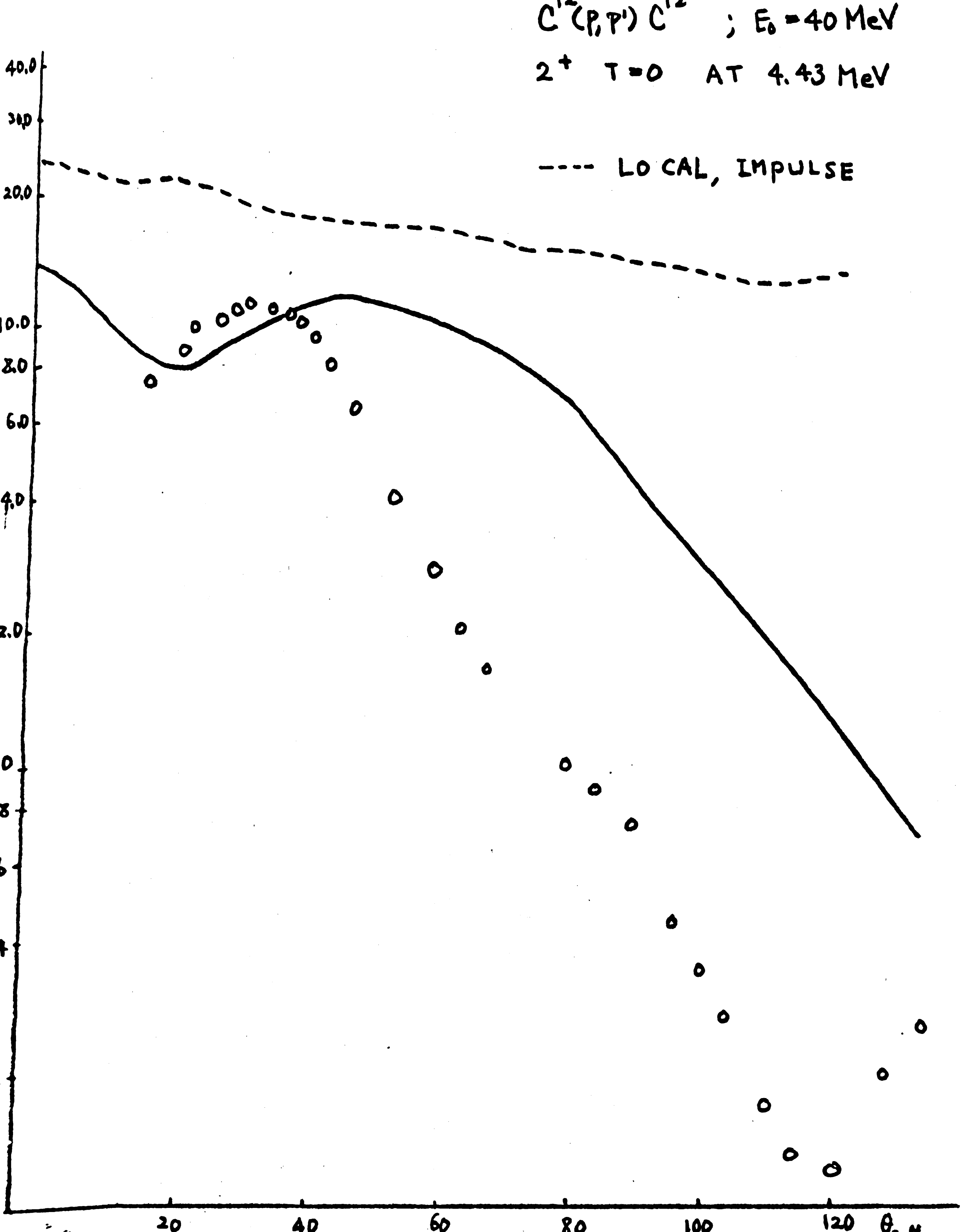
$C^{12}(p,p')C^{12*}$; $E_0 = 40$ MeV
2^+ T = 0 AT 4.43 MeV
---- LOCAL, IMPULSE
40.0
30.0
20.0
10.0
8.0
6.0
4.0
2.0
20
40
60
80
100
120
$\theta_{c.m.}$

FIG. 60

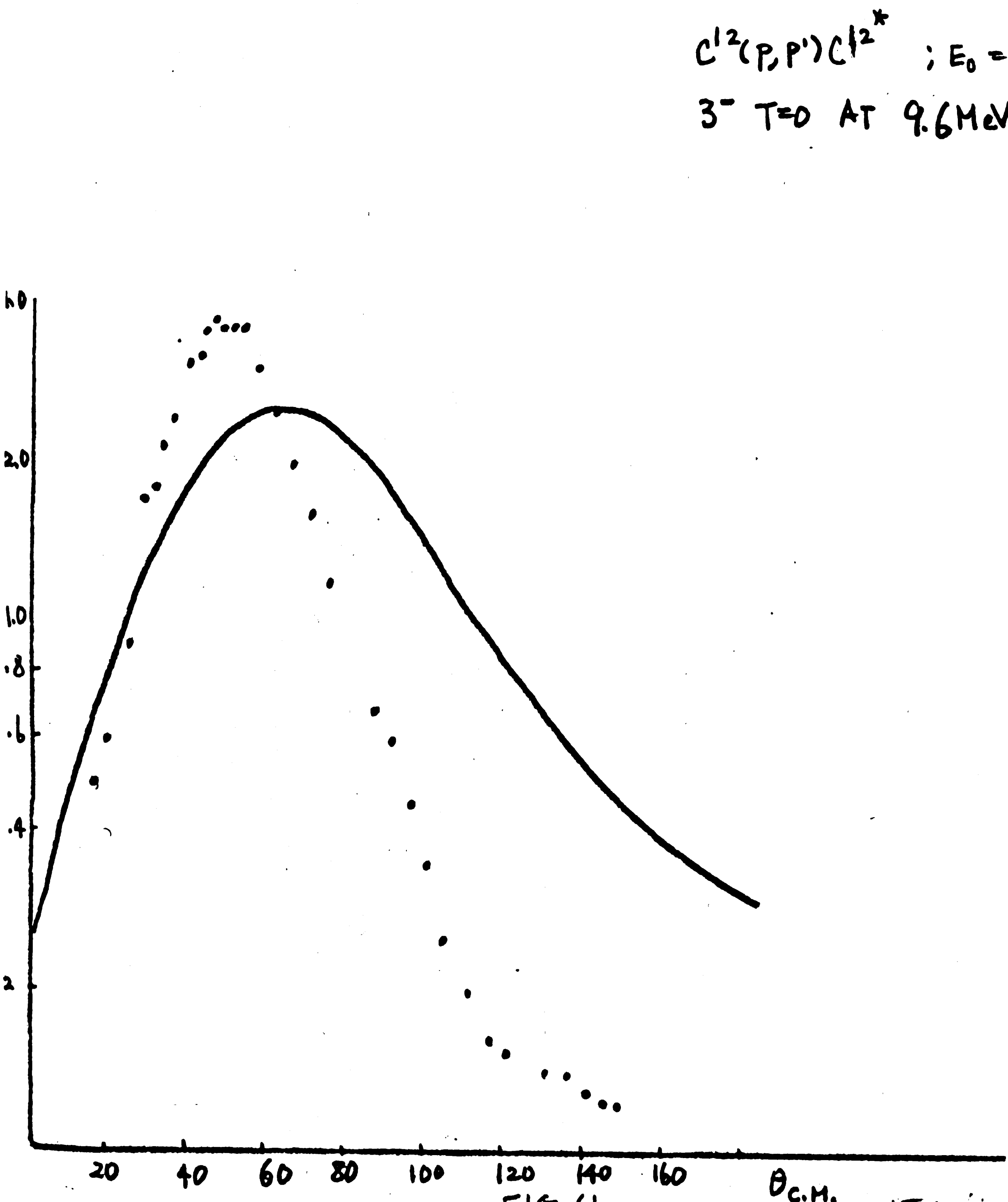
$C^{12}(p,p')C^{12*}$; E_0 = 40MeV
3⁻ T=0 AT 9.6MeV
1.0
2.0
.8
.6
.4
.2
20
40
60
80
100
120
140
160
$\theta_{C.M.}$

FIG. 61

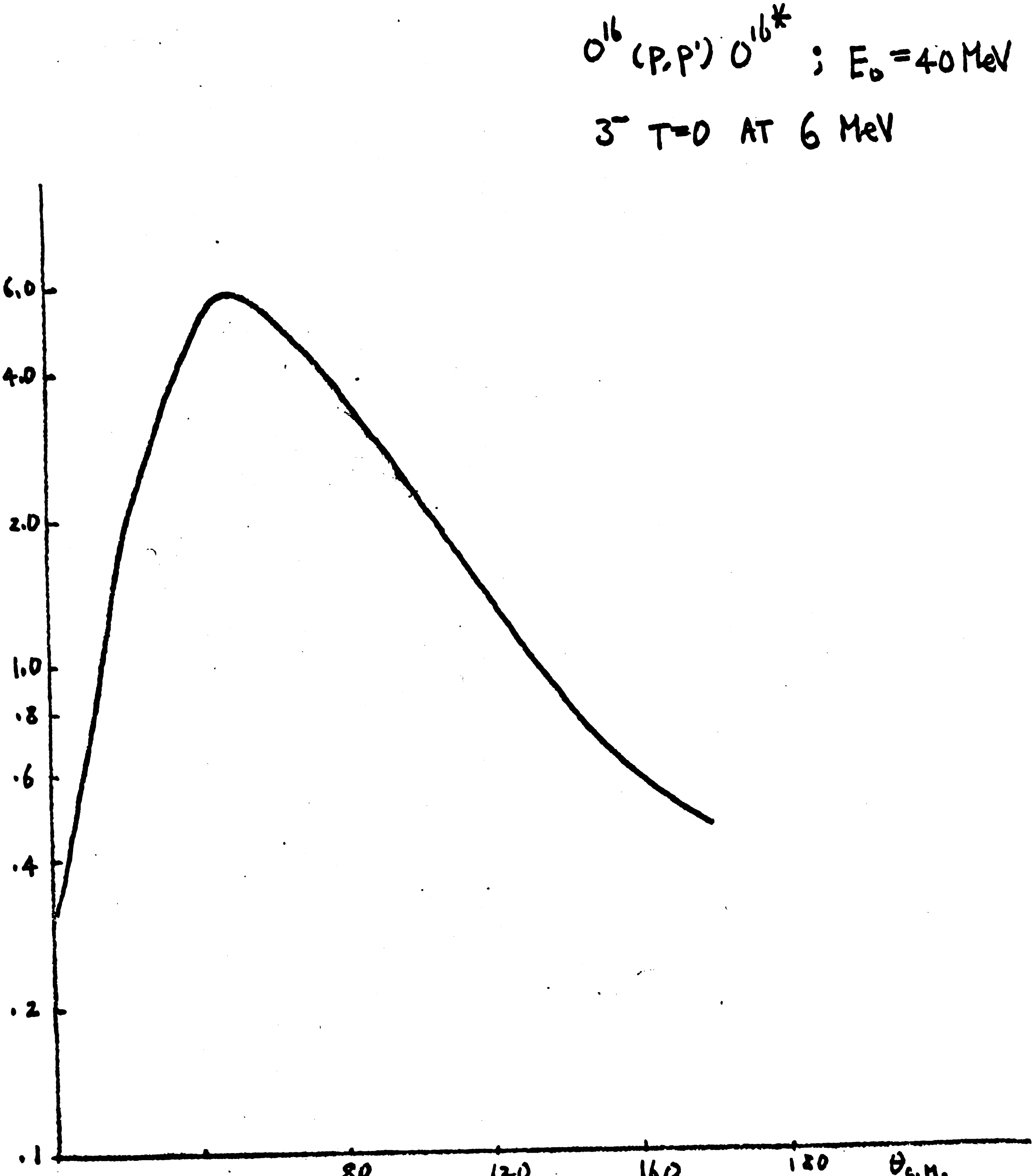
$O^{16}(p,p')O^{16*}$; $E_0 = 40$ MeV
3^- T=0 AT 6 MeV
6.0
4.0
2.0
1.0
.8
.6
.4
.2
.1
80
120
160
180
$\theta_{c.m.}$